

**SORPTION BEHAVIOR OF RADIOIODINE ON
ORGANIC RICH SOIL, ALUMINA AND CLAY
MINERALS**

**A THESIS
SUBMITTED TO THE DEPARTMENT OF CHEMISTRY
AND THE INSTITUTE OF ENGINEERING AND SCIENCES
OF BILKENT UNIVERSITY
IN PARTIAL FULFILLMENT OF THE REQUIREMENTS
FOR THE DEGREE OF
MASTER OF SCIENCE**

**By
SHOELEH ASSEMI
June 1992**

SORPTION BEHAVIOR OF RADIOIODINE ON
ORGANIC RICH SOIL, ALUMINA AND CLAY
MINERALS

A THESIS

SUBMITTED TO THE DEPARTMENT OF CHEMISTRY
AND THE INSTITUTE OF ENGINEERING AND SCIENCES
OF BILKENT UNIVERSITY
IN PARTIAL FULFILLMENT OF THE REQUIREMENTS
FOR THE DEGREE OF
MASTER OF SCIENCE

By

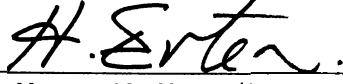
SHOELEH ASSEMI

June 1992

B 209.5

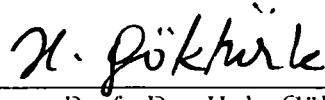
GD
547
A87
1992

I certify that I have read this thesis and that in my opinion it is fully adequate, in scope and in quality, as a thesis for the degree of Master of Science.



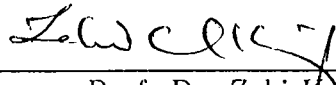
Prof. Dr. Hasan N. Erten(Principal Advisor)

I certify that I have read this thesis and that in my opinion it is fully adequate, in scope and in quality, as a thesis for the degree of Master of Science.



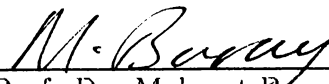
Assoc. Prof. Dr. Hale Gökürk

I certify that I have read this thesis and that in my opinion it is fully adequate, in scope and in quality, as a thesis for the degree of Master of Science.



Prof. Dr. Zeki Kuruoğlu

Approved for the Institute of Engineering and Sciences:



Prof. Dr. Mehmet Baray
Director of Institute of Engineering and Sciences

ABSTRACT

SORPTION BEHAVIOR OF RADIOIODINE ON ORGANIC RICH SOIL, ALUMINA AND CLAY MINERALS

SHOELEH ASSEMI

M.S. in Chemistry

Supervisor: Prof. Dr. Hasan N. Erten

June 1992

Sorption behavior of radioiodine on organic rich soil, alumina, chlorite-illite clay mixture, kaolinite and bentonite have been studied using the batch method. ^{131}I was used as tracer.

Characterization of samples were done by FTIR, X-ray diffraction spectrometry and particle size distribution by Andreason pipette method.

The grain size of the samples used were all below $38\mu\text{m}$ and the experiments were performed at room temperature. The aqueous phase used in all experiments were synthetic ground water with a composition similar to the underground waters of the regions where the samples were obtained.

Stock solutions containing ^{131}I tracer, were prepared using synthetic ground-water. Initial concentration of inactive iodide ion in the solutions ranged from 10^{-8} to 10^{-3} mmole/ml.

The influence of contact time, solution/solid ratio, pH of synthetic ground-water, biomass of soil and I^- ion concentration on the sorption of radioiodine on the organic rich soil were investigated. The effect of I^- ion concentration

and complexing agents on the sorption behavior of radioiodine on alumina and clay minerals were also studied.

A rather slow kinetics was observed for the adsorption of radioiodine on the organic rich soil, tending saturation within 14 days. It was observed that distribution ratio increased with increasing ratio of the volume of solution to the mass of soil (V/m ratio) and reached a plateau after V/m=50. Distribution ratio did not change very much by changing the pH of the solution. Comparison of Eh-pH behavior of the solutions with the standard Eh-pH graph of iodine-water system indicated that in the whole pH range, iodine is mostly present in I^- form. To observe the effect of soil biomass soil samples were sterilized by heat and ^{60}Co gamma-ray source and the results were found to be much lower than the control sample.

Increasing the concentration of iodide ion in the solution, caused a decrease in R_d values. Desorption was observed only for low initial iodine concentrations ($[I^-]_0 \leq 1 \times 10^{-6} \text{ mmol/ml}$), for organic rich soil which suggests that at least two sites and/or mechanisms are involved in the sorption.

The sorption data were fitted to Freundlich and Dubinin-Radushkevich isotherms. The slope of Freundlich isotherm was found to be less than 1 which indicates the non-linearity of the isotherm. The mean free energy of adsorption was calculated from the slope of Dubinin-Radushkevich isotherm and was found as about 11 kJ/mol. The distribution of sites on organic rich soil was calculated using the Freundlich and Dubinin-Radushkevich constants, considering Cl^- as the competing ion with I^- in the solution. The affinities of sites were found to be about three times higher for Cl^- than I^- .

Among the clay minerals, the highest R_d value was found for chlorite-illite clay mixture but the R_d values found for alumina and the other samples were well below those found for the organic rich soil. The sorption data were fitted to Freundlich and Dubinin-Radushkevich isotherms. All the Freundlich isotherms were non-linear (slope < 1), except for alumina (slope = 0.98), since the alumina sample used was 99% Al_2O_3 .

The mean energies of adsorption calculated for these samples, were in the

range of 9-11 kJ/mol. The site distribution curves were also obtained for these samples and the affinities of sites were found to be at least three times higher for Cl^- than I^- .

Clay samples were pretreated with complexing agents EDTA (Ethelene Diamine Tetra Acetic acid) and TPAI (Trimethyl Phenyl Ammonium Iodide). Very low or zero R_d values were found for treated samples.

Keywords: Sorption, Desorption, Radioiodine, Organic rich soil, Alumina, Clay minerals, Batch method, Isotherms, Sorption energy, Site distribution, Competing ion, Soil biomass, Complexing agents.

ÖZET

RADYOAKTİF İYOD'UN ORGANİK TOPRAK, ALUMİNA VE KİL MİNERALLERİNDE TUTULMASI

SHOELEH ASSEMI

Kimya Bölümü Yüksek Lisans

Tez Yöneticisi: Prof. Dr. Hasan N. Erten

Haziran 1992

Bu çalışmada radyoaktif iyodun organik kısmı yüksek(%70) olan toprakta, alumina, klorit-illit kil karışımı, bentonit ve kaolinit de tutulması araştırılmıştır.

Örneklerin yapısal karakterizasyonu, FTIR, X-ışını kırınımı spektrometresi ve Andreason pipet metodu ile tanecik büyüklüğü dağılımı deneyleri ile yapılmıştır.

Baç yöntemi ile yapılan deneylerde, örnekler tanecik büyüklüğüne göre ayrıldıktan sonra tanecik büyüklüğü, 0-38 μ m arası olanlardan belirli ağırlıklar alınmış ve polipropilen tüplerde değişik zaman aralıklarında, bilinen hacim ve I⁻ iyonu derişiminde, izleyici ¹³¹I içeren çözeltilerle çalkalanmış, sıvı ve katı fazlar santrifüj yolu ile ayrılmış ve sıvı fazdaki ¹³¹I aktivite değişikliği izlenmiştir.

Deneyler boyunca sulu faz olarak örneklerin elde edildiği bölgelerdeki yeraltı sularına uygun olarak hazırlanmış sentetik yeraltı suyu kullanılmıştır. ¹³¹I içeren çözeltilerde, aktif olmayan I⁻ iyonu, 10⁻⁸–10⁻⁶mmol/ml arası derişimlerle kullanılmıştır.

Topraktaki tutulmanın zaman, hacim/kütle oranı, solüsyonun pH değeri, topraktaki mikroorganizmalar ve solüsyondaki I⁻ iyonu derişimi ile bağımlılığı,

incelenmiştir. Alumina ve killerde ise I^- iyonu derişimi ve kompleks yapan maddelerin tutulma üzerindeki etkisi saptanmıştır.

Toprakla yapılan kinetik deneyde, tutulmanın çok yavaş ilerlediđi ve doyunluk deđerine en az 14 gün sürede ulaşıldığı görölmüştür. Hacım/kütle oranı(V/m), arttıkça, dağılım katsayısının yükseldiđi ve V/m=50 den sonra sabit kaldığı görölmüştür. Dağılım katsayısı, R_d , sentetik yeraltı suyunun pH deđişimi ile fazla deđişiklik göstermemiştir. Bu solüsyonlardaki Eh deđerleri, iyot-su sistemi Eh-pH diyagramı ile karşılaştırmca, tüm pH aralıklarında, iyodun çoğunlukla I^- iyon şeklinde olduđu belirlenmiştir. Topraktaki biokütlenin tutulma üzerindeki etkisini görmek için, toprak numuneleri ısı ve ^{60}CO kaynađı ile sterilize edilmiş ve dağılım katsayılarının sterilize olmayan topraktan çok daha düşük olduđu gözlenmiştir.

Sıvıdaki aktif olmayan iyodun derişimindeki artış, dağılım katsayısındaki düşüşe neden olmuş ve salıverilme (desorpsiyon), sadece düşük iyot derişimlerinde ($[I^-]_0 \leq 1 \times 10^{-6} mmol/ml$) görölmüştür. Bu davranış, iyodun toprakta en az iki mekanizma veya tutulma bölgelerince meydana geldiđini göstermektedir.

Tutulma izotermi Freundlich ve Dubinin-Radushkevich izoterm modellerine uygulanmıştır. Bu uygulamadan ise, tutulma enerjisi yaklaşık 11 kJ/mol bulunmuştur. Ayrıca Cl^- iyonunu, I^- iyonuna rakip iyon olarak kabul ederek, tutulma bölgelerinin çözeltideki I^- ve Cl^- iyonlarının tercih etmelerine göre, tutulma bölgelerin dağılımı bulunmuştur. Tutulma bölgeinin Cl^- 'u I^- 'da üç kat daha fazla tercih ettikleri hesaplanmıştır.

Killerde, en fazla tutulma katsayısı, Klorit-Illit kil karışımı için bulundu. Alumina ve diđer kil örneklerdeki tutulma katsayıları organik toprađa göre çok daha düşük bulunmuştur. Izotermi Freundlich ve Dubinin-Radushkevich izoterm modellerine uygulanmış ve tutulma enerjisi alumina ve killer için 8-12 kJ/mol arasında hesaplanmıştır. Freundlich izotermi eğrileri killer için 1'den az bulunmuştur. Alumina için ise, Freundlich sabiti 0.98 olarak bulunmuştur. Bu deđer alüminanın saf (%99) Al_2O_3 olduđundan kaynaklanıyor.

Tutulma enerjileri alumina ve killer için 8.5-11 kJ/mol olarak hesaplanmıştır. Bu örnekler için tutulma bölgelerin dağılım eğrileri elde edilmiştir. Bu örneklerde

de tutulma bölgelerinin Cl^- iyonunu I^- iyonuna en az üç defa daha fazla tercih ettikleri belirlenmiştir.

Alumina ve kil örnekleri, EDTA (Etilen Diamin Tetra Asetik asit) ve TPAI (Trimetil Fenil Amonyum İyodur) ile denge haline getirilmiştir. Bu örnekler için çok düşük veya sıfır R_D değerleri elde edilmiştir.

Anahtar Kelimeler: Tutulma, Salıverilme, Radyoaktif iyot, Organik toprak, Alumina, Kil, Baç yöntemi, İzotermiler, Tutulma enerjisi, Bölge dağılımı, Rakip iyon, Topraktaki canlı kütle, Kompleks yapan madde.

ACKNOWLEDGEMENT

I would like to express my gratitude towards Prof. Dr. Hasan Erten, for his unceasing contribution, guidance and encouragement throughout the development of this thesis.

I debt special thanks to Mr. Eray Aşansu, Yelda Sargin, Ayşın Solak and Nihan Nugay for their valuable helps in different steps of this work.

All my friends in Bilkent and Middle East Technical Universities are gratefully acknowledged for their continuous interest, help and morale support.

My last but not least thanks goes to Soheyl and my family who never left me alone and supported me by every means.

Contents

1	INTRODUCTION	1
1.0.1	Radioactive Waste Management	1
1.0.2	Iodine	7
1.0.3	Clay Minerals	11
1.0.4	Soils	19
1.0.5	Soil Organic Matter(SOM)	21
1.0.6	The Sorption Process	22
1.0.7	The R_d Concept	24
1.0.8	Isotherm Models	25
1.0.9	Previous Work	27
2	Experimental	31
2.0.10	Size Fractionation	31
2.0.11	Synthetic Groundwater	33
2.0.12	Tracer Containing Stock Solutions	34
2.0.13	Sorption-Desorption Experiments	35
3	Results and Discussion	38
3.1	Characterization of Samples	38

3.2	Bolu-Yeniçağ Soil	45
3.2.1	Kinetic Experiment	45
3.2.2	Variation of Distribution Ratio with the Ratio of Volume of the Solution to Mass of the Solid	48
3.2.3	The Effect of pH on the Adsorption of Iodine	49
3.2.4	Loading Experiments	52
3.2.5	Adsorption Isotherms	56
3.2.6	Site Distribution	59
3.2.7	Effect of Sterilization	61
3.3	Clay Minerals	63
3.3.1	Sorption Experiments	63
3.3.2	Adsorption Isotherms	66
3.3.3	Site Distribution	73
3.3.4	Effect of Complexing Agents	76
4	Discussion of Results	77

List of Figures

1.1	The Radioactivity of Heavy Nuclides in Spent Nuclear Fuel . . .	6
1.2	The Migration Pathway of Radioiodine from an Underground Repository to the Environment	8
1.3	Doses to Nearby Residents for Scenario A of Swedish Program .	10
1.4	Diagrammatic Sketch showing (a) A Single Octahedral Unit and (b) The Sheet Structure of the Octahedral Units.	11
1.5	Diagrammatic Sketch showing (a) A Single Silica Tetrahedron and (b) The Sheet Structure of the Tetrahedrons Arranged in a Hexagonal Network.	12
1.6	Schematic Representation of The Atom Arrangement in Unit cells of (a) A 2:1 Layer Mineral (b) A 1:1 Layer Mineral	13
1.7	Diagrammatic sketch of the structure of the kaolinite layer . . .	14
1.8	Schematic Representation of The Structure of Montmorillonite .	16
1.9	The Diagrammatic Sketch of The Structure of Chlorites	17
1.10	Schematic Representation of The Structure of illites	18
3.1	The FTIR spectrum of Bolu-Soil and the Spectrum of Standard Humic Acid	39
3.2	The FTIR Spectrum of Chlorite-Illite Clay mixture and the Spectrum of Standard Chlorite and Illite	39
3.3	The FTIR Spectrum of Bentonite Clay and the Spectrum of Standard Montmorillonite	40

3.4	The FTIR Spectrum of Kaolinite Clay and the Spectrum of Standard Kaolinite	40
3.5	The FTIR Spectrum of Alumina and the Spectrum Gibbsite . .	41
3.6	The X-Ray Diffraction Pattern of Bolu Soil	41
3.7	The X-Ray Diffraction Pattern of CHlorite-Illite Clay Mixture .	42
3.8	The X-Ray Diffraction Pattern of Bentonite	42
3.9	The X-Ray Diffraction Pattern of Kaolinite	43
3.10	The X-Ray Diffraction Pattern of Alumina	43
3.11	Particle Size Distribution Below $38\mu m$ of Bolu-Soil and Minerals	44
3.12	The Change of Distribution Ratio with Time for Bolu-Yeniç Soil	46
3.13	Plot of Remaining Activity in the Solution versus Time for the Adsorption of Radioiodine on Bolu-Yeniçağ Soil	47
3.14	Change of R_d with V/m Ratio for Bolu-Yeniçağ Soil	49
3.15	The Change of Distribution Ratio with pH of the Solution for Bolu-Yeniçağ Soil	50
3.16	Eh-pH Diagram for Iodine-Water System	51
3.17	The Change of Distribution Ratio with the Iodine Loading for Pretreated and untreated Bolu-Yeniçağ Soil	52
3.18	Loading curve for Exchange of Radioiodine on Bolu-Yeniçağ soil	54
3.19	Freundlich Isotherms for Adsorption of Radioiodine on Bolu-Yeniçağ Soil. Initial Iodine Concentration $1 \times 10^{-3} mmol/ml < [I^-]_i^0 < 1 \times 10^{-3} mmol/ml$	56
3.20	The Dubinin-Radushkevich Isotherm for Adsorption of Radioiodine on Bolu-Yeniçağ Soil. Initial Iodine Concentration $1 \times 10^{-3} mmol/ml < [I^-]_i^0 < 1 \times 10^{-3} mmol/ml$	57
3.21	The Site Distribution on Bolu-Yeniçağ Soil, Considering Cl^- as the Competing Ion	61

3.22 Loading Curves for sorption of radioiodine on Chlorite-Illite Clay Mixture	64
3.23 Loading Curves for sorption of radioiodine on Bentonite	65
3.24 Loading Curves for sorption of radioiodine on Kaolinite	65
3.25 Loading Curves for sorption of radioiodine on Alumina	66
3.26 Freundlich Isotherms for Sorption of Radioiodine on Chlorite-Illite Clay Mixture	67
3.27 Freundlich Isotherms for Sorption of Radioiodine on Bentonite	67
3.28 Freundlich Isotherms for Sorption of Radioiodine on Kaolinite .	68
3.29 Freundlich Isotherms for Sorption of Radioiodine on Alumina . .	68
3.30 Dubinin-Radushkevich Isotherms for sorption of Radioiodine on Chlorite-Illite Clay Mixture	69
3.31 Dubinin-Radushkevich Isotherms for sorption of Radioiodine on Bentonite	69
3.32 Dubinin-Radushkevich Isotherms for sorption of Radio iodine on Kaolinite	70
3.33 Dubinin-Radushkevich Isotherms for sorption of Radio iodine on Alumina	70
3.34 The Site Distribution on Chlorite-Illite, for the adsorption of iodine, Considering Cl^- as Competing Ion	73
3.35 The Site Distribution on Bentonite, for the adsorption of iodine, Considering Cl^- as Competing Ion	74
3.36 The Site Distribution on Kaolinite, for the adsorption of iodine, Considering Cl^- as Competing Ion	74
3.37 The Site Distribution on Alumina for the adsorption of iodine, Considering Cl^- as Competing Ion	75

List of Tables

1.1	Some Methods Used For The Disposal of Radioactive Waste	2
1.2	Radioactive Waste Categories	3
1.3	The Chemical Forms of Radioiodine in Trench, Well and Spring Waters Around a Low-Level Waste Disposal	9
1.4	Risk of Cancer Mortality for Some Radionuclides in Radioactive Wastes	10
1.5	Alumina Types	19
1.6	Climate Classification of Soils	20
1.7	Categories of Adsorption Process	23
1.8	Experimental Results in Literature for Adsorption of Radioiodine on Soil Samples	29
1.9	Experimental Results in Literature for Adsorption of Radioiodine on Chlorite, Illite, Chlorite-Illite mixture, Bentonite and Alumina	30
1.10	Experimental Results in Literature for Adsorption of Radioiodine on Soil and Bentonite Pretreated with Inorganic Complexing Agents (HDTMA ⁺ : Hexadecyl Trimethyl Amonium ion, HDPY ⁺ :Hexadecyl Pyridinium ion, BE ⁺ :Benzethonium ion.) . .	30
2.1	Composition of the Synthetic Groundwater Used	33
2.2	Composition of the Stock Solutions Used	33
3.1	Results of Chemical Analysis of Bolu-Yeniçağ Soil	44

3.2	Concentration of some trace elements in Bolu-Yeniçağ Soil	45
3.3	The Results of Kinetic Experiment for Bolu-Yeniçağ Soil	46
3.4	The Experimental Results Showing the Change of Distribution Ratio with V/m for Bolu-Yeniçağ Soil	48
3.5	The Experimental Results Showing the Effect of pH on Distribution Ratio for the sorption of radioiodine on Bolu-Yeniçağ Soil	51
3.6	Sorption, Desorption and Exchange Distribution Ratios and percentages of Adsorption(%A), Desorption (%D), Reversibility (%R) and Exchange (%E),for adsorption of radioiodine on Bolu-Yeniçağ Soil	55
3.7	The Constants Found from Fitting the Sorption and Exchange Data to Freundlich and Dubinin-Radushkevich Isotherms for the Adsorption of Iodine on Bolu-Yeniçağ Soil	57
3.8	The Theoretical R_d values Obtained From The Isotherm Constants, for Bolu-Yeniçağ soil. $R_{d,(exp.)}$: Experimental R_d , $R_{d,(D-R.)}$: R_d obtained from Dubinin-Radushkevich Isotherm, $R_{d,(Fru.)}$: R_d obtained from Freundlich Isotherm	59
3.9	Effect of Sterilization on Sorption of Iodine on Bolu-Yeniçağ Soil	62
3.10	Experimental and Theoretical R_d Values for the Adsorption of Radioiodine on Clay Minerals. $R_{d,(exp.)}$: Experimentally obtained R_d values, $R_{d,(D-R.)}$: R_d Calculated from Dubinin-Radushkevich Isotherm, $R_{d,(Fru.)}$: R_d Calculated from Freundlich Isotherm	71
3.11	The Constants Found From Fitting the Sorption Data to Isotherm Models for Clay Minerals	72
3.12	Adsorption Energies Calculated from the Dubinin-Radushkevich Isotherm Constant K ($E = (2K)^{-1/2}$) for the Minerals	72
3.13	The Parameters Used to Calculate the Site Distribution Functions of Minerals and the Affinities Found from These Parameters for the Adsorption of Iodine on Clay Minerals	75
3.14	R_d Values for the Sorption of Radioiodine on Clay Mineral Samples Pretreated With EDTA and TPAI $[I]_i^0 = 1 \times 10^{-8} mmol/ml$	76

4.1 Comparison of Distribution Ratios with the Number of OH^- ion in The Unit Cells of Clay Minerals	78
--	----

Chapter 1

INTRODUCTION

1.0.1 Radioactive Waste Management

Usage of radionuclides in nuclear power plants, reprocessing of spent fuel, medical applications and research fields in ever increasing quantity , leads to the problem of radioactive waste which is potentially harmful to man and to the environment. They range in activity from near natural background as those used in radio-medicine, to very high activity from nuclear reactor fuel wastes[1].

Internationally different conceptual methods for the disposal of radioactive wastes has been proposed . Some of these methods with comments on their feasibility are given in Table-1.1[2].

Underground disposal seems to be the most preferred way of management of the radioactive wastes, because of both economical and technological points of view. The most important consideration is the safety of the environment. In this sense nuclear wastes are charachtarized into five categories by International Atomic Energy Agency (Table-1.2) [3].

The high-level wastes (spent fuel and high-level liquid wastes) may be stored for a suitable period to allow shorter lived radioactivity to decay . Then they can be encapsulated in metals or ceramic. The liquid waste must be immobilized by conversion to solid. The adequate heat dissipation must also be considered to prevent unacceptably high temperatures.

Methods	Comments
Supervised storage	Does not constitute a final solution
Launching into space	Technology not available
Separation and transmutation	Technology not available
Deep geological disposal	Possible in bedrock
Disposal in deep-sea sediments	Requires available sites
Injection into isolated deep geological formations	Suitable areas are required
Disposal under inland ice sheets or under permafrost	Area of sufficient extent are required

Table 1.1: Some Methods Used For The Disposal of Radioactive Waste

Waste Category	Important Features
High-level Long-lived	High beta/gamma Significant alpha High radio toxicity High heat output
Intermediate-level Long-lived	Intermediate beta/gamma Significant alpha Intermediate radiotoxicity Low heat output
Low-level Long-lived	Low beta/gamma Significant alpha Low/Intermediate radiotoxicity Insignificant heat output
Low-level Short-lived	Low beta/gamma Insignificant alpha Intermediate radiotoxicity Low heat output
Low-level Short-lived	Low beta/gamma Insignificant alpha Low radiotoxicity Insignificant heat output

Table 1.2: Radioactive Waste Categories

The intermediate level, long-lived radioactive wastes result from spent fuel elements, the cladding hulls, the associated hardware and the insoluble dissolver residues. For their disposal the undissolved fuel, the associated fission product and the actinide radioactivity sources must be removed from the cladding hulls. The mechanical compaction of spent fuel, incorporation in cement or metal or placement in cement canisters must also be done. Concrete, polymers and bitumen are also used for immobilization of this type of waste.

The gaseous wastes are also included in this category. The most important ones are: ^{85}Kr , ^{129}I and ^{14}C . ^{85}Kr should be compressed in metal gas bottles or incorporated in a number of metals and other solid materials. It can also be removed and concentrated, then isolated for about 100 years, to decay to acceptable levels before releasing to the environment. The ways of immobilization of ^{129}I over a long period is being studied. A detailed review of the works done and the importance of radioiodine is given in the next section. For ^{14}C marine dilution is an alternative. Ways of immobilization of this radionuclide is also being studied. Contaminated soil also appears in this category. For their disposal, incorporation in cement or bitumen or plastic resins or sealing with an adherent coating must be done.

The gaseous wastes and contaminated soil appear also in short-lived low and intermediate level wastes. Their treatment is the same as explained above.

The low level liquid wastes and the alpha contaminated wastes with low beta/gamma radioactivity level are in the category of low-level, long-lived wastes. For low level liquid wastes, treatments such as precipitation, ion-exchange, distillation, sorption, solvent extraction and filtration are used for immobilization. The residues are immobilized and the fluids are discharged to the environment. The combustible wastes contained in alpha contaminated wastes with low beta/gamma radioactivity level group, are oxidized to reduce volume and flammability. The resulting ash may be leached to remove plutonium and residues may be conditioned and prepared for disposal. These wastes

can also be added to the wastes of previous categories (the high and intermediate, long-lived wastes). The noncombustible wastes must be decontaminated as far as possible to enable their disposal with short-lived radioactive wastes.

The tritium contaminated wastes are in the intermediate-level, short-lived wastes category. For a large volume of waste with low concentration of tritium, the treatment ways consist of: dilution and direct discharge into aqueous environment including oceans, deep well injection and hydraulic fracturing. For the more concentrated wastes with lower volume of tritium, immobilization in a packaged solid (with or without impregnation by polymer resins, silica gel, activated alumina, hydrated calcium sulphate, molecular sieves, organic hydrogenous compounds, metal hydrides) and burial are suggested. Another way is their disposal in a packaged and solidified form on the ocean floor.

In summary IAEA (International Atomic Energy Agency) considers five major options for underground disposal of radioactive wastes as followings[4]:

- 1) Disposal in shallow ground
- 2) Disposal in rock cavities
- 3) Disposal in deep geological formations
- 4) Disposal by liquid injection
- 5) Disposal by hydraulic fracturing

The underground disposal must be done in such a way that during a long period of time, the radioactive waste will remain isolated and from the environment. From a long period we mean about at least 10^7 years which is the time for reducing the total activity in spent fuel from 10^{16} bq/tonne uranium to 10^{11} bq/tonne. For a better illustration, the radioactivity of heavy nuclides in spent fuel is shown in Fig. 1.1 [2].

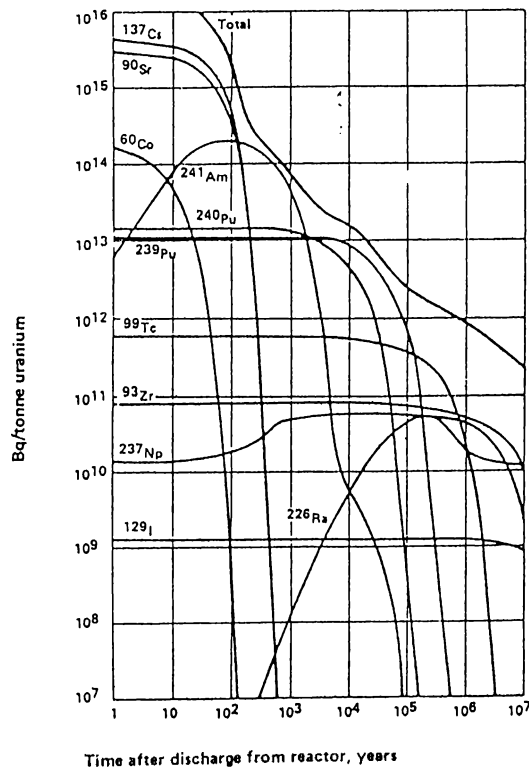


Figure 1.1: The Radioactivity of Heavy Nuclides in Spent Nuclear Fuel

Although the access of water to the emplaced waste and transport from a repository are not likely in most cases, a long term safety program should model conceivable scenarios in which this access and transport of water could nevertheless occur. In this sense the following parameters are important in transport of radionuclides by ground water and/or sorption or desorption of them by backfills, clays or soils:

- Aerobic/anaerobic conditions
- Variation of Eh and pH
- Grain size of clay or soil
- Formation of colloids
- Radionuclide concentration
- The contact time
- Solubility of the elements
- Temperature
- Soil organics
- Complexing agents

1.0.2 Iodine

Iodine is an electronegative element with a large ionic radius of 0.22 nm. Its oxidation states in aqueous medium are -1 , 0 , $+1$, $+3$, $+5$ and $+7$. Its most abundant states in the environment are -1 , 0 and $+5$. The common forms of iodine are I^- , IO_3^- , IOH , IO^- , I_2 and I_3^- [5, 6]. Generally iodine is present in aqueous systems as iodide or iodate. In acidic solution, I_2 and the polyiodide ion I_3^- may also become important. I_2 can be stabilized in solution to some extent by combining with I^- to form I_3^- species [7]. This anion forms stable salts with large cations such as Cs^+ [8]. Iodide can interact with solid material by complex formation.

Iodine has two important isotopes with respect to radioactive wastes. ^{129}I with a half-life of ($t_{1/2} = 1.57 \times 10^7$ y) and ^{131}I with a half-life of ($t_{1/2} = 8.04$ d). The long half-life of ^{129}I and the high specific activity of pure ^{131}I (1.23×10^4 ci/g), make them important contaminants of environment in the long and short terms respectively. They are produced during the operation of nuclear power plants, the reprocessing of nuclear fuel and testing of nuclear weapons [9]. ^{129}I is also a naturally occurring isotope of ^{127}I . The terrestrial equilibrium ratio of ^{129}I to ^{127}I is in the range of $2.2 - 3.3 \times 10^{-15}$ [10]. Iodine can transfer easily in the environment because of its volatility and concentrates in thyroid gland and tissues in human being. The biological half-life of iodine in the adult thyroid is about 140 days and the quantity of iodine in human thyroid is about 7 milligrams [11].

The major pathways of released ^{129}I migrating from a geological waste disposal site to the biosphere has been derived, based on the migration behavior of iodine in nature and the global circulation model [11]. This pathway is illustrated in Fig. 1.2.

The chemical speciation of radioiodine in trench, well and spring waters around the low-level waste disposal site at Battelle, have been determined by Robertson et al. [12]. The results are summarized in Table-1.3.

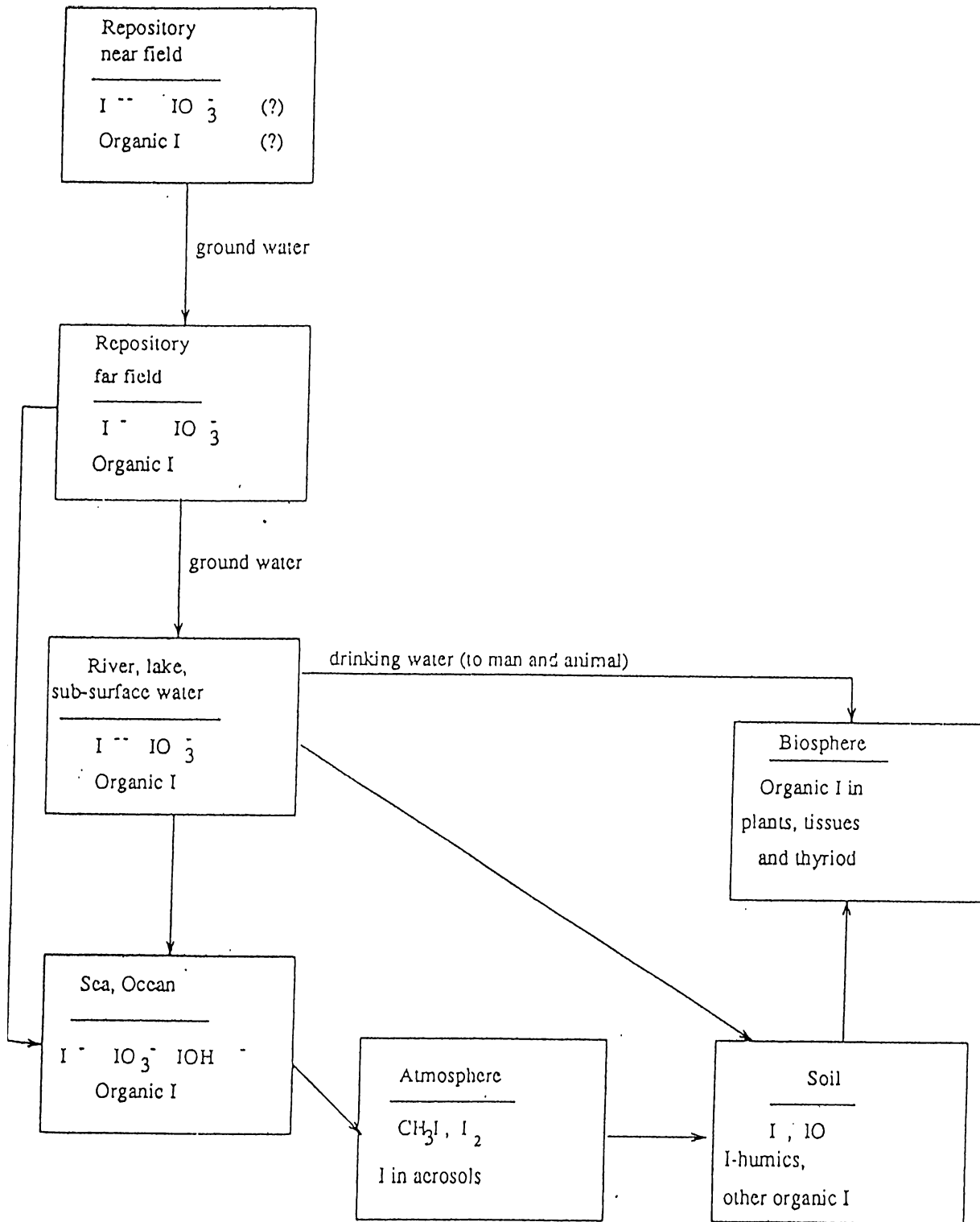


Figure 1.2: The Migration Pathway of Radioiodine from an Underground Repository to the Environment

Sample	Date	Chemical Forms of ^{131}I	% of total
Trench water	26-1-83	I^-	48
		IO_3^-	3
		Organic I	49
Well#1 water	27-1-83	I^-	46
		IO_3^-	2
		Organic I	52
Spring water	31-1-83	I^-	42
		IO_3^-	1
		Organic I	57

Table 1.3: The Chemical Forms of Radioiodine in Trench, Well and Spring Waters Around a Low-Level Waste Disposal

Weber et al [13] and von Gunten[14] have measured the radionuclides resulting from fallout from Chernobyl accident in the river Glatt at Switzerland and in the adjacent shallow groundwater stream. Their results show that more than 95% of the ^{131}I activity is found in solution, either as soluble iodide or possibly bound to very small colloids of diameter less than $0.05 \mu\text{m}$. 90% of the ^{131}I is present as iodide and only 10% could be precipitated as lead iodate.

^{129}I has a very low specific activity due to its long half-life, so it is much less toxic compared to other radioactive waste nuclides. But it survives over a long time, migrates easily in the environment and concentrates in a critical organ. The total dose contributed by ^{129}I to the global population per unit of electricity generated from a nuclear power plant is 0.005 man-Gy per Mw per year(=0.5 rad/Mw.y). This should be compared with the total dose to the global population from radionuclide release, which is 0.025 man-Gy per Mw per year(=2.5 rad/Mw.y)[15].

The risk of cancer mortality¹ for children below 10 years of age, upon ingestion of soluble radionuclides is assessed by Staley et al.[17]. The potential hazard of ^{129}I is demonstrated in these numbers when compared to the other

¹The cancer risk is calculated by $\sigma = D^n/C$, where σ is the cancer coefficient, D is the dose to each person and C is the cancer deaths from dose D [16]

radionuclides (Table-1.4).

Radionuclide	Risk of cancer mortality (risk/ μ ci radionuclide)
^{129}I	2×10^{-4}
^{238}Pu ^{239}Pu ^{240}Pu	1×10^{-6}
^{90}Sr	2×10^{-8}

Table 1.4: Risk of Cancer Mortality for Some Radionuclides in Radioactive Wastes

The cement of the technical barrier used in an underground repository is assumed to be decomposed to compacted sand after about 10^4 years. The radionuclides are conservatively assumed to pass without delay from the solid phase into pore water and migrate into the geosphere. Due to the long half-life of ^{129}I , it will be a major contaminant after this period. This is illustrated in Fig. 1.3, which shows the doses to nearby residents in a period of 10^{10} years, from a scenario A of Swedish program for underground disposal of radioactive waste.[18]

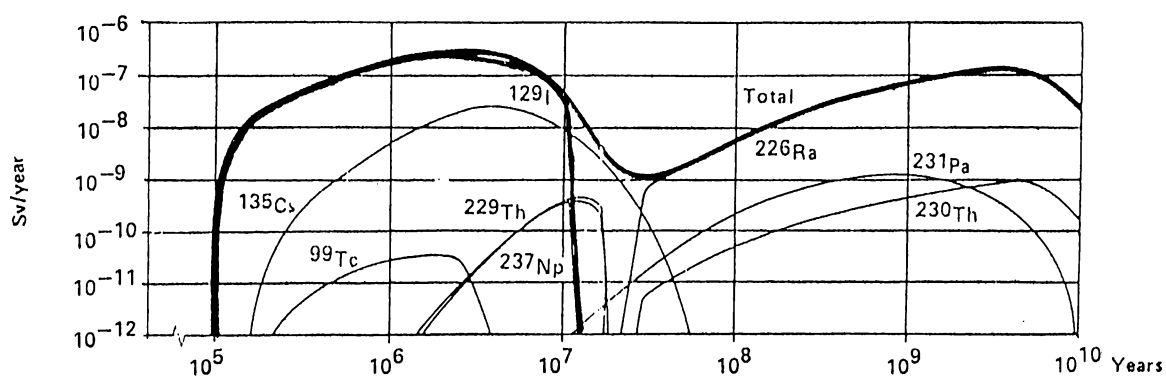


Figure 1.3: Doses to Nearby Residents for Scenario A of Swedish Program

1.0.3 Clay Minerals

Clay minerals are described as aluminum or magnesium silicates with stacked layer structure. Unit layers consist of sandwiches of octahedral and tetrahedral sheets.

Octahedral sheets consist of two layers of oxygen atoms (or hydroxyl group), in a hexagonal close packed arrangement with aluminum, iron or magnesium atoms at the octahedral sites, so that they are equidistant from from six oxygens or hydroxyls (Fig. 1.4). When aluminum is present, only two thirds of the possible positions are filled to balance the structure, which is the *gibbsite* structure and has the formula $\text{Al}_2(\text{OH})_6$. When magnesium is present, all the positions are filled to balance the structure, which is the *brucite* structure and has the formula $\text{Mg}_3(\text{OH})_6$. The normal O-to-O distance is 2.6\AA and a common OH-to-OH distance is about 3\AA , but in this structural unit the OH-to-OH distance is 2.94\AA and the space available for the ion in the octahedral coordination is about 0.61\AA . The theoretical thickness of the distorted unit is 5.05\AA in clay mineral structures.

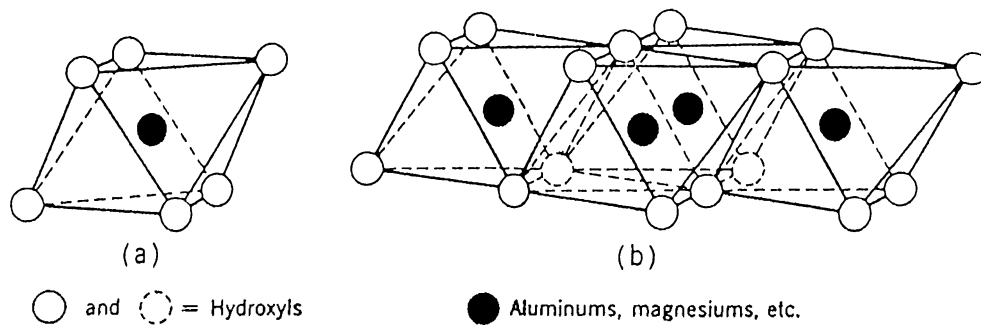


Figure 1.4: Diagrammatic Sketch showing (a) A Single Octahedral Unit and (b) The Sheet Structure of the Octahedral Units.

In tetrahedral or silicate sheets, silicon atoms are surrounded by four oxygen atoms in tetrahedral arrangement. In each tetrahedron a silicon atom is

equidistant from four oxygens, or hydroxyls if needed to balance the structure, arranged in the form of a tetrahedron with a silicon atom at the center. The silica tetrahedral groups are arranged to form a hexagonal network which is repeated indefinitely to form a sheet of composition $\text{Si}_4\text{O}_6(\text{OH})_4$ (Fig. 1.5). The tetrahedrons are arranged in a way that all tips of them point to the same direction and their bases are all in the same plane. The open hexagonal network can be considered as composed of three strings of oxygen atoms intersecting at angles of 120° . The O-O distance in the silica tetrahedral sheet is 2.55\AA and the space available for the ion in the tetrahedral coordination is about 0.55\AA . The thickness of the undistorted unit is 4.65\AA in clay mineral structures. Each of these units presents a center-to-center height of about 2.1\AA . [19]

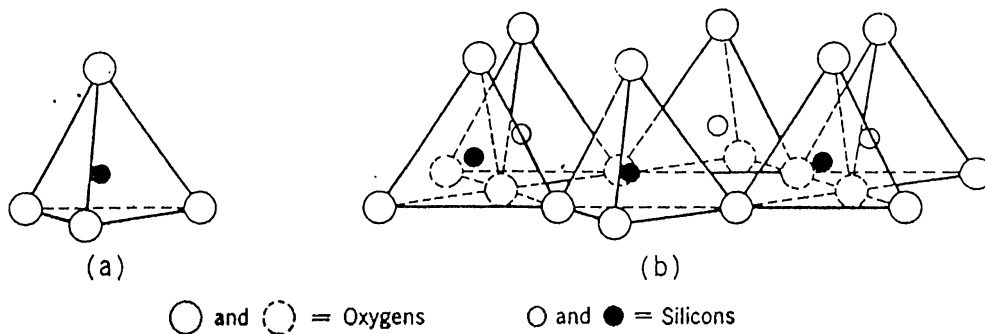


Figure 1.5: Diagrammatic Sketch showing (a) A Single Silica Tetrahedron and (b) The Sheet Structure of the Tetrahedrons Arranged in a Hexagonal Network.

The analogous symmetry and the almost identical dimensions in the tetrahedral and the octahedral sheets, allow the sharing of oxygen atoms between these sheets. The fourth oxygen atom protruding from the tetrahedral sheet is shared by the octahedral sheet. This sharing of atoms may occur between one silica and one aluminum sheet, as in the case of so called 1:1 layer minerals. In the 2:1 layer minerals, one alumina sheet shares oxygen atoms with two silica sheets, one on each side. The combination of an octahedral sheet and one or two tetrahedral sheets is called a layer. Most clay minerals are consisted of such layers which are stacked parallel to each other.

There exists a certain unit in each layer which repeats itself in a lateral direction and referred to as *unit cell*. The total assembly of a layer plus inter-

layer material is also referred to as a *unit structure*. An schematic representation of the atom arrangement in a unit cell for 1:1 (T-O) and 1:2 (T-O-T) layers are shown in Fig. 1.6.

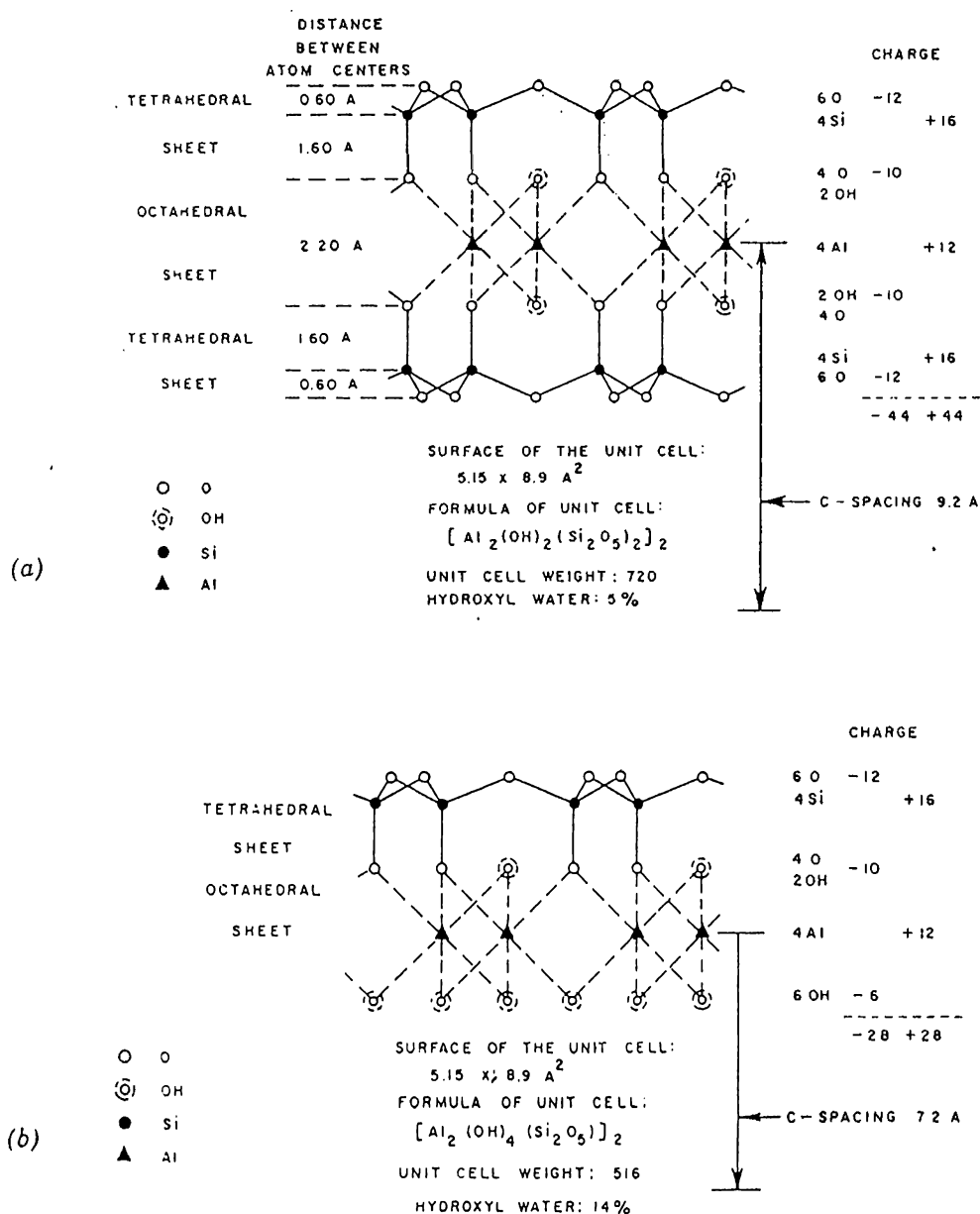


Figure 19. Atom arrangement in the unit cell of a 1:1 layer mineral (schematic).

Figure 1.6: Schematic Representation of The Atom Arrangement in Unit cells of (a) A 2:1 Layer Mineral (b) A 1:1 Layer Mineral

The interlayer consists of layers of water and/or interlayers or surface of cations (to compensate the negative charge). These cations may be exchangeable and interlayer water may be absorbed by a dry clay causing it to swell. Two main clay groups are kaolinite and montmorillonite groups which have 1:1 and 1:2 layer structures. Their structures will be discussed in the following parts.

Kaolinite:

Kaolinite has a two layer structure with one gibbsite and one silica sheet. The conventional formula for kaolinite $Al_4Si_4O_{10}(OH)_8$ is clearly a condensation of the layer arrangement described. In the layer common to the octahedral and tetrahedral groups, two-thirds of the atoms are shared by the silicon and aluminum and then they become O instead of OH. Only two-thirds of the possible positions for aluminum in the octahedral sheet are filled and there are three possible plans of regular population of the octahedral layer with aluminums. The aluminum atoms are considered to be so placed that two aluminums are separated by an OH above and below, thus making a hexagonal distribution in a single plane in the center of the octahedral sheet. The OH groups are placed so that each OH is directly below the perforation of the hexagonal net of oxygens in the tetrahedral sheet (Fig. 1.7).

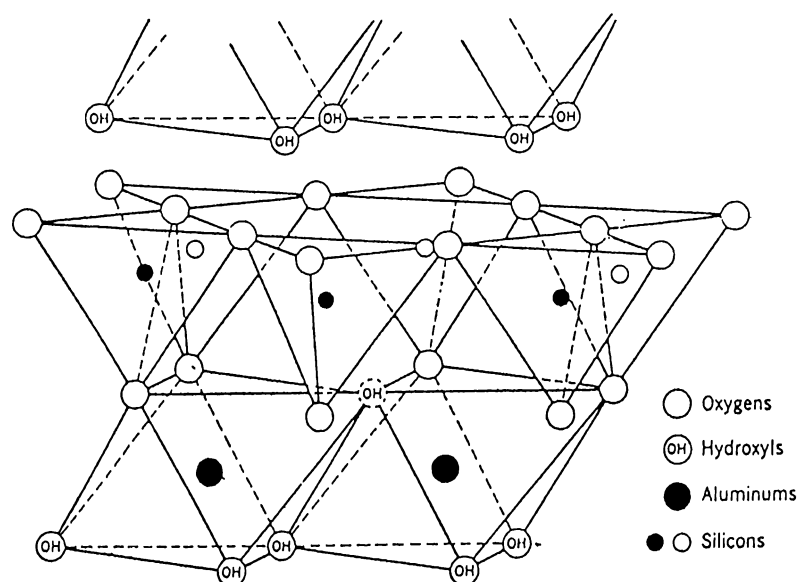


Figure 1.7: Diagrammatic sketch of the structure of the kaolinite layer

The main difference between various species is in layer stacking geometry. Members of the kaolinite group are kaolinite, dickite, nacrite and halloysite. In water these minerals are not expandable. The cohesive energy in kaolinites is primarily electrostatic, augmented by van der Waals attraction and a certain degree of hydrogen bonding between the hydroxyl groups of one layer and the oxygen atoms of the adjoining layer.

Bentonite:

Bentonite is a rock term and the clay mineral montmorillonite is the dominant mineral which determines the properties of a bentonite. Therefore it is necessary to understand the composition and structure of montmorillonite. Montmorillonite is a fine particle size hydrous aluminum silicate and is one of the three layer minerals. The three layers are as followings:

- 1) A silicate tetrahedral layer with each silica tetrahedron composed of a silicon atom surrounded by four oxygen atoms.
- 2) An aluminum (iron, magnesium, etc.) octahedral layer made up of octahedrons that has an aluminum (iron, magnesium, etc.) surrounded by six hydroxyl atoms.
- 3) The same as layer 1.

Aluminum can replace silicon in tetrahedron and magnesium, iron, zinc and other ions can replace the aluminum in the octahedral units. When Al^{+3} ions replace Si^{+4} ions in the tetrahedron, this is the substitution of a trivalent for a quadrivalent ion and leaves a charge deficiency in the tetrahedral layer. To satisfy this tetrahedral charge deficiency, cations such as Ca^{+2} , Na^{+} , Mg^{+2} and H^{+} are commonly held in the interlayer position. (Fig. 1.8).

Substitution of divalent ions for trivalent aluminum in the octahedral layer results in a weaker surface charge because of the increased distance from the charge center to the surface. Therefore although the cations are held in the interlayer positions, the attraction is much weaker.

Some bentonites swell many times their original dry volume when placed in water. Sodium bentonites swell 10 to 20 times whereas calcium bentonites

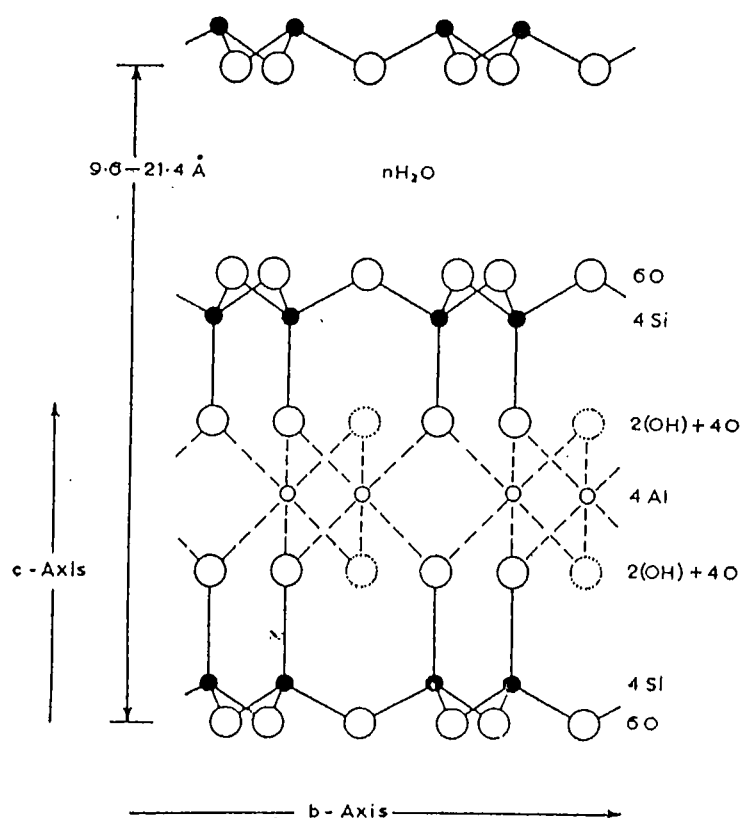


Figure 1.8: Schematic Representation of The Structure of Montmorillonite

swell only 2 to 5 times their original volume. This is related to the location of charge (tetrahedral or octahedral) and to the type of cation in the interlayer position. Bentonites have a relatively high surface area (50 to 80 m²/g) when compared to most of other natural materials. Sodium bentonites generally have a higher surface area than calcium bentonites[20]. The formula of bentonite is : $Na_{0.67}(Al_{3.33}Mg_{0.67})[Si_8O_{20}(OH)_4]$. It's density has been reported as 2.5 g/cm³ and for natural bentonites as 2.7-2.8 g/cm³.

Chlorites:

Chlorites are clay minerals which are structurally related to 2:1 layer clays. In these minerals the charge compensating cations between montmorillonite type clays are replaced by an octahedral magnesium hydroxide sheet, formally called brucite sheet. Owing to some replacement of Mg^{+2} by Al^{+3} in the hydroxide sheet , this sheet carries a net positive charge. Since the cation exchange capacities of chlorites are very low, the positive charge of the hydroxide sheet practically compensates the net negative charge of the layers.

Krauskopf refers chlorites and illites as mixed-layer clays. The chlorite mineral is considered as regular alternation of mica and brucite layers and illite as a repetition of mica and montmorillonite [21]. In chlorites the mica and brucite layers are continuous in a and b dimensions and are stacked in c direction with basal cleavage between the layers. The mica-like layers are trioctahedral with general composition of $(OH)_4(Si, Al)_8(Mg, Fe)_6O_{20}$. The brucite like layer has the general composition of $(Mg, Al)_6(OH)_2$. The mica layer is unbalanced by substitution of Al^{+3} for Si^{+4} and this deficiency of charge is balanced by an excess charge in the brucite sheet as a consequence of substitution Al^{+3} for Mg^{+2} . The diagrammatic sketch of the structure of chlorites is illustrated in Fig. 1.9. The formula of chlorites is: $(Mg, Fe)_6(Si, Al)_8O_{20}(OH)_4$

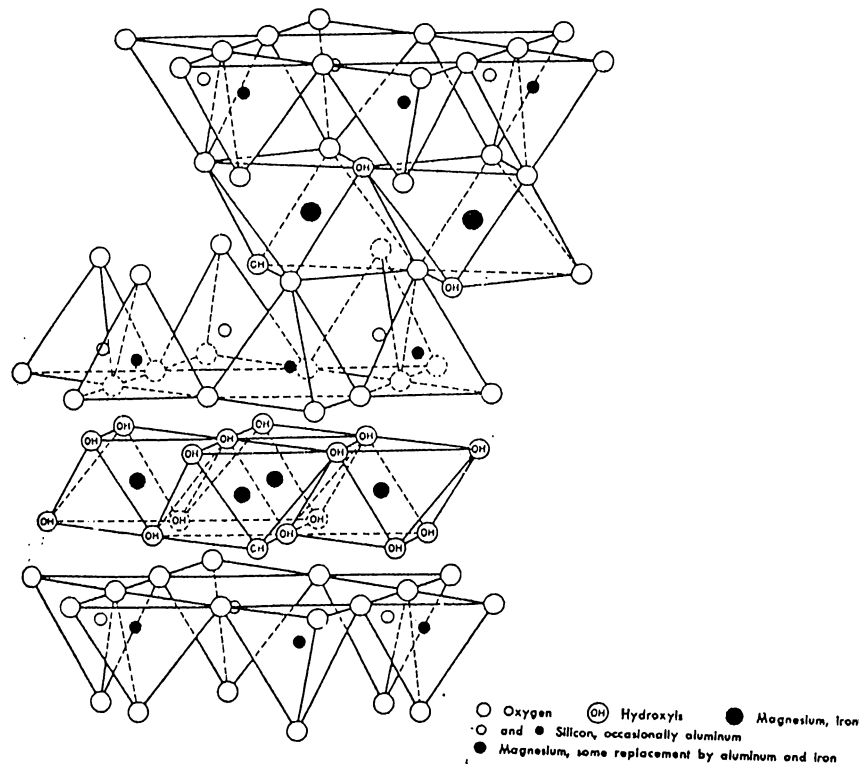


Figure 1.9: The Diagrammatic Sketch of The Structure of Chlorites

Illites:

Clays which have a deficiency of positive charge due largely to substitution in the tetrahedral sheets, (hence close to the surface of the layers) held the K^+ especially tightly, so that only part of it is replaceable by other ions. These clays with successive layers held together by K^+ ions, have properties different from montmorillonite and are given the name *illite* (it is also named

hydromica). The illite structure is similar to muscovite, in which the amount of K^+ is greater and bears a constant relation to the amounts of *Si* and *Al*. The difference in structure between montmorillonite, illite and muscovite, may be symbolized by the ideal formulas:

montmorillonite	$Al_4Si_8O_{10}(OH)_4$
illite	$K_{0-2}Al_4(Si_{6-8}Al_{0-2})O_{20}(OH)_4$
Muscovite	$K_2Al_4(Si_6, Al_2)O_{20}(OH)_4$

The basal spacing of illites is about 10\AA which is the same as that of montmorillonites with potassium ions as exchange ions in the dry state. The total net negative layer charge which results from the substitution and therefore the amount of compensating K^+ ions is usually larger than for most montmorillonites. Since only the external cations of illite clays are exchangeable, the cation exchange capacity of illites is smaller than that of montmorillonites despite the higher degree of isomorphous lattice substitution in the illites (Fig. 1.10).

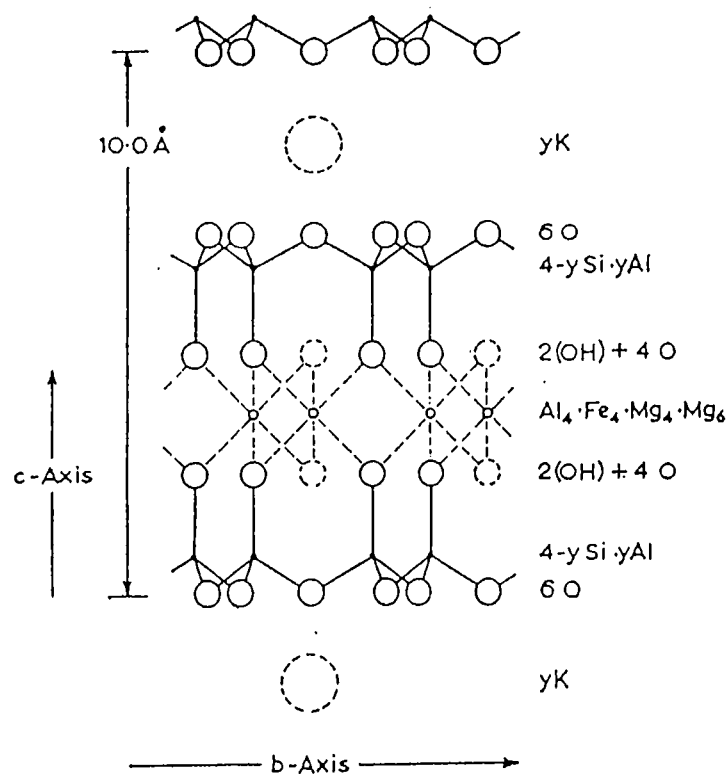


Figure 1.10: Schematic Representation of The Structure of illites

Alumina:

Alumina is not a clay mineral but it is a constituent of clay minerals. It occurs in crystalline form as corundum and the less pure emery. It also occurs hydrated as bauxite, diaspore and gibbsite. Alumina itself has two forms α and γ -Alumina. α -Alumina has a trigonal crystalline form. It is strictly the high temperature form but does not change to γ -Alumina at low temperatures. γ -Alumina is produced by controlled low temperature dehydration of hydrates at temperatures up to 500°C. On strong heating it is converted reversibly to α form at 1150-1200°C. Its crystalline form is hexagonal. β -Alumina is sodium aluminate with a composition of $Na_2O.11Al_2O_3$ or $Na_2O.12Al_2O_3$. Alumina types are listed in Table-1.5[22].

Formula	Name
Al_2O_3	Corundum (α -Alumina)
$Al_2O_3.H_2O$	Bohemite
$Al_2O_3.H_2O$	Diaspore
$Al_2O_3.3H_2O$	Gibbsite

Table 1.5: Alumina Types

1.0.4 Soils

Classification of soils is rather difficult since they differ in so many ways such as: grain size, composition, plasticity, mechanical strength, color, fertility, permeability, parent material and nature of profile. An easy classification based primarily on the climate factors of soil development is considered here[21]. The soils can be divided to humid and arid region soils. The humid region soils are characterized by a concentration of iron oxide and aluminum silicates in B-horizon and these soils are accordingly often referred to as *pedalfer* soils. Soils of arid regions show concentration of calcium salts and are designated as *pedocal* soils. Zonal humid or *pedalfer* soils are further subdivided according to temperature and the zonal aridic soils due to degree of aridity. The classification is shown in Table-1.6.

Average Rainfall inch/year	Soil Type	Classification
Over 25	Pedalfer	Laterite(tropics) Podzol (temperature Zone) Tundra (arctic Zone)
Less than 25 12-25 10-15 less than 10	Pedocal	Chernozem Chestnut-Brown Desert and Saline

Table 1.6: Climate Classification of Soils

The most widespread of the zonal humid soils are *podzols* and their relatives, soils typical of the humid parts of the temperature zones. The word *podzol* refers to forest soils in the northern part of the temperature zone. Abundant vegetation makes the soil water acid, pH values reaching 4 to 4.5 in the clayey part of the soil and 3.5 in the humus. The clay in *podzols* is typically kaolinite as would be expected from the acid environment and the depletion of lime and magnesia. The color of A horizon of *podzol* is gray-white.

Laterite is a very different kind of soil formed in humid tropics. The chief characteristics are a red color, enrichment of iron oxide and aluminum oxide through the profile, a depletion in silica and removal of most of the alkaline and alkaline earth ions. *Laterite* has a red color.

North of forested area of *podzol* are the tree-less plains of Arctic, the *tundra* which gives its name to the typical cold humid soils. Such soils have a great abundance of organic matter because the cold climate slows decay. The clay mineral content of *tundra* soils is frequently rather low.

Zonal aridic soils are characterized by concentration of calcium salts in the profile. *Chernozem* or black earth is a soil colored black by an abundance of organic matter and having an ill-defined zone of lime enrichment at depth. It is the best of all agricultural soils because of its content of organic matter and

unleached cations. With increasing dryness, the soil becomes thinner and light colored. Varieties are often designated by color terms such as *chestnut* and *red-brown*. When dryness is extreme, the soil may retain very soluble salts such as sodium chloride and is accordingly described as a *saline* soil.

1.0.5 Soil Organic Matter(SOM)

Soil organic matter is defined by Hayes and Swift as following: “ The complete soil organic fraction is made up of live organisms and their undecomposed, partly decomposed and completely transformed remains ”. SOM is the term used to refer more specifically to the non-living components which are a heterogenous mixture composed largely of products resulting from microbial and chemical transformations of organic debris. These transformations known collectively as the humification process, give rise to humus, a mixture of substances which have a degree of resistance to further microbial attack [23].

SOM is usually subdivided into non-humic and humic substances. Non-humic substances include those with still recognizable chemical characteristics such as: carbohydrates, proteins, peptides, pyridimines, fatty acids , waxes, resins , pigments and other low molecular weight organic substances. In general all these compounds are relatively easily degraded in soils and have short life spans.

Humic substances are amorphous, dark-colored, partly aromatic, mainly hydrophilic, chemically complex, polyelectrolyte-like materials which range in molecular weight from a few hundred to several thousands and are more resistant to biological degradation[24, 25].

Humic substances are defined operationally by their solubilities. Fulvic acids are the fraction which are soluble at all pH values and humic acids are soluble above a pH range of approximately 3.5 and humin is the fraction insoluble at all pH values [26].

1.0.6 The Sorption Process

Sorption reactions are referred to interactions among all phases present in a subsurface system and at the interfaces between these phases. Solutes which undergo sorption are commonly termed *sorbates*, the sorbing phase, the *sorbent* and the primary phase from which the sorption occurs, the *solution* or *solvent*.

Sorption results from a variety of different types of attractive forces between solute, solvent and sorbent molecules. Such forces usually act together, but one type or another is more significant than others in any particular situation.

There are two broad categories of sorption, adsorption and absorption. They can be differentiated by the degree to which the sorbate molecule interacts with and is free to migrate between the sorbent phase. In adsorption solute accumulation is generally restricted to a surface or interface between the solution and adsorbent. In contrast absorption is a process in which solute is transferred from one phase to another, interpenetrates the sorbent phase by at least several nanometers.

Adsorption processes such as dissolution of a relatively immiscible phase into an aqueous phase or accumulation of a lipophilic substance in an organic phase, involve exchange of molecular environments. So the energy of an individual molecule is altered by its interactions with solvent and sorbent phases. Its distribution between phases results from its relative affinity for each phase, which in turn relates to the nature of the forces which exist between molecules of the sorbate and those of solvent and sorbent phases. So these forces are rather similar to those which arise in chemical reactions. Adsorption also involves intermolecular forces but in this case it is for the molecules at the surface of the sorbent rather than bulk phase molecules. Adsorption can be categorized into three classes according to the class of attraction force which predominates. Some features of these classifications are summarized in Table-7.

Category	Forces Involved	Characteristics	Example
<i>Physical adsorption</i>	non-specific attraction forces involving the entire electron shells of radioelement and adsorbing substrate	<ul style="list-style-type: none"> -pH Dependant -rapid -reversible -temperature independent -independent of composition of the sorbent -independent of ionic strength and composition of the solution -influenced by complexing agents -characteristic energy 4.2-8.4 kJ/mol 	sorption of tri and tetravalent actinide complexes on metal oxide surfaces near natural pH
<i>Electrostatic adsorption</i>	coulombic forces of attraction between charged solute species and the adsorbing substrate	<ul style="list-style-type: none"> -rapid -largely reversible -temperature dependant -strongly dependant on the composition of the sorbent -strongly dependant on ionic strength -strongly dependant on the composition of the solution -characteristic energy 8-16 kJ/mol 	<ul style="list-style-type: none"> -ion exchange -adsorption of Cs⁺ on clays
<i>Chemical substitution</i>	Specific chemical forces involving chemical bonding	<ul style="list-style-type: none"> -slow -partly reversible -highly solute selective -temperature dependant -highly dependant on composition of the sorbent -highly dependant on the concentration of solute -characteristic energy 100-500 kJ/mol 	Interaction of Am with surfaces of phosphate minerals

Table 1.7: Categories of Adsorption Process

1.0.7 The R_d Concept

The distribution coefficient is a macroscopic expression of the various processes involved simultaneously in the distribution of elements between solid and liquid phases. It represents the ratio of the concentration in the solid phase over the concentration in the liquid phase for a given element C :

$$R_d = \frac{[C]_s}{[C]_l} \quad (1.1)$$

The unit of R_d is ml/g since the units of $[C]_s$ and $[C]_l$ are g/g *solid* and g/ml *of solution* respectively.

Since the physico-chemical properties of the elements will not change for all isotopes of an element (stable or radioactive), in a discussion of sorption behavior, R_d can be expressed for any specific isotope of an element or even simply for that element. It can be determined experimentally and can be used to calculate the retardation in transport processes. It must be noticed that measured sorption characteristics for a trace element are related to a large number of chemical and physical parameters such as composition of the solid and liquid phases, temperature, contact time, colloid formation and presence of organic macromolecules. Composition of the liquid phase is referred to the radionuclide concentration, concentration of other anions and cations, pH and redox potential. From composition of the solid phase we mean the chemistry and mineralogy of the solid phase, its surface properties, crystallinity, surface to volume ratio, etc.

Generally the distribution ratio increases with the contact time since new surfaces become available for sorption in the solid phase as the dissolved components penetrate into pores and microfissures. Distribution ratios determined experimentally constitute the sum of all contributions from different sorption processes and therefore not element specific quantities. However laboratory experiments under simulated natural conditions, have given acceptable agreement in cases where field observations concerning trace element transport are

available.

1.0.8 Isotherm Models

Models for characterizing the equilibrium distribution of a solute among the phases and interfaces of an environmental system, typically relate the amount of solute, sorbed per unit of sorbing phase or interface to the amount of solute remained in the solvent phase. An expression of this type, evaluated at a fixed system temperature is termed as a *sorption isotherm*. To obtain an isotherm, usually all the conditions are kept constant and the only changing parameter is the aqueous concentration of the trace element of interest. The most frequently used isotherm relationships are *Langmuir*, *Fruendlich* and *Dubinin-Radushkevich* models.

1) *Langmuir Isotherm*

This model was developed originally for the adsorption of gas molecules onto the surface of homogenous solids and systems which leads to deposition of a single layer of solute molecules on the surface of a sorbent. This model is predicted on the assumptions that the energy of sorption for each molecule is the same and independent of surface coverage and that the sorption occurs only on localized sites and involves no interactions between sorbed molecules. The Langmuir equation can be written as :

$$X = \frac{bX_m C}{1 + bC} \quad (1.2)$$

Where:

- X : Amount of solute adsorbed per unit mass of solid (g/g)
- X_m : Maximum amount of solute which can be sorbed by the solid (g/g)
- C : Equilibrium solute concentration of sorbate (g/ml)
- b : Constant related to the energy of adsorption (ml/g)

This relationship becomes linear at very low sorbate concentrations. The equation can be written also as:

$$X = X_m - \frac{1}{b} \times \frac{X}{C} \quad (1.3)$$

Then by plotting X versus X/C , b can be found from the slope as $1/b$ and X_m from the intercept. R_d (defined as X/C , can be computed for any C value over the range in which the relationship holds:

$$R_d = \frac{bX_m}{1 + bC} \quad (1.4)$$

Langmuir isotherm is not good in describing the actual adsorption on heterogeneous soils and sediments. Nevertheless there are some cases that it successfully describes such as trace adsorption by natural substrates[27].

2) *Fruendlich Isotherm*

The Freundlich model is perhaps the most widely used non-linear sorption equilibrium model. The model has the general form of:

$$X = KC^N \quad (1.5)$$

Where:

X : Amount of solute adsorbed per unit mass of solid (g/g)

C : Equilibrium solute concentration of sorbate (g/ml)

K, N : Positive valued empirical parameters with $0 < N < 1$

The parameter K is related to sorption capacity and N to the sorption intensity. The logarithmic form of this equation is generally used to determine these coefficients:

$$\log X = \log K + N \log C \quad (1.6)$$

3) *Dubinin-Radushkevich isotherm*

Dubinin-Radushkevich isotherm was developed to model adsorption of trace aqueous constituents and it is more general than Langmuir model since it does not require homogenous adsorption sites or constant adsorption potential. The Dubinin-Radushkevich equation is given as following:

$$X = X_m e^{-KE^2} \quad (1.7)$$

Where:

X : Amount of solute absorbed per unit weight of solid (mmol/g)

X_m : Sorption capacity of adsorbent per unit weight (mmol/g)

E : Polanyi potential = $RT \ln(1 + 1/C)$ (J/mol)

C : Equilibrium solute solution concentration (mmol/ml)

R : Gas constant (J/K.mol)

T : Temperature (K)

K : Constant related to the sorption energy (mol^2/KJ^2)

The linearized Dubinin-Radushkevich equation is:

$$\ln X = \ln X_m - KE^2 \quad (1.8)$$

A plot of $\ln X$ versus E^2 , allows the estimation of $\ln X_m$ as the intercept and $-K$ as the slope.

Assuming a very small subregion of sorption surface to be uniform in structure and energetically homogenous and by applying the Langmuir isotherm as a local isotherm, the mean energy of sorption can be calculated from Dubinin-Radushkevich parameters. The mean energy of sorption is the free energy change when one mole of ion is transferred to the surface of the solid from the infinity in the solution. The magnitude of E can indicate the type of sorption occurring. It can be calculated from the following relation[28]:

$$E = (2K)^{-1/2} \quad (1.9)$$

1.0.9 Previous Work

Many investigations have been previously done experiments on the sorption behavior of radioiodine on different matrixes.

Using colorimetric methods, Whithead have found that soil organic matter are the major sorbents of iodide above $\text{pH}=6$ and below that pH , ferric and aluminum oxides are the most effective compounds in the sorption process. He has also related the sorption capacity of soil to the dryness of the soil, the equilibrium time, pH of the soil and temperature.[29] He has reported that iodine could not be adsorbed by kaolinite, montmorillonite, chalk or limestone[30].According to Torstenfelt, who has used bentonite in diffusion experiments, iodine diffuses in bentonite by two different mechanisms and has related this phenomena to different species of iodine in the form of I^- and HIO or IO_3 and the pore-size effects in the clay[31]. Sheppard and Thilbault [32] have stated that the organic soils had higher K_d values for iodine adsorption than the mineral soils. They also emphasized on the effect of soil/solution ratio and the concentration of pore water as well as the presence and concentration of cations.

Rançon has used four methods (batch and column methods as laboratory processes, lysimetry and direct field experiments), to study the behavior of radioiodine in soils and he concluded that the sorption properties of the aluminum silicates are not sufficient to ensure iodine containmennt. From batch and column experiments he has found that some lead and copper minerals could inhibit iodine migration. He also concludes that the iodine behaviour in the soil is very different whether it is present in trace amounts or in higher concentrations. [33]

Beherens found that in fresh surface waters most of the organic radioiodine compounds are soluble, while in soils most of the radioiodine is associated with insoluble organic substances. He suggested that the organic complexation reactions occuring, involve exteracellular oxidation of iodine with subsequent incorporation of elemental iodine into organic compounds.Christiansen and

Carlsen have studied the enzymatically controlled iodination reactions in the terrestrial environment and in the presence of enzymes of peroxidase group and hydrogen peroxide, they were able to iodinate humic acids with either iodide or elemental iodine [34]. The effect of soil organics and biomass and some inorganic complexing agents has been also studied by Bors and he showed that these species have a high effect in the adsorption of radioiodine. He observed an increase in the distribution ratio by adding glucose directly to soil. Addition of some complexing agents such as hexadecylpyridinium ion (HDPY⁺) and benzethonium ion (BE⁺), increased the R_d value several orders of magnitude than those in clays[31,43-45]. The results of some experiments for the sorption of iodine in the literature is summarized in Tables 1.8-1.10.

Sorbing Matrix	Aqueous Phase	$R_{d,ad}$ (ml/g)	Comments	Reference
Surface Soil 22 types collected in Minnesota, Oregon and Washington pH 3.6-8.9	0.01 M CaCl ₂ Solution	0.8-53	Tracer ¹³¹ I	Wildung [35]
Cadarache Soil (Eq. pH 7.6) Grain Size<0.1 mm	Water	1.3 1.3	After 1 Day After 2 Days (Tracer ¹³¹ I)	Rançon [33]
Chernozem (Clay Silt Soil) Grain Size<2mm pH 7.5	Synthetic Soil Water Bidistilled Water	250 135	Tracer ¹²⁵ I	Bors [36]
Podzol (Humus Sandy Soil) Grain Size<2mm pH 6.5	Synthetic soil Water Bidistilled Water	80 47	Tracer ¹²⁵ I	Bors [36]

Table 1.8: Experimental Results in Literature for Adsorption of Radioiodine on Soil Samples

Sorbing Matrix	Aqueous Phase	R_d (ml/g)	Comments	Reference
Chlorite Illite	Pre Equilibrium Water	3		Strickert [37]
	Synthetic Ground Water	0	pH=7	Relyea [38]
Chlorite-Illite (Org.C 1.27%)	NaCl soln.(0.01-0.5 M)	0-0.01	$5.6 \leq pH \leq 6.8$	Meyer [39]
	Water	0.5	1-3 Days	Rançon[33]
	Synthetic Soil Water	5.0	$R_{d,des}$ 18.2(ml/g)	Bors [36]
	Bidistilled Water	1.4	$R_{d,des}$ 6.2(ml/g)	
Kaolinite (Org.C 0.04%)	Synthetic Ground Water	0	pH=7	Relyea [38]
	Water	4	1-3 Days	Rançon [33]
	Synthetic Soil Water	0.6	$R_{d,des}$ 1.7(ml/g)	Bors [36]
	Bidistilled Water	0.5	$R_{d,des}$ 1.4(ml/g)	
Bentonite	Water	0.001	$[I^-]=1 \times 10^{-13}$	Torstenfelt [31]
	Water	1.5	1 Day	Rançon [33]
Alumina	Nacl Solution 0.01-0.5 M	0-12.2		Meyer [39]

Table 1.9: Experimental Results in Literature for Adsorption of Radioiodine on Chlorite, Illite, Chlorite-Illite mixture, Bentonite and Alumina

Sorbing Matrix	Complexing Agent	R_d (ml/g)	Reference
Soil	HDTMA ⁺	215	Bors [40]
	HDPY ⁺	900	
	BE ⁺	990	
Bentonite	-	6	Bors [40]
	HDTMA ⁺	12	
	HDPY ⁺	1500	
	BE ⁺	800	

Table 1.10: Experimental Results in Literature for Adsorption of Radioiodine on Soil and Bentonite Pretreated with Inorganic Complexing Agents (HDTMA⁺: Hexadecyl Trimethyl Amonium ion, HDPY⁺:Hexadecyl Pyridinium ion, BE⁺:Benzethonium ion.)

Chapter 2

Experimental

The following types of soil or clay minerals were used in the experiments:

- 1) Bolu-Yeniçağ soil
- 2) Seydişehir Alumina
- 3) Afyon Chlorite-Illite
- 4) Giresun Bentonite
- 5) Sındırgı Kaolinite

The soil samples were taken from the Soil Department of Ankara University and the mineral samples were obtained from M.T.A (Maden Teknik Arama) institute in Ankara.

2.0.10 Size Fractionation

The samples were separated into different particle sizes by dry sieving and the fraction below $38\mu\text{m}$ was used in the experiments. The particle size distribution of samples below $38\mu\text{m}$ were determined using the Andreason pipette method [41, 42]. The procedure applied was as follows:

A certain amount of clay or soil sample was dried at 110°C overnight. Ten grams of this sample was suspended in one liter of distilled water by

stirring with a magnetic stirrer for twelve hours. To prevent agglomeration, $Na_4P_2O_7$ was added as a dispersing reagent. After twelve hours, the solution was introduced into the Andreason pipette and samples of 10 ml were taken at different intervals. These samples were dried and the amount of solid was determined. The size of particles then were calculated using Stoke's Law:

$$V = \frac{gd^2(\rho_s - \rho_l)}{18\eta} = \frac{h}{t} \quad (2.1)$$

Where:

- V :Settling velocity (cm/s)
- η :Viscosity of the liquid (g/cm.s)
- ρ_s :Density of clay (g/cm³)
- ρ_l :Density of the liquid (g/cm³)
- g :Gravitational constant (cm/s²)
- h :Height of the taken sample (cm)
- t :Time from start of the experiment (s)

The fraction of particles in the suspension which were finer than the given size was calculated from the following formula[43, 44]:

$$\%FT = (W_s - \frac{C \cdot V_a}{1000}) \cdot \frac{V_t}{V_a} \cdot \frac{1}{W_t} \cdot 100 \quad (2.2)$$

Where:

- W_s :Weight of clay plus defloculant in the beaker (g)
- C :Concentration of defloculant in suspension (M)
- V_a :Volume of aliquot (ml)
- V_t :Total suspension volume in pipette (ml)
- W_t :Total weight of clay in pipette (g)

2.0.11 Synthetic Groundwater

To approximate natural conditions, the experiments were carried out, using synthetic groundwater which simulated the composition of groundwater in the region where solid samples were taken. The composition of the groundwater used in the sorption experiments is given in Table-2.1:

Ion	Concentration (meq/l)
Na ⁺	2.17
Ca ²⁺	3.90
Mg ²⁺	3.10
CO ₃ ²⁻	
HCO ₃ ⁻	7.06
Cl ⁻	0.60
SO ₄ ²⁻	1.75
K ⁺	0.24

Table 2.1: Composition of the Synthetic Groundwater Used

The composition of the stock solutions used to prepare the synthetic groundwater is given in Table-2.2:

Component	Concentration g/L
Ca(NO ₃) ₂ ·4H ₂ O	46.04
Mg(SO ₄ ·7H ₂ O	21.573
Mg(NO ₃) ₂ ·6H ₂ O	9.615
Mg(Cl ₂ ·6H ₂ O	6.094
KNO ₃	2.427
NaNO ₃	18.422

Table 2.2: Composition of the Stock Solutions Used

10 milliliters of each stock solution was taken and diluted to one liter using deionized water. To avoid the change in composition and pH of the synthetic

groundwater by CO₂ present in air, the solutions were equilibrated with air for four days till a constant pH of about 5.8 was reached.

2.0.12 Tracer Containing Stock Solutions

The iodine tracer used in the sorption experiments was ¹³¹I, in the form of NaI and with a specific activity of 25 mci/ml. Six stock solutions of inactive iodine were prepared with the following concentrations.:

Solution	I ⁻ Concentration mmole/ml
I ₁	1×10^{-1}
I ₂	1×10^{-2}
I ₃	1×10^{-3}
I ₄	1×10^{-4}
I ₅	1×10^{-5}
I ₆	1×10^{-6}

One milliliter of the active NaI solution were diluted to 100 milliliters. From this solution, portions of 100 microliters were taken into glass beakers and one milliliter of the corresponding inactive solution was added and diluted to hundred milliliters to reach the following concentrations of the tracer containing solutions:

Solution	I ⁻ Concentration mmole/ml
A ₁	1×10^{-3}
A ₂	1×10^{-4}
A ₃	1×10^{-5}
A ₄	1×10^{-6}
A ₅	1×10^{-7}
A ₆	1×10^{-8}

2.0.13 Sorption-Desorption Experiments

All sorption experiments were performed using the batch method. Weighed amounts of duplicate samples were suspended in polypropylene centrifuge tubes in certain volumes of tracer containing solutions. The tubes were shaken for desired preset times at room temperature. The two phases were separated by centrifugation at 12000 rpm for 30 minutes and the activity of the supernatant was determined using a NaI detector.

The experimental procedure was as followings: The plastic tubes were cleaned and dried at 60 °C overnight. They were then cooled and weighed. In the pretreatment part four milliliters of synthetic groundwater were added to the tubes and were shaken for six days, using a rotational shaker at 150 rpm. The tubes were centrifuged and the phases were separated. The reason for pre-treatment is to obtain an equilibrium condition between the sorbing material and the synthetic groundwater, prior to the sorption experiments. The next step was the addition of four milliliters tracer containing solution to the solid phase. The samples were again shaken in the same conditions for the desired times and the phases were separated by centrifugation again. One milliliter of the liquid phase was transferred to a clean tube and was counted to observe the loss in activity of supernatant and the distribution ratio R_d was calculated as followings:

$$R_d = \frac{[I]_s}{[I]_l} \quad (2.3)$$

The concentration of iodine species on the solid phase can be calculated as:

$$[I]_s = \frac{V([I]_l^0 - [I]_l)}{W_s} \quad (2.4)$$

Then R_d can be calculated as :

$$R_{d,ads} = \frac{(V[I]_i^0 - [I]_l)}{W_s \times [I]_l} \quad (2.5)$$

Since the iodine tracer activities correspond to iodine concentrations in solution, $R_{d,ad}$ can be calculated as following :

$$R_{d,ad} = \frac{V \times A_0 - A_{1,ad}(V + \Delta W_{pt})}{W_s \times A_{1,ad}} \quad (2.6)$$

Where:

- $R_{d,ad}$: Adsorption distribution ratio (ml/g).
- A_0 : Initial activity of the solution (cpm).
- $A_{1,ad}$: Activity of the solution after sorption (cpm).
- V : Volume of the liquid phase (ml).
- W_s : Weight of the solid phase (g).
- ΔW_{pt} : Weight of the pretreatment solution remained in the solid phase after pretreatment (g).
- $[I]_i^0$: Initial iodine concentration in the liquid phase (mmole.ml⁻¹).
- $[I]_s$: Iodine concentration in the solid phase at the end of the experiment (mmole.g⁻¹).
- $[I]_l$: Iodine concentration in the liquid phase at the end of the experiment (mmole.ml⁻¹).

For desorption experiments, following the adsorption step, the two phases were separated and four milliliters of synthetic groundwater were added to the sample tube and shaken for the desired time. Again the phases were separated by centrifugation and the activity of one milliliter of the supernatant was counted. $R_{d,des}$ was calculated according to the relation:

$$R_{d,des} = \frac{V(A_0) - V(A_{1,ad} + \Delta W_{ad})}{W_s \times A_{1,des}} \quad (2.7)$$

Where:

$R_{d,des}$: Desorption distribution ratio (ml/g).

ΔW_{ad} : Amount of liquid remaining in the centrifuge tube after sorption step (g).

Adsorption, desorption, reversibility and exchange percentages were calculated using the following relations:

$$\%Adsorption = \frac{VA^0 - A_{1,ad}(V + \Delta W_{pt})}{VA^0} \times 100 \quad (2.8)$$

$$\%Desorption = \frac{A_{1,de}(V + \Delta W_{ad}) - A_{1,ad} \times \Delta}{VA^0 - A_{1,ad}(V + \Delta W_{pt})} \times 100 \quad (2.9)$$

$$\%Exchange = \frac{VA^0 - A_{1,ex}(V + \Delta W_{pt})}{VA^0} \times 100 \quad (2.10)$$

$$\%Reversebility = \frac{\%Des}{100 - \%Ads} \times 100 \quad (2.11)$$

Chapter 3

Results and Discussion

3.1 Characterization of Samples

The soil and clay samples were characterized by X-Ray Diffraction, FTIR analysis and particle size distribution .

The FTIR analysis of the samples were in good agreement with the standards given in the literature[45]. For Bolu soil no standard data was available but the spectrum was compared with the IR spectrum of standard humic acid since this soil is known to contain high amount of organic matter. Comparison of both spectra, shows that most of the peaks occur in the same wave number. The FTIR spectra of the minerals and the spectra of standards are given in Figs. 3.1-3.5.

The X-Ray Diffraction patterns are given in Figs. 3.6-3.10 . The main peaks were compared to those given in literature[46] and the peaks were found to be in good agreement with the patterns of standard samples. Alumina was found to be of *corundum* type.

The particle size distribution of the particles were obtained using the Andreason pipette method and the results are shown in Fig. 3.11. It is seen from the graph that about 23% of the minerals (70% for bentonite), have a grain size below 1 μm which is the beginning of the colloidal size range[21].

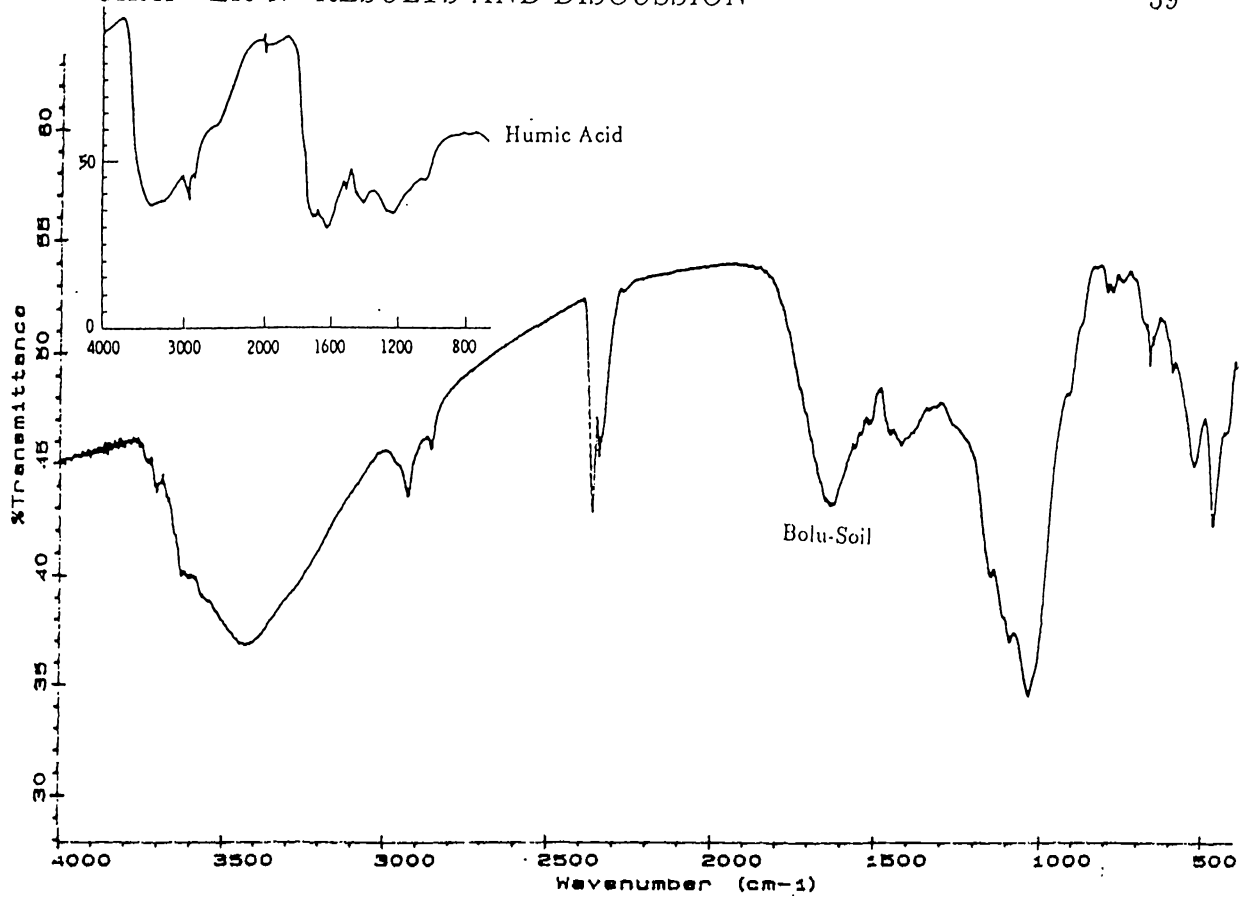


Figure 3.1: The FTIR Spectrum of Bolu-Soil and the Spectrum of Standard Humic Acid

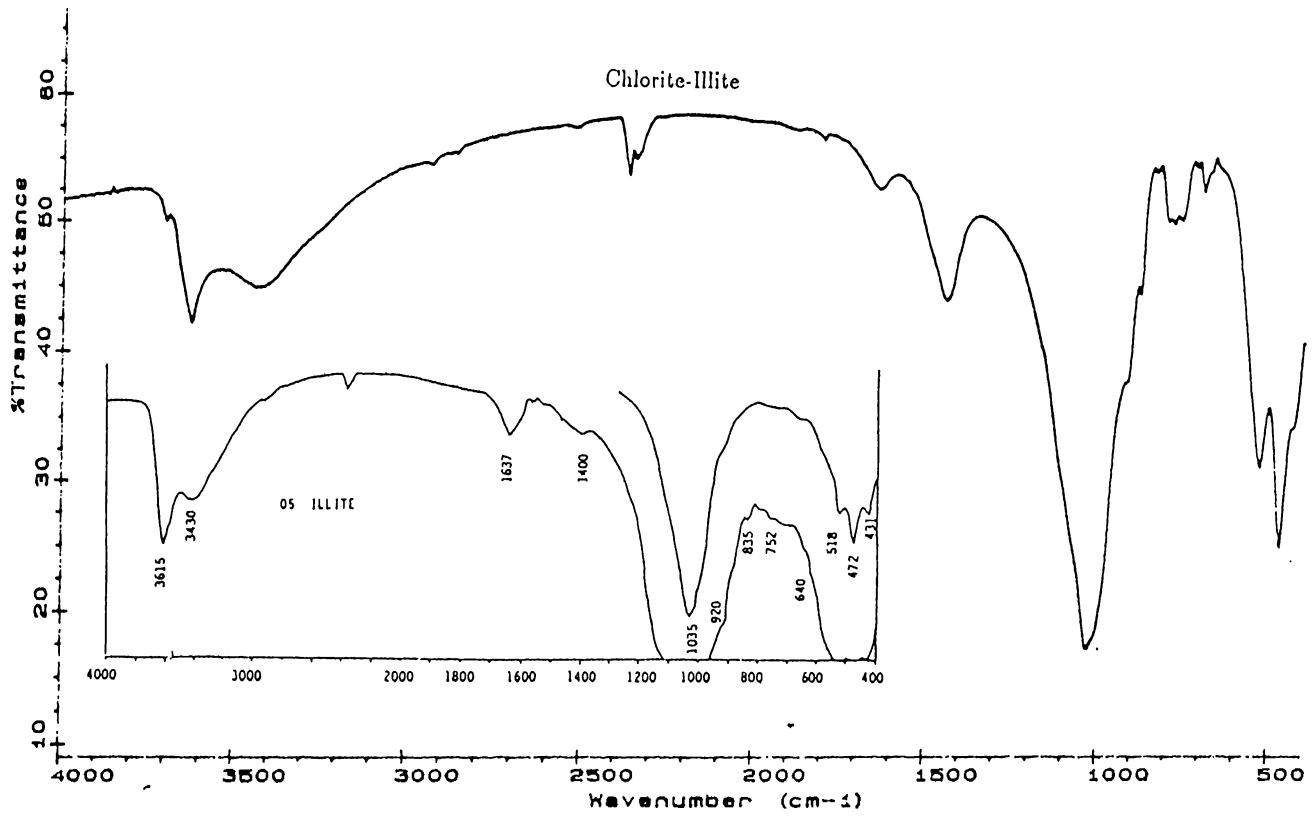


Figure 3.2: The FTIR Spectrum of Chlorite-Illite Clay mixture and the Spectra of Standard Chlorite and Illite

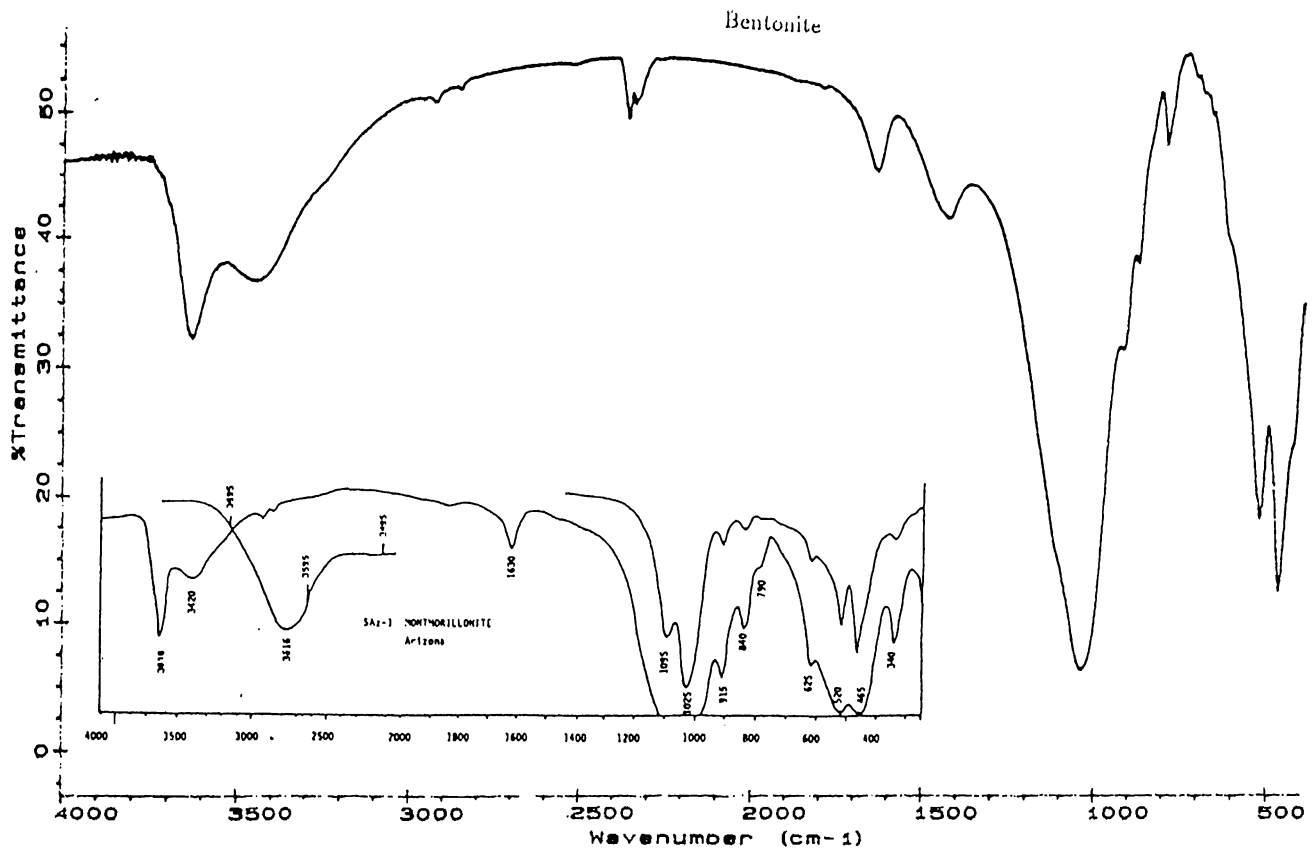


Figure 3.3: The FTIR Spectrum of Bentonite Clay and the Spectra of Standard Montmorillonite

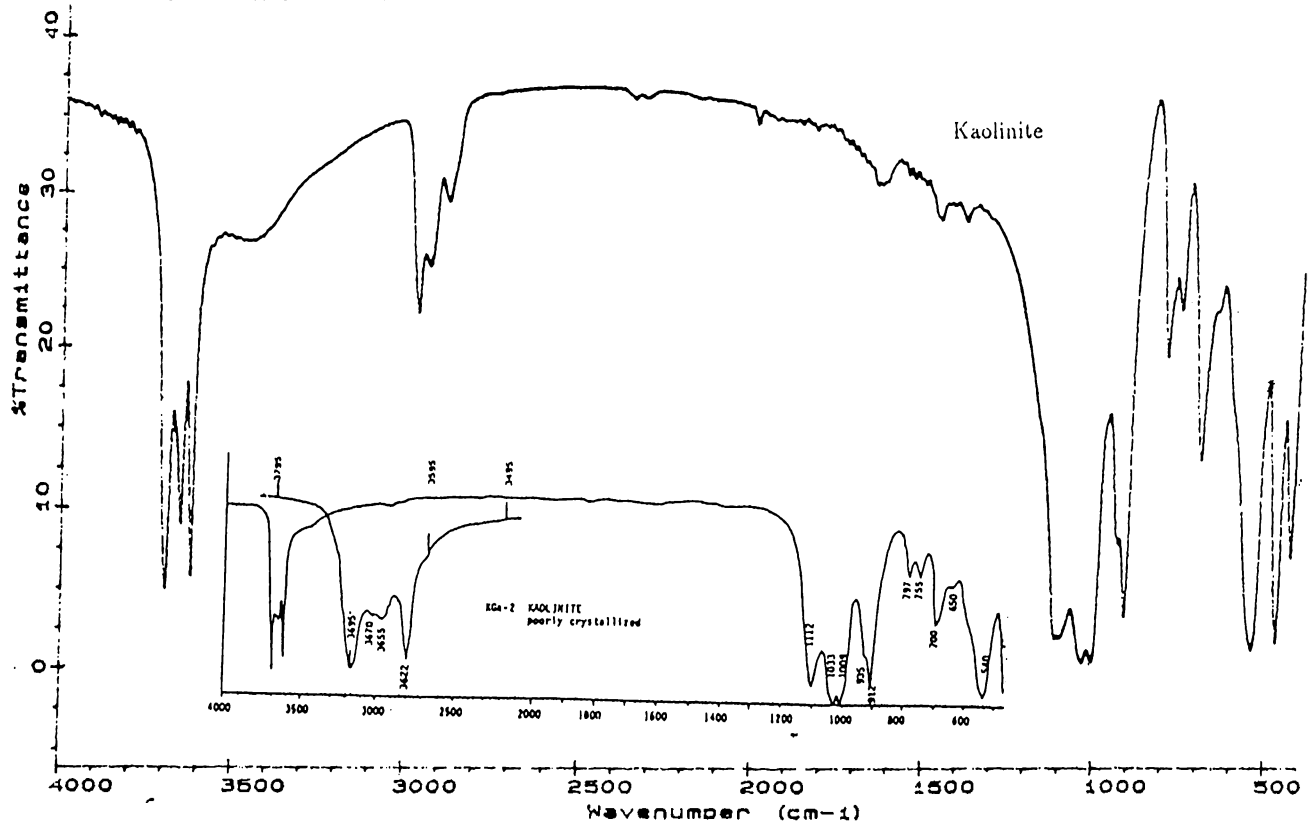


Figure 3.4: The FTIR Spectrum of Kaolinite Clay and the Spectrum of Standard Kaolinite

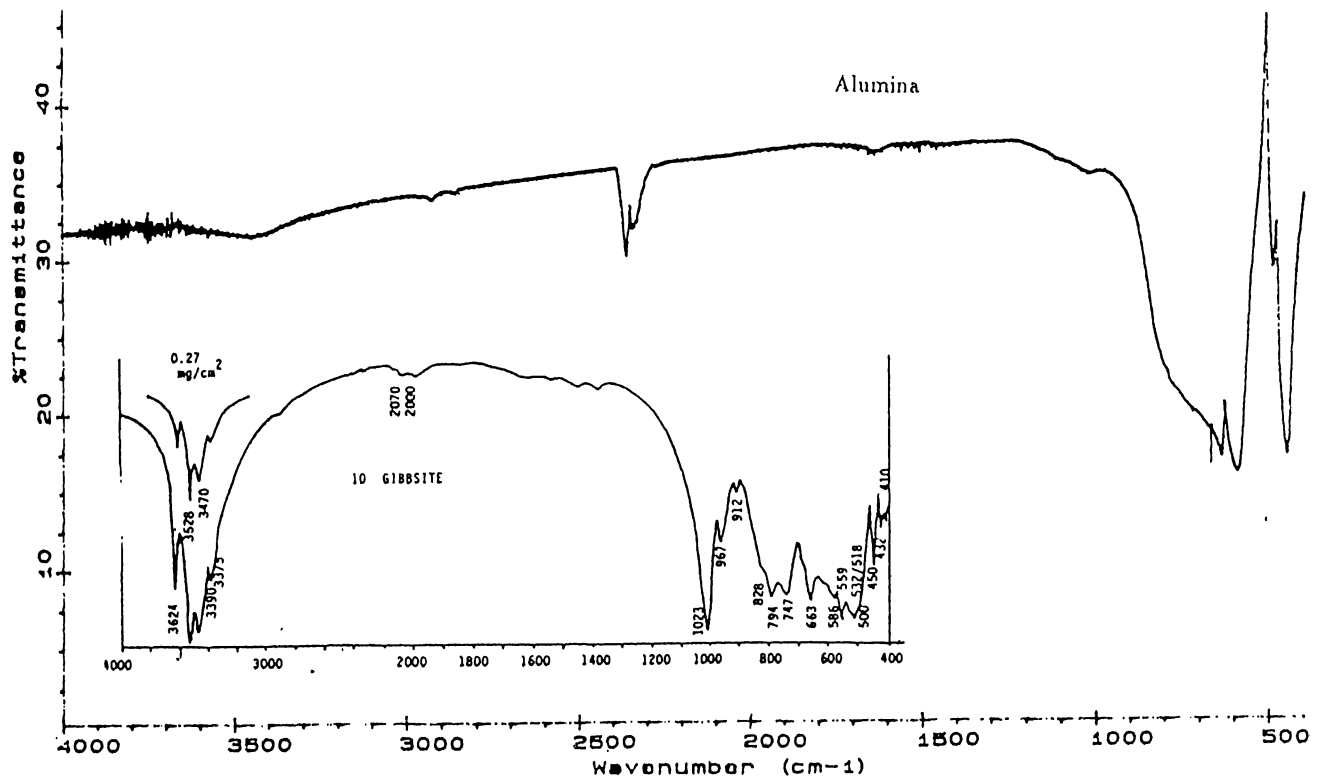


Figure 3.5: The FTIR Spectrum of Alumina and the Spectrum of Gibbsite

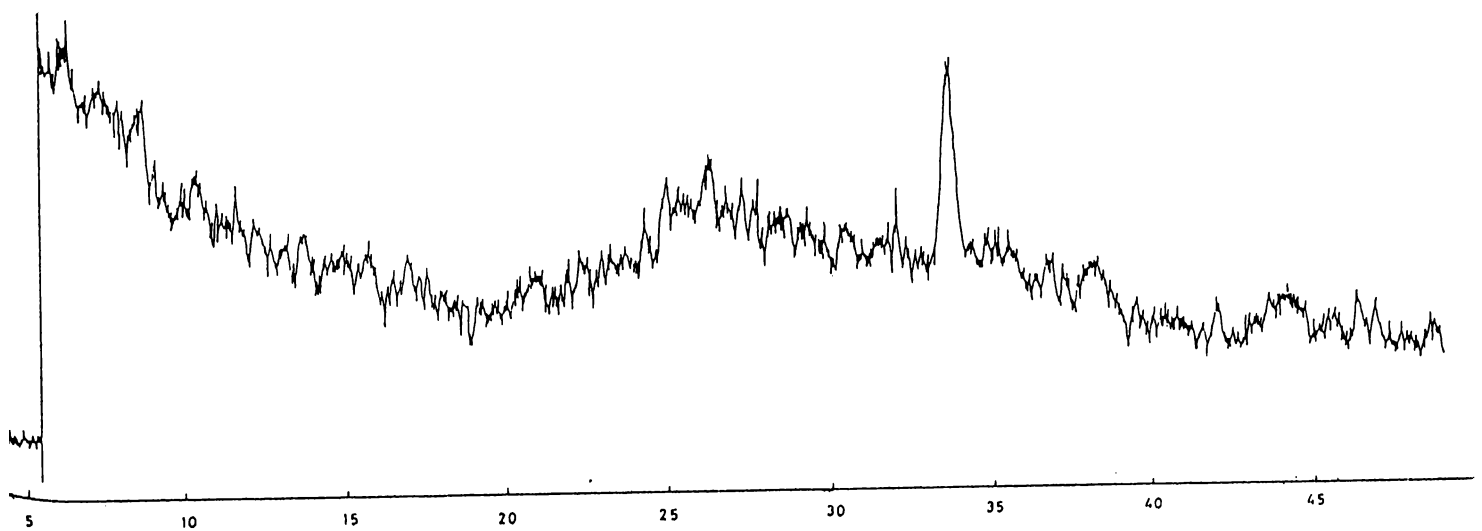


Figure 3.6: The X-Ray Diffraction Pattern of Bolu Soil

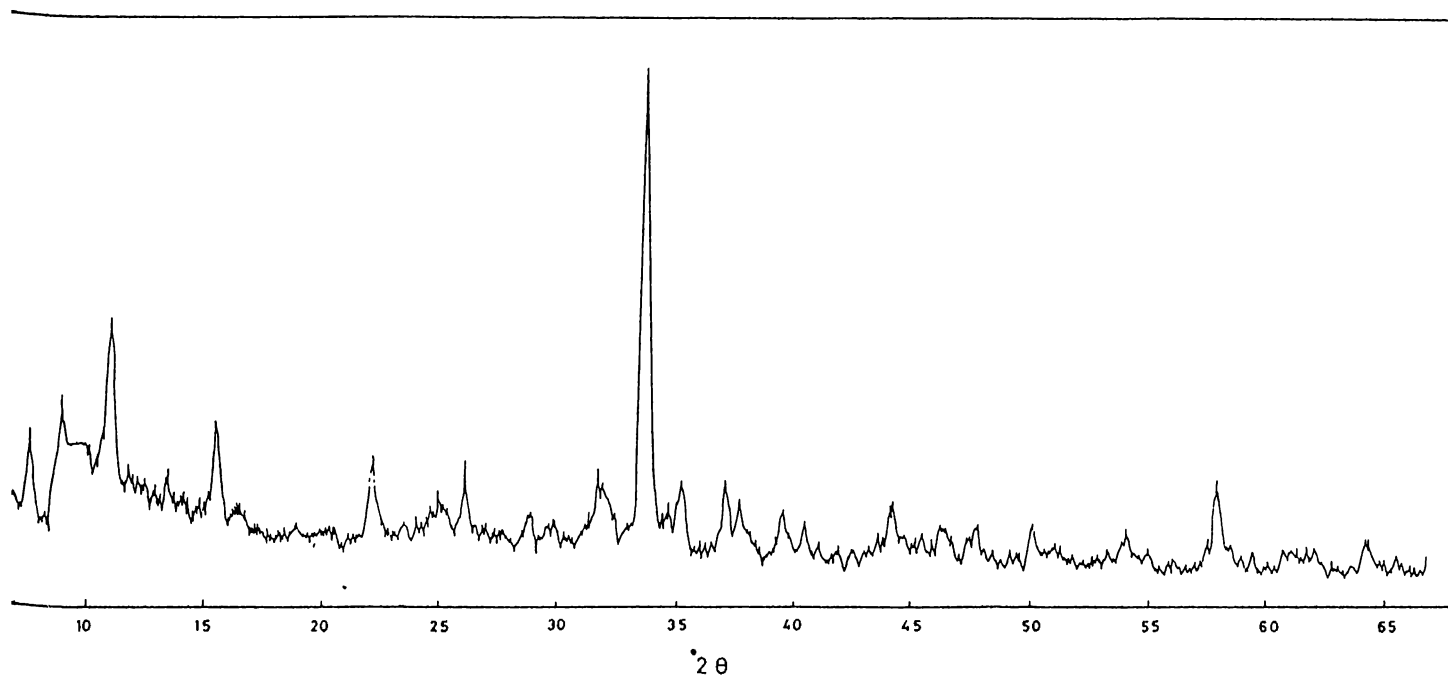


Figure 3.7: The X-Ray Diffraction Pattern of Chlorite-Illite Clay Mixture

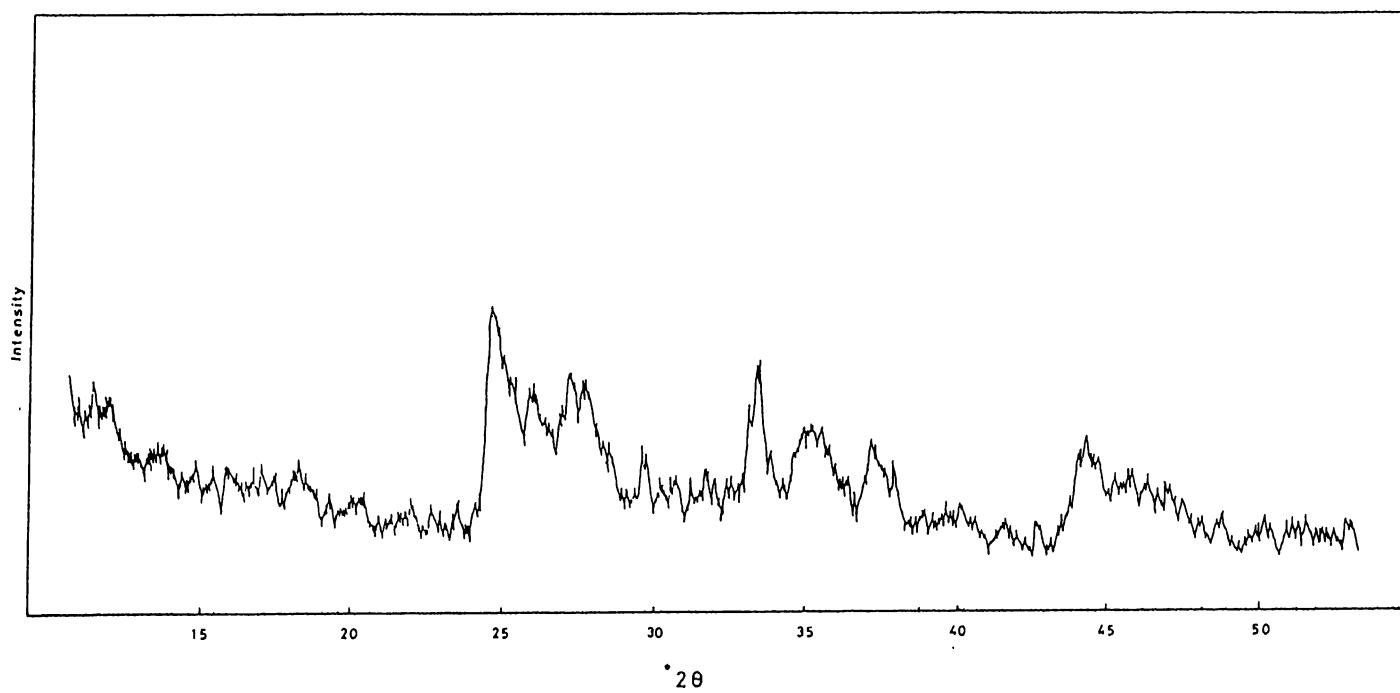


Figure 3.8: The X-Ray Diffraction Pattern of Bentonite

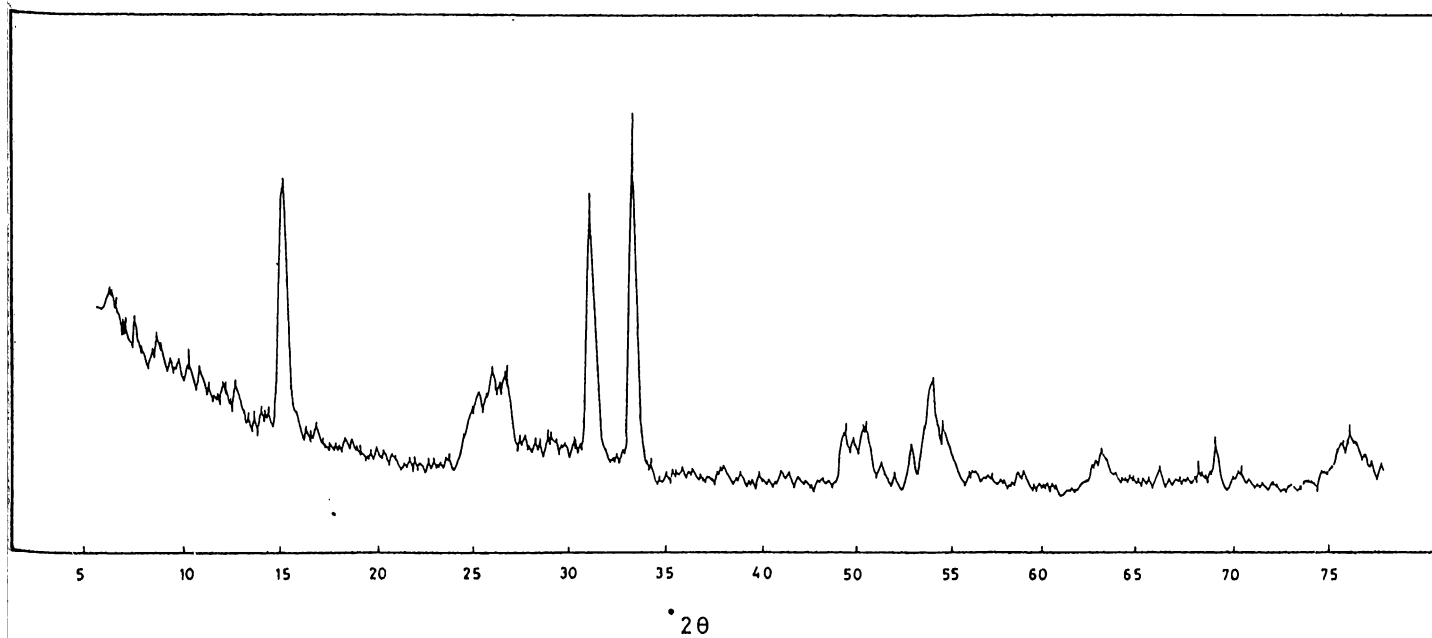


Figure 3.9: The X-Ray Diffraction Pattern of Kaolinite

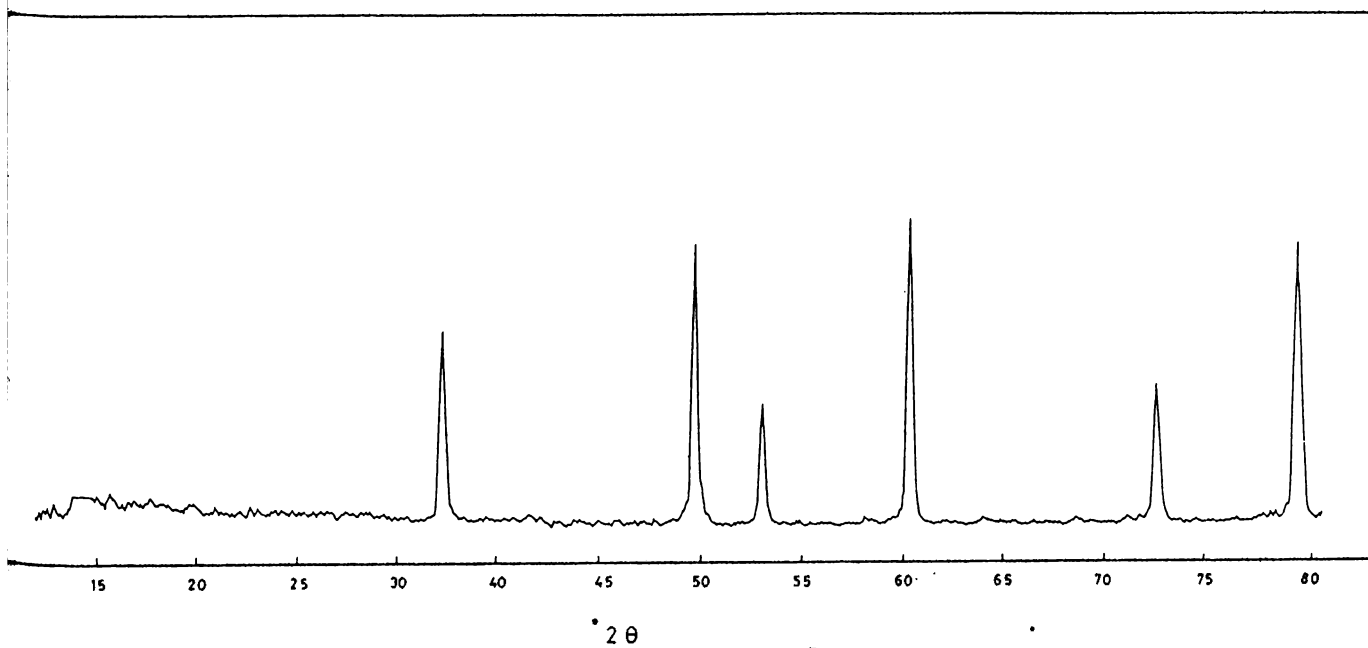


Figure 3.10: The X-Ray Diffraction Pattern of Alumina

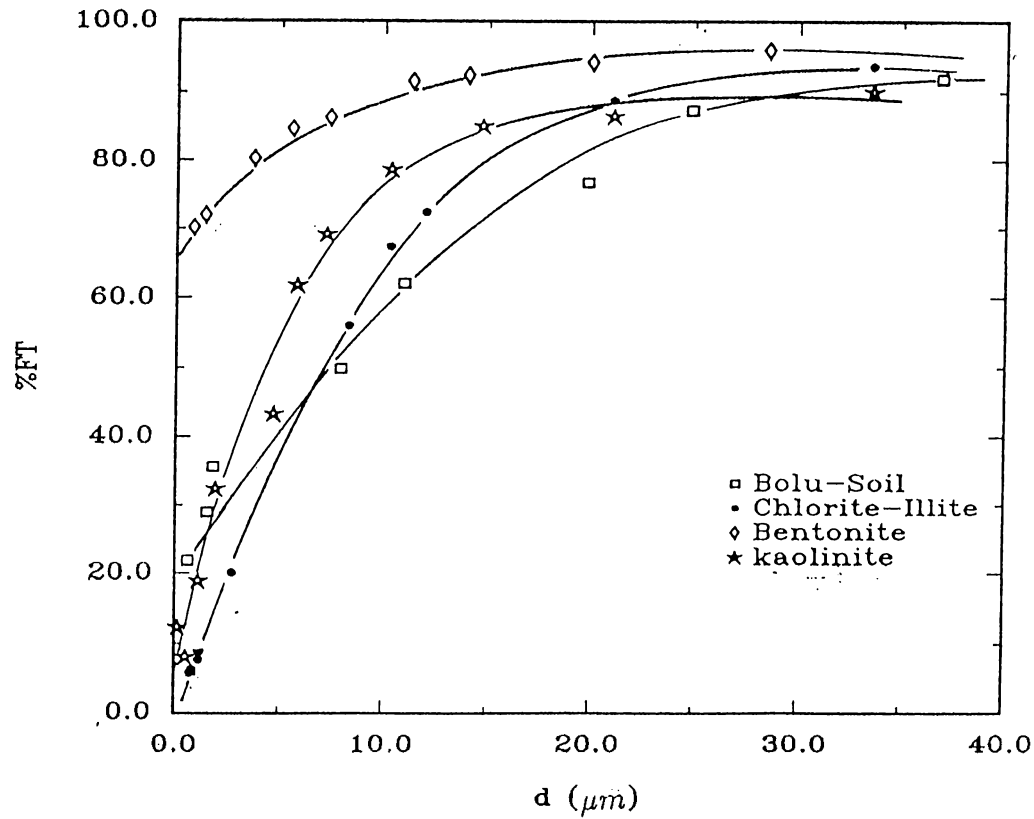


Figure 3.11: Particle Size Distribution Below $38\mu m$ of Bolu-Soil and Minerals

The complete analysis of Bolu-Yeniçağ soil has been done by G.Çaycı as a part of his Ph.D Thesis [47]. Some of the useful data are given in Table-3.1 :

Analysis	Result
Density	1.88 g/cm ³
Porosity	85.34
Organic matter	69.21%
Free Carbonates	4.71%
Conductivity	3.54 mS/cm
Cation Exchange Capacity	142.52 meq/100 g

Table 3.1: Results of Chemical Analysis of Bolu-Yeniçağ Soil

The trace elements present in the soil have also been analyzed and the concentrations given in Table-3.2 :

Element	Concentration of the element (ppm)
Ca	462
Mg	170
K	12.5
Na	94.33
Fe	.59
Mn	1.27
Zn	0.45
Cu	0.47

Table 3.2: Concentration of some trace elements in Bolu-Yeniçağ Soil

3.2 Bolu-Yeniçağ Soil

3.2.1 Kinetic Experiment

The change of distribution ratio with time was studied using an initial concentration of $[I^-]_i^0 = 1 \times 10^{-6}$ M at room temperature. The grain size of the samples used were below $38\mu m$.

The resulting curve is shown in Fig.-3.12 . The sorption behavior was rather slow and tends to saturation within about 14 days. This long saturation time can be explained by the complex and heterogeneous structure of the soil, since it includes clay and organic(living or non-living) parts and they may have a total effect in the adsorption of radioiodine. The results in the literature also show that by increasing the amount of organics in the soil the saturation time increases [36].

The experimental results obtained are given in Table-3.3:

Time (day)	R_d (ml/g)
0.042	0.1
0.5	1.1
1	1.6
2	3.6
4	9.0
10	101.8
14	174.5

Table 3.3: The Results of Kinetic Experiment for Bolu-Yeniçağ Soil

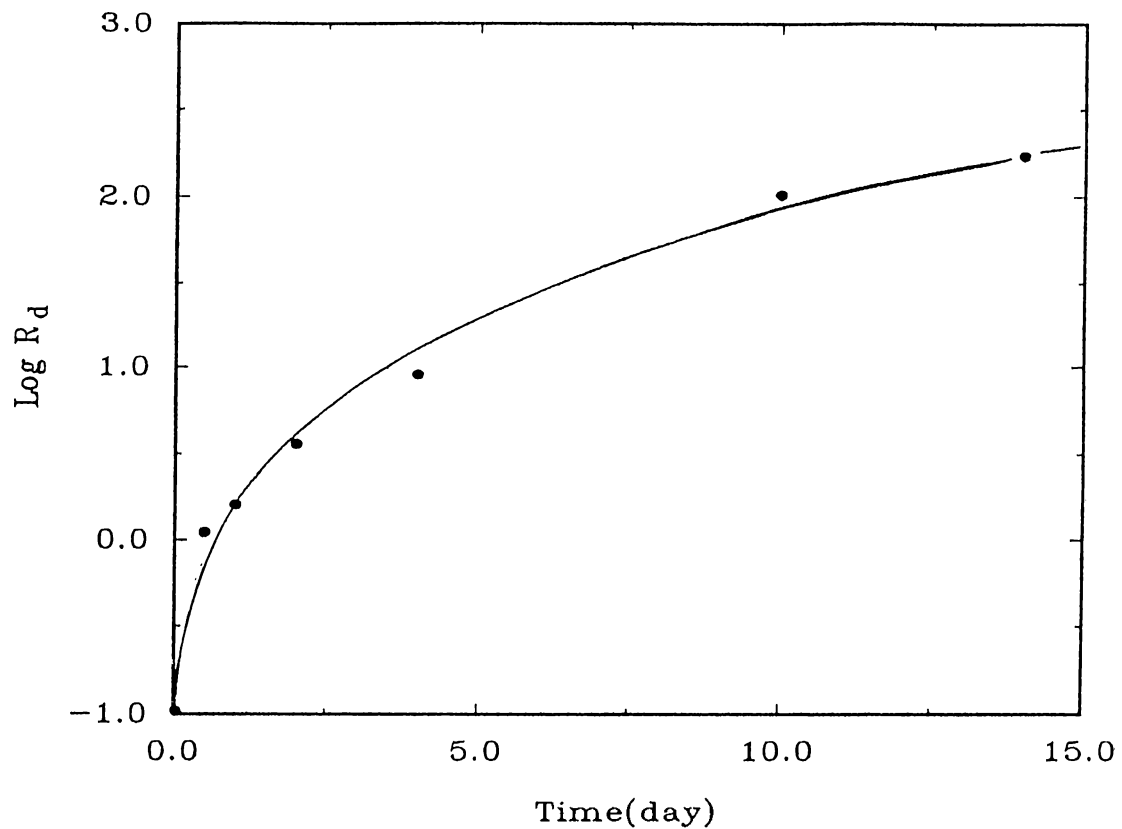


Figure 3.12: The Change of Distribution Ratio with Time for Bolu-Yeniç Soil

If the sorption process is considered to be of first order, the plot of logarithm of the activity remaining in the solution versus time, should give a straight line according to the equation $A = A_0 e^{-kt}$, where A is the remained activity in the solution after the desired time t and A_0 is the initial activity of the tracer containing solution. A and A_0 . The curve obtained, (Fig.-3.13), may be fitted to a straight line. The slope has been calculated as -0.212, so the rate constant k is equal to 0.212

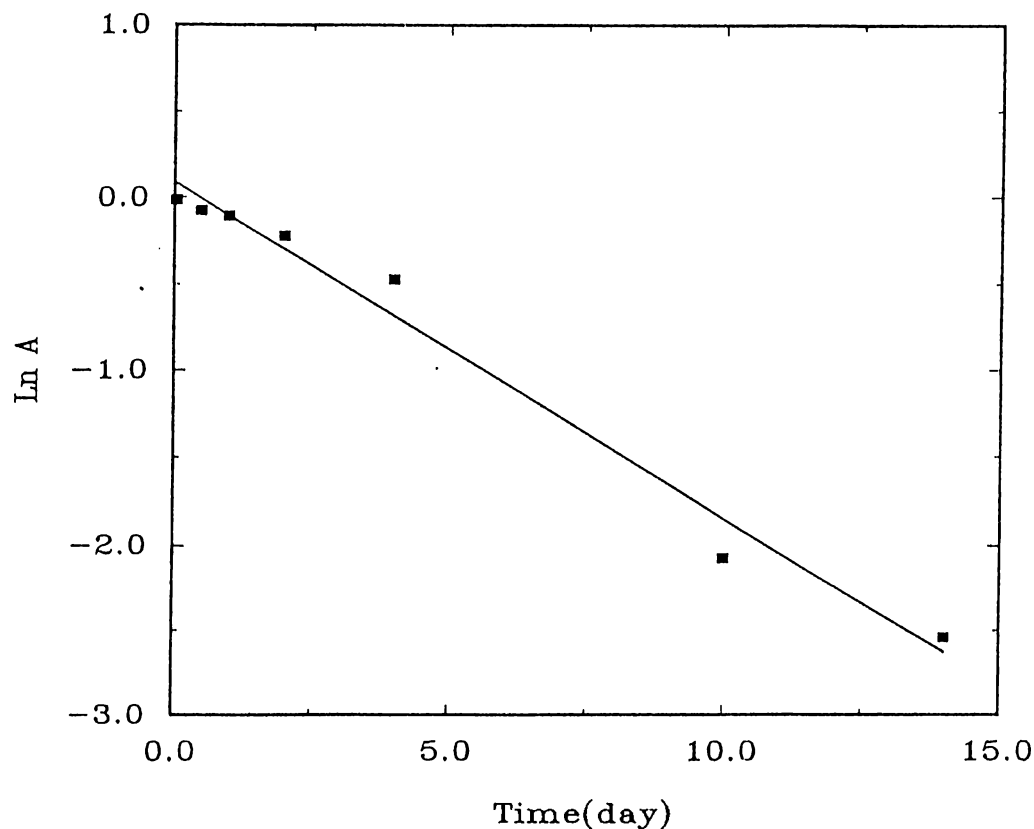


Figure 3.13: Plot of Remaining Activity in the Solution versus Time for the Adsorption of Radioiodine on Bolu-Yeniçağ Soil

These facts imply that although there may be different mechanisms or sites involved in the sorption, their rates are not comparable and most of the iodine is adsorbed by a slow reaction. As will be discussed later, this slow mechanism is supposed to be the one which corresponds to the organic part of the soil. Erten and Bors have performed sorption experiments with podzol ($C_{org} = 1.4\%$, Biomass $142\mu g/g$) and chernozem ($C_{org} = 2.4\%$, Biomass $317\mu g/g$) type soils they have observed faster initial sorption rate for the podzol type soil and have stated that the sorption process for the chernozem was more gradual and

to be present at higher amounts and in dynamic activity in chernozem soil [36].

3.2.2 Variation of Distribution Ratio with the Ratio of Volume of the Solution to Mass of the Solid

The effect of V/m (the ratio of volume of tracer containing solution to that of the mass of sorbent) was studied using an initial iodide concentration of $[I^-]_i^0 = 1 \times 10^{-6} M$ at room temperature. The results are given in Table-3.4 and the curve obtained is illustrated in Fig.-3.14.

V/m	R_d (ml/g)
10	48.5
15	53.4
20	113.6
50	278.5
100	447.7
120	357.5
200	325.2
250	340.9

Table 3.4: The Experimental Results Showing the Change of Distribution Ratio with V/m for Bolu-Yeniçağ Soil

An initial strong dependence of the distribution ratio, R_d , on V/m is observed between $V/m=$ to about 50. A plateau region is observed after $V/m \simeq 50$. Increasing the volume to mass ratio, probably results in better dispersion of the soil particles and their organic components in the soil. As a result the inner surfaces become more exposed to the solution and can interact more with iodine. When almost all of the sorption sites are filled with iodine, increasing the V/m ratio does not change the R_d very much and reaches a plateau.

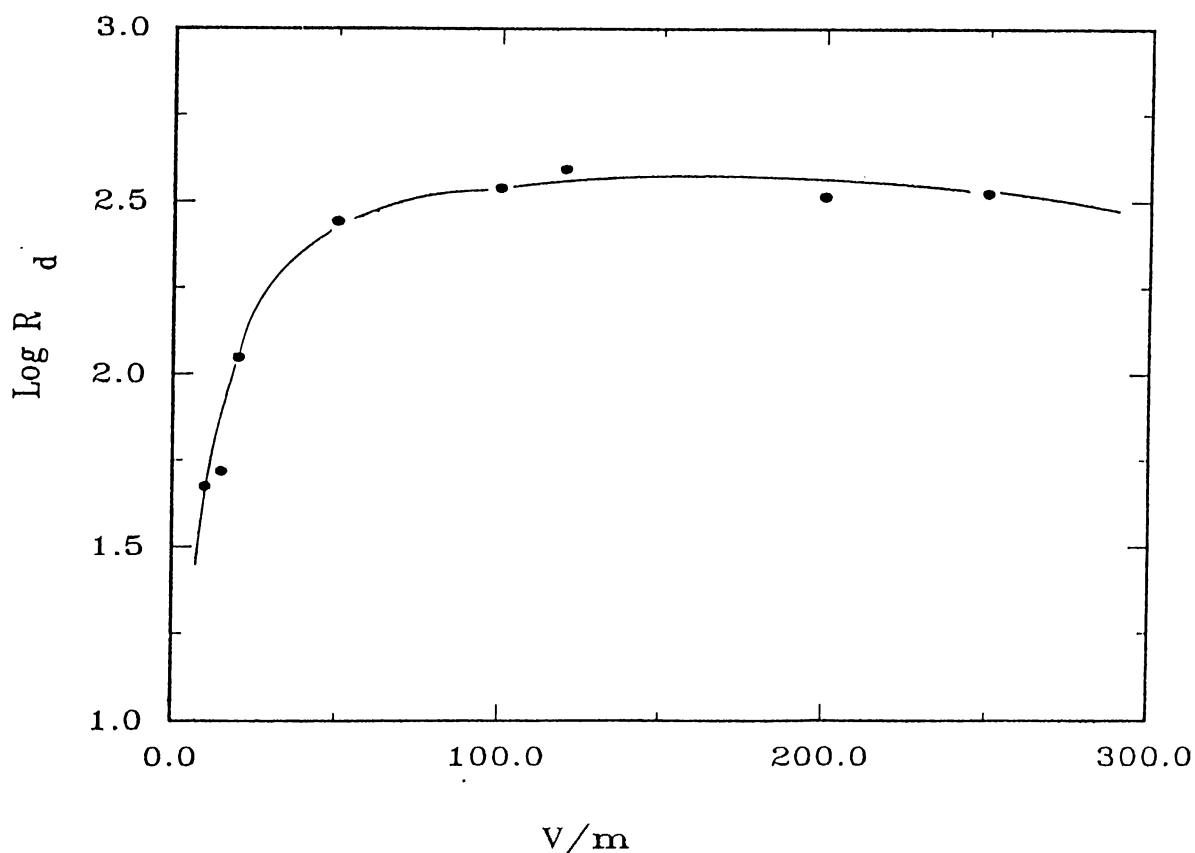


Figure 3.14: Change of R_d with V/m Ratio for Bolu-Yeniçağ Soil

Meier et al.[48], have studied the dependence of sorption and desorption distribution coefficients on solution-to-rock ratios in detail, using a lower range of V/m ($0.8 < V/m < 9$). They have explained the increase of distribution ratios by increasing V/m , as a result of successive compensation of adsorption sites. They have also indicated that the change of R_d with V/m ratio may be due to a change in the electrical double layer of the surface of the sediments. Erten and Bors [40], have examined the same effect on two soil types within a range of $2 < V/m < 110$ and have reported that after a $V/m \approx 10$, the distribution ratio did not change significantly but a gradual increase has been observed for the higher organic carbon and biomass containing soil (Chernozem).

3.2.3 The Effect of pH on the Adsorption of Iodine

The pH dependence of the distribution ratio for the adsorption of radioiodine on Bolu-Yeniçağ Soil, is shown in Fig.3.15 and the results are given in

Table-3.5. It is seen that the distribution ratio have fluctuations below $pH=7$ and after that pH , the changes are not very significant.

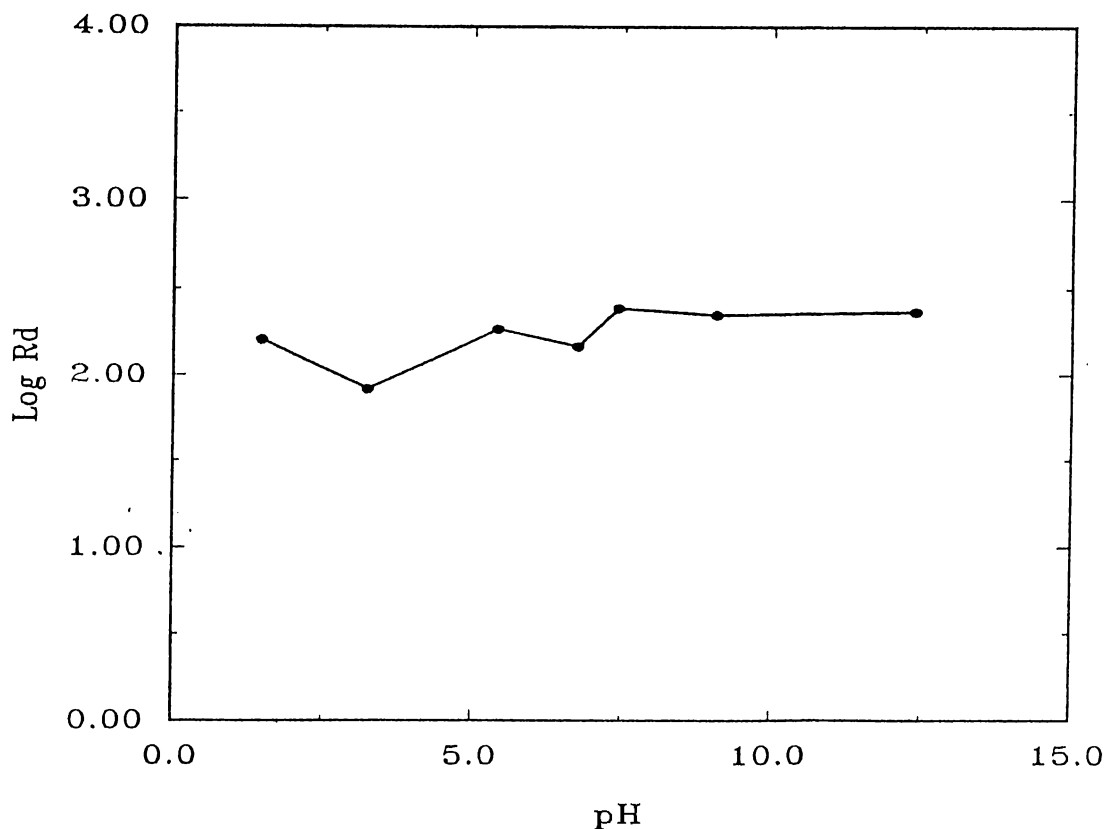


Figure 3.15: The Change of Distribution Ratio with pH of the Solution for Bolu-Yeniçağ Soil

According to the Eh-pH diagram of iodine-water system (Fig. 3.16), iodine is stable over a wide range of Eh and pH [11, 21]. The other iodine species were not determined in this study but the Eh of the synthetic groundwater was measured as 0.047 volts which is mostly in I^- region. Eh was measured for a pH range of $\simeq 1$ to $\simeq 12$ for a solution with $[I]_i^0 = 1 \times 10^{-8} M$ range and the Eh values observed were in the range of 0.289 volts to -0.268 volts. In the whole range iodine is in I^- form in the solution due to Fig. 3.16. However, other iodine species such as IO_3^- , and IO^- , can be formed in the solution in low amounts. It must be noticed that change in the pH of the solution can effect the adsorption sites as well as the iodine species. It is possible that at $pH < 7$, the sites are less available to iodine than $pH > 7$. This low effect of pH on distribution Ratio of radioiodine has been observed also by Sheppard and Thibault [32].

pH	R_d (ml/g)
1.47	161.0
3.24	84.1
5.42	185.6
6.76	148.5
7.44	247.0
12.40	233.2

Table 3.5: The Experimental Results Showing the Effect of pH on Distribution Ratio for the sorption of radioiodine on Bolu-Yeniçağ Soil

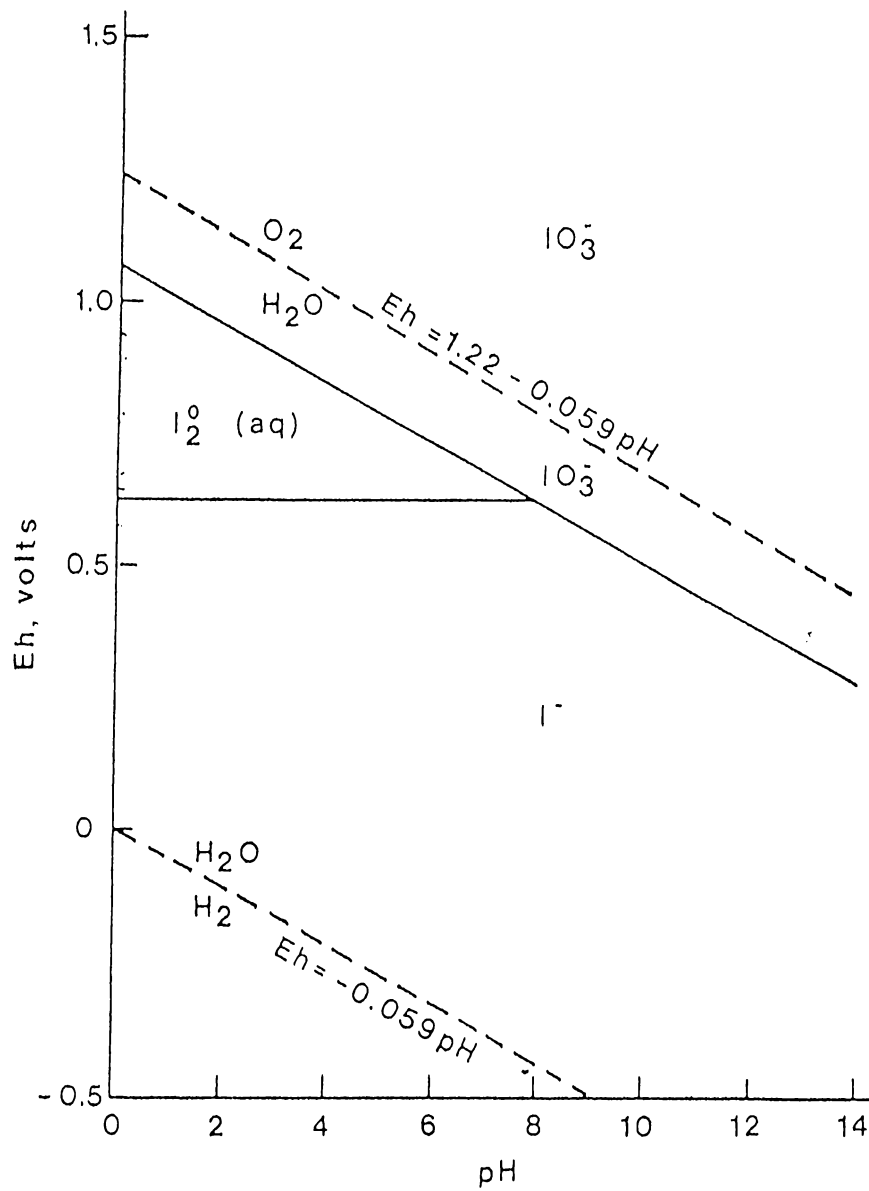


Figure 3.16: Eh-pH Diagram for Iodine-Water System

3.2.4 Loading Experiments

The effect of initial I^- ion concentration in the tracer solution on the immobilization of radioiodine by soil is shown in Fig. 3.17. It was observed that the distribution ratio increases by decreasing the initial iodine concentration and desorption is achieved in the low iodine concentration ($[I]_i \leq 1 \times 10^{-6} \text{ mmol/ml}$). The desorption R_d values are higher compared to those obtained for adsorption, which indicates a partly reversible adsorption.

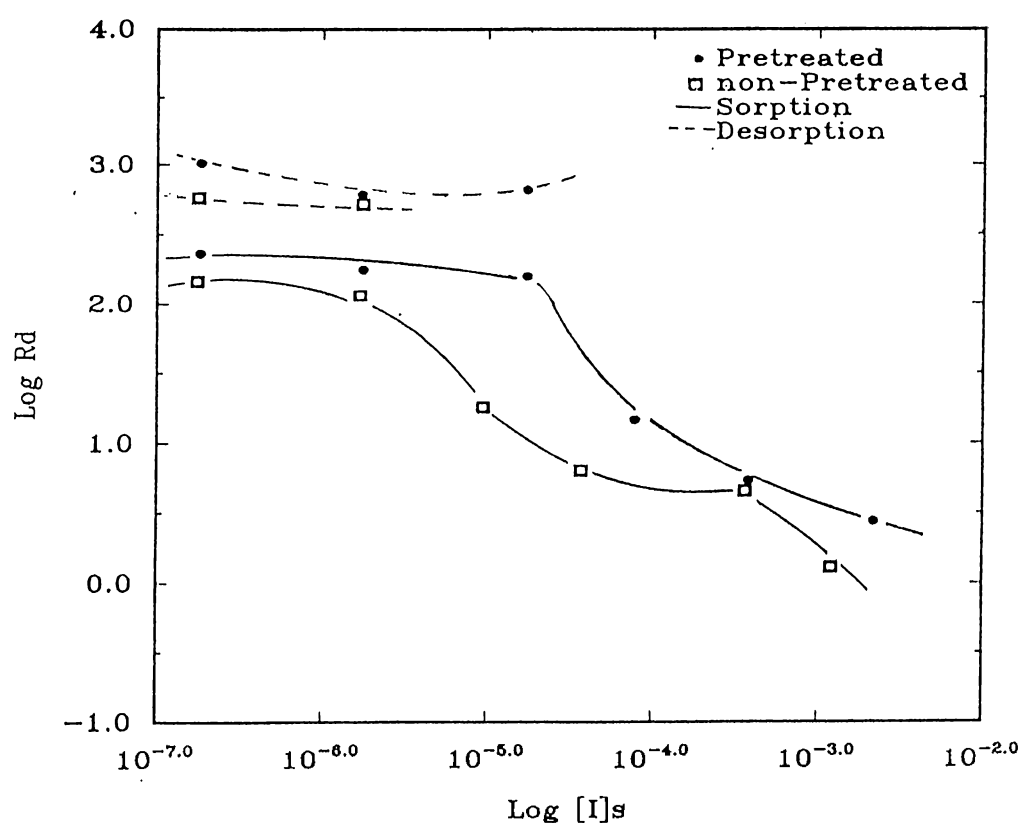


Figure 3.17: The Change of Distribution Ratio with the Iodine Loading for Pretreated and untreated Bolu-Yeniçağ Soil

A constant R_d region is observed in the loading curve for $[I]_s \leq 5 \times 10^{-5} \text{ mmol/g}$ and after that point, a gradual decrease in R_d values is observed. By extrapolating this part, a saturation value of $[I]_s \simeq 1 \times 10^{-2} \text{ mmol/g}$ may be estimated. This value can be referred as the anion-exchange capacity if ion exchange is considered to be the most effective mechanism of the adsorption.

Desorption is observed just in the constant R_d region, with low percentages.

It is possible that the adsorption process in this region, is a semi-reversible one. The second assumption is that the mechanism by which desorption takes place, is unique and different from the main adsorption mechanism (which is probably completely irreversible).

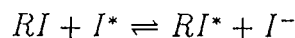
The fact that desorption occurs only at low iodine concentrations, suggests that some of the bonds formed are so weak that they can easily be replaced by cations or anions of the synthetic ground water and result in the removal of iodine from the adsorbed site. Iodine desorption at high R_d regions, suggests that the probability of an adsorption mechanism including more than one layer is higher in this region. So the loosely bounded ions in the exterior layers are desorbed. Another possibility is that most of the iodine adsorbed is fixed by the soil and the non-fixed part is desorbed. It is stated by Grim[49] that the exchanged ions can be fixed either completely or incompletely and the reaction might not be reversible.

In the case of untreated soil, lower distribution ratios are observed and the loading curve has two constant R_d regions in the ranges $2 \times 10^{-6} < [I]_s < 2 \times 10^{-7}$ and $5 \times 10^{-5} < [I]_s < 6 \times 10^{-4}$. If the curve is extrapolated, a saturation value of $[I]_s \simeq 1 \times 10^{-2} \text{ mmol/ml}$ can be estimated which is the same of the value obtained for the pretreated soil. Desorption values were obtained just for the region $2 \times 10^{-6} < [I]_s < 2 \times 10^{-7} \text{ mmol/ml}$. Pretreatment has a significant effect on the adsorption of radioiodine because the adsorption site are equilibrated with the ions in the synthetic groundwater and the adsorption can be related just to the radioiodine after addition of tracer containing solution.

The sorption and desorption distribution ratios, as well as the percentages of adsorption, desorption and reversibility are given in Table-3.6. Adsorption percentages increase by decreasing the initial iodine concentration in the solution.

To observe the extent of exchange of radioiodine in the solution with inactive iodine bounded to the sorption sites, sorption experiments were performed with soil samples pretreated with $0.1M$ inactive NaI . The exchange reaction

would be as following:



The loading curve for the exchange experiment is seen in Fig. 3.18. Also the experimental results and exchange percentages are given in Table-3.6.

Higher exchange is seen in lower iodine concentrations ($[I]_i^0 \leq 1 \times 10^{-6}$) and the exchange percentages are close to the reversibility percentages in $[I]_i^0 \leq 1 \times 10^{-7}$ iodine concentrations. This may be an indication of the fact that iodine is sorbed at least partly by the surface ions. Erten and Bors[36] have also found very low R_d values (between 0.2 and 0.5 ml/g) for exchange experiments on two soil types and they have stated that no much exchange seems to take place between radioactive I^- and inactive I^- ion.

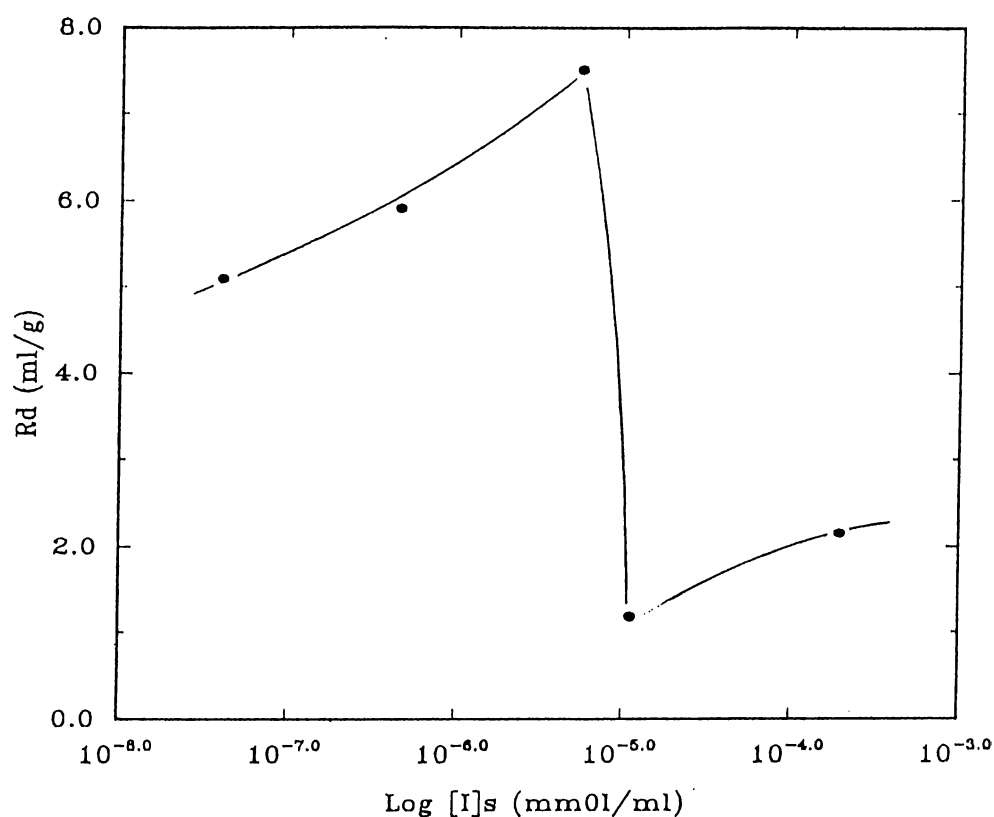


Figure 3.18: Loading curve for Exchange of Radioiodine on Bolu-Yeniçağ soil

$[I]_i^0$ (mmole/ml)	$R_{d,ads}$ (ml/g)	$R_{d,des}$ (ml/g)	$R_{d,ex}$ (ml/g)	%A	%D	%R	%E
1×10^{-3}	2.8 ± 1.2	0	0	11.0	0	0	0
1×10^{-4}	5.4 ± 0.53	0	2.2 ± 0.97	19.2	0	0	9.7
1×10^{-5}	17.8 ± 5.95	0	1.2 ± 0.78	39.4	0	0	5.5
1×10^{-6}	157.6 ± 14.67	651.0	7.3 ± 1.48	87.4	1.5	12.3	2.3
1×10^{-7}	175.7 ± 3.13	605.0	5.9 ± 0.70	88.7	2.1	18.5	22.8
1×10^{-8}	232.4 ± 9.63	1032.2	5.1 ± 0.62	91.2	1.4	16.5	20.3

Table 3.6: Sorption, Desorption and Exchange Distribution Ratios and percentages of Adsorption (%A), Desorption (%D), Reversibility (%R) and Exchange (%E), for adsorption of radioiodine on Bolu-Yeniçağ Soil

3.2.5 Adsorption Isotherms

The sorption and exchange data were fitted to Freundlich and Dubinin-Radushkevich isotherm models. The Freundlich isotherm is given in Fig. 3.27. The value of N was found to be less than one which indicates the non-linearity of the isotherm for both sorption and exchange experiments.

The Dubinin-Radushkevich isotherm is given in Fig. 3.28. This curve is also non-linear and it seems that the slope of the curve changes after $E^2 \simeq 10 \times 10^6$ for the sorption data. The value of X_m , the maximum adsorbed amount, can be calculated from the intercept of this isotherm and if the exchange mechanism is assumed to be the most effective one, it can be considered as anion exchange capacity.

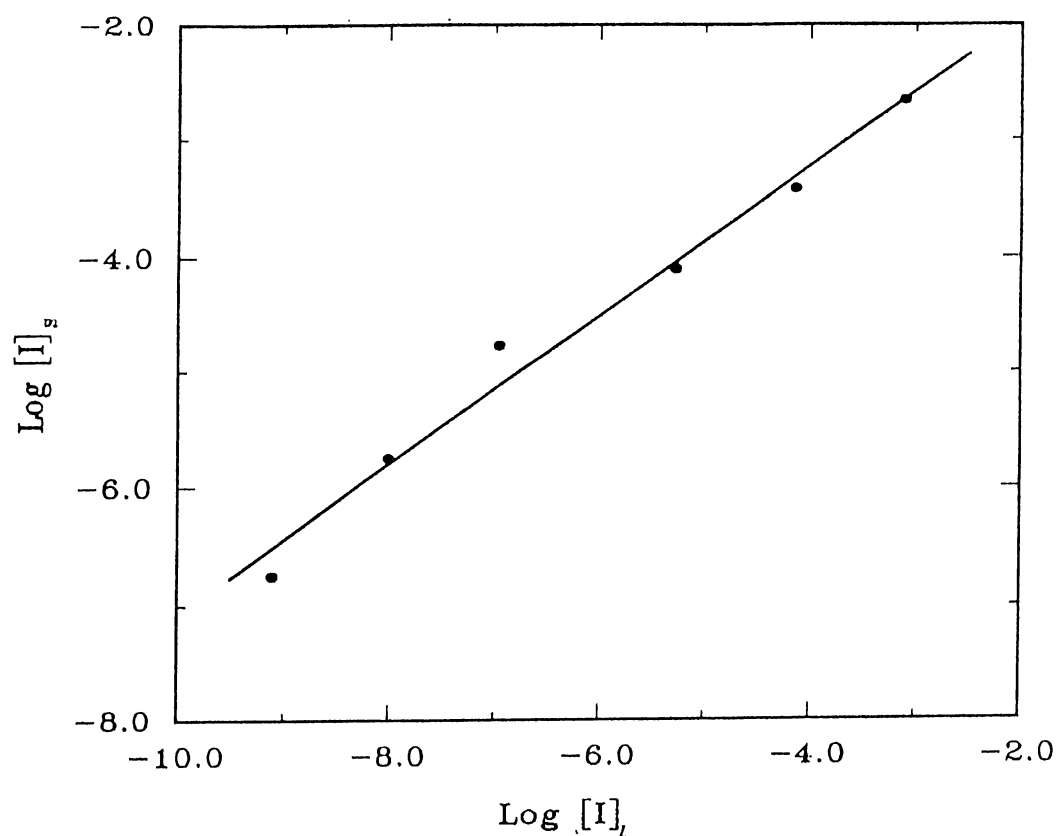


Figure 3.19: Freundlich Isotherm for Adsorption of Radioiodine on Bolu-Yeniçağ Soil. Initial Iodine Concentration $1 \times 10^{-3} \text{ mmol/ml} < [I^-]_l^0 < 1 \times 10^{-3} \text{ mmol/ml}$

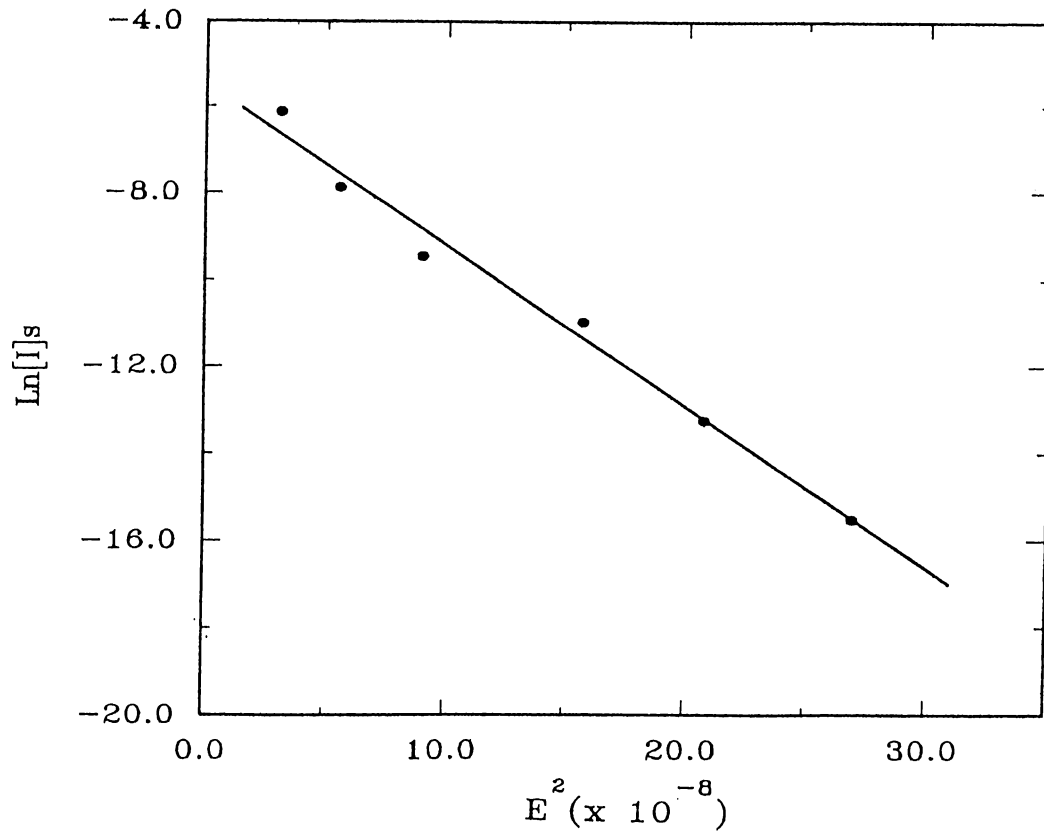


Figure 3.20: The Dubinin-Radushkevich Isotherm for Adsorption of Radioiodine on Bolu-Yeniçağ Soil. Initial Iodine Concentration $1 \times 10^{-3} \text{mmol/ml} < [I^-]_i < 1 \times 10^{-3} \text{mmol/ml}$

The constants found from fitting the sorption and exchange data to these isotherms, are given in Table-3.7.

Experiment	Fruendlich		Dubinin-Radushkevich	
	N	A	X_m (meq/g)	K
Sorption	0.644	0.225	4.102×10^{-3}	3.71×10^{-9}
Exchange	0.86	0.48	1.629×10^{-3}	4.96×10^{-9}

Table 3.7: The Constants Found from Fitting the Sorption and Exchange Data to Fruendlich and Dubinin-Radushkevich Isotherms for the Adsorption of Iodine on Bolu-Yeniçağ Soil

The mean energy of adsorption can be calculated from Dubinin-Radushkevich isotherm. The mean energy of adsorption is defined as the free energy change when one mole of ion is transferred to the surface of the solid from the infinity

in the solution. It can be calculated from the equation: $E = (2K)^{1/2}$ [28]. The magnitude of E was calculated as 11kJ/mol for adsorption of radioiodine on Bolu-Yeniçağ soil. This value is in the energy range for ion-exchange reactions (8-16 kJ/mol). No data is available in the literature for the adsorption energy estimation of radioiodine.

The calculated R_d values for the sorption experiments can be obtained by using the constants found from the isotherms using the following equations:

$$R_{d,(Fru.)} = KC^{N-1} \quad (3.1)$$

$$R_{d,(D-R.)} = 1/C X_m (-K(RT \ln(1 + 1/C)^2)) \quad (3.2)$$

Where:

- $R_{d,(Fru.)}$: Distribution ratio calculated from the curve fitting constants of Freundlich isotherm (ml/g)
- C : Solute Equilibrium solution concentration (mmol/ml)
- K,N : Constants found from the Freundlich isotherm
- $R_{d,(D-R.)}$: Distribution ratio calculated from the curve fitting constants of Dubinin-Radushkevich isotherm (ml/g)
- X_m : Sorption capacity of adsorbent per unit weight (mmol/g)

The experimental R_d values are compared with those calculated from the curve fitting of Freundlich and Dubinin-Radushkevich isotherms, in Table-3.10 . The experimental R_d values are closer to those calculated from Freundlich isotherm in the whole range. Differences between the experimental R_d values and those calculated from Dubinin-Radushkevich isotherm is observed at extreme points.

$[I]_i^0$ (mmol/ml)	$R_{d,(D-R.)}$ (ml/g)	$R_{d,(Fru.)}$ (ml/g)	$R_{d,(exp.)}$ (ml/g)
1×10^{-3}	0.6	2.9	2.8
1×10^{-4}	7.2	6.7	5.4
1×10^{-5}	26.8	17.0	14.7
1×10^{-6}	107.0	67.4	157.6
1×10^{-7}	180.0	158.0	175.7
1×10^{-8}	235.0	393.0	232.4

Table 3.8: The Theoretical R_d values Obtained From The Isotherm Constants, for Bolu-Yeniçağ soil. $R_{d,(exp.)}$: Experimental R_d , $R_{d,(D-R.)}$: R_d obtained from Dubinin-Radushkevich Isotherm, $R_{d,(Fru.)}$: R_d obtained from Freundlich Isotherm

3.2.6 Site Distribution

Sposito has used the empirical Freundlich constants to obtain information about the heterogeneity of the adsorbing sites, in case of a binary exchange reaction where one of the species is adsorbed in trace amounts[50]. He has made assumptions, stating that the adsorption sites may be grouped into classes, each characterized by the number of sites it contains and by the relative affinity it possesses for the exchanging species and describing exchange reaction in each class of sites, by Langmuir equation. The site distribution function is given as following :

$$m(q) = m_{max} \frac{2 \cos(\pi N) \exp[N(q_m - q)]}{1 + 2 \cos(\pi N) \exp[N(q_m - q)] + \exp[2N(q_m - q)]} \quad (3.3)$$

where:

- $m(q)$: number of sites of class q
- q : The class of adsorption sites
- m_{max} : The value of $m(q)$ at its maximum
- q_m : The value of q when $m_q = m_{max}$
- N : Freundlich exponent

q is related to the affinity parameters of species A and B and it is defined as:

$$q \equiv \ln(K_A/K_B) \quad (3.4)$$

m_{max} is calculated from the equation:

$$m_{max} = \frac{M}{2\pi} \ln(\pi N/2) \quad (3.5)$$

where M is the total number of adsorption sites. The value of q_m is calculated from the following equation:

$$q_m = (1/N) \ln \alpha \quad (3.6)$$

The parameter α is calculated from :

$$\alpha = A c_B^N / M \quad (3.7)$$

A and N are the Freundlich constants and c_B is the average value of the concentration of species B, in the solution.

For the adsorption of radioiodine in the soil, the competing ion was considered as Cl^- , since its size and charge are close to that of iodide and both are in the same group. The sites in the soil were found to have a greater affinity to Cl^- ion than I^- and the ratio obtained was $K_{Cl^-}/K_{I^-} = 3.32$. The parameters used to obtain this curve are as followings:

$$N=0.644$$

$$A=0.225$$

$$c_B=6 \times 10^{-4}$$

$$M=4.1^{-3} \text{ (meq/ml)}$$

$$\alpha=0.462$$

$$q_m = -1.199$$

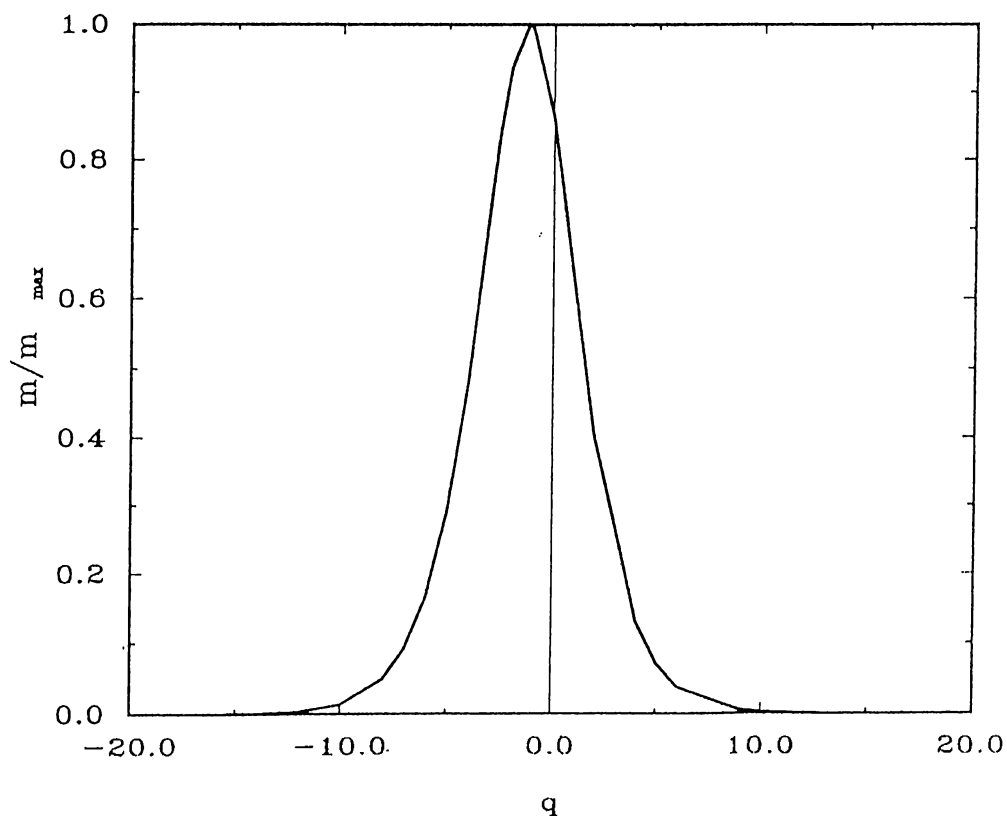


Figure 3.21: The Site Distribution on Bolu-Yeniçağ Soil, Considering Cl^- as the Competing Ion

It is observed in the curve that most of the sites have a greater affinity to Cl^- ion than I^- . The reason may be the smaller size of Cl^- . But there are also a number of sites in the positive region of the curve (that have a higher affinity to I^- than Cl^-).

3.2.7 Effect of Sterilization

The microorganisms are known to be very effective in iodine sorption [36, 51]. We have performed experiments to study the effect of microorganisms on the adsorption of radioiodine.

Soil samples were sterilized by heat ($180^{\circ}C$ for 2 hrs.) and gamma irradiation, using a ^{60}Co source ($3.7 \times 10^4 rad/hr$), till a dose of 2.7×10^6 rad. This

with the values given in literature which are about 10^2 to 10^5 rad[52]. Sorption experiments were performed using the sterilized and a control sample. The distribution ratios found, are given in Table-3.9 .

Soil Sample	R_d (ml/g)
sterilized by heat	8.3
sterilized by ^{60}Co radiation	26.5
control soil	138.2

Table 3.9: Effect of Sterilization on Sorption of Iodine on Bolu-Yeniçağ Soil

The difference between the R_d values of sterilized and not sterilized samples are quite striking. The results indicate the strong influence of microorganisms in the sorption of iodine.

The soil samples sterilized with ^{60}Co gamma source, have somewhat higher R_d values compared to those sterilized by heat. The reason may be due to the structural defects in soil, brought about as a result of over drying by heat. Cleavage of some bonds by the gamma radiation can also effect the adsorption of iodine.

Bors et.al.[36], have reported also the decrease of R_d value of soil, when sterilized by heat or CH_3Cl fumigation. Strack and Milton have reported that autoclaving reduced the immobilization of iodine[53]. They also stated that thermal treatment has an effect also on the inorganic soil matrix and the non-living organic substances and may vary the physico-chemical properties of soil.

Experiments were also performed to study the sorption of iodine by pure microorganisms in the solution. Microorganisms were isolated from soil by cultivation in a nutrient medium. Very low or zero R_d values were obtained in these studies . We relate the results to the conditions of the experiment. Since each bacteria lives in certain conditions of pH, temperature, nutrient media, etc, the optimization of these living conditions for the microbial part of the soil is very important. Also we observed that the isolated bacteria were

in these studies . We relate the results to the conditions of the experiment. Since each bacteria lives in certain conditions of pH, temperature, nutrient media,etc, the optimization of these living conditions for the microbial part of the soil is very important. Also we observed that the isolated bacteria were very sensitive to centrifugation and filtration is probably a better way to separate them from the liquid part. It may be said that the sorption experiments attempted with living microorganisms had negative results, probably because at the experimental conditions the microorganisms were not alive.

3.3 Clay Minerals

3.3.1 Sorption Experiments

Sorption experiments were performed using Alumina and four types of Clay minerals as described before. For all the experiments the concentration of iodide ion in the tracer containing solution was $1 \times 10^{-8}M$ and the experiments were done at the room temperature and at the pH of synthetic ground water ($pH \simeq 5.8$) using a V/m of 50. The loading curves for the adsorption of radioiodine on clay minerals¹ are given in Figs. 3.22-3.25 and the sorption values are given in Table-3.12 .

The Chlorite-Illite clay-mixture, had higher R_d values than the other minerals. A constant R_d region is observed where $[I]_s \leq 5 \times 10^{-5}mmol/g$. The distribution ratio then decreases and remains constant where $[I]_s \geq 1 \times 10^{-4}mmol/g$ This behavior indicates the existence of more than one adsorption sites and/or mechanisms for the adsorption of radioiodine on this sample. Since Chlorite-Illite is a clay mixture, this behavior may be related to its heterogeneous nature. Also this sample is a natural soil taken from Afyon and it is possible that it has contain organic parts which lead to higher adsorption of radioiodine.

¹Although alumina is not a clay mineral, but from now on it is mentioned in this group, for convenience.

Bors and Erten have reported the R_d value for Chlorite-Illite clay mixture as 5 ml/g using synthetic soil water as tracer containing solution and 1.4 ml/g when bidistilled water is used[36]. Strickert has reported a R_d value of 3 ml/g for chlorite[37]. Relyea [38], Meyer and Burtch [39] and Rançon [33] have examined the adsorption of iodide ion on illite and have reported R_d values as 0, 0.01 and 0.5 respectively. The higher R_d value found in this study may be related to the the effect of organic part as mentioned before.

Bentonite, kaolinite and Alumina showed low adsorption of radioiodine and the loading curves obtained do not resemble the loading curves of Chlorite-Illite. Torstenfelt[31] and Rançon[33] have reported distribution ratios as 0.001 and 1.5 respectively for the adsorption of iodide ion on bentonite. For kaolinite the R_d values found by Relyea[38], Meyer and Burtch[39], Erten and Bors[36] and also Rançon[33], are between 0 and 4 ml/g. The adsorption of radioiodine on Alumina has been studied by Meyer and Burtch[39], using NaCl solution as the aquas phase and he has found distribution ratios between 0 ml/g (at 0.5 M NaCl soln.) and 12.2 ml/g (at 0.01 M NaCl soln.)

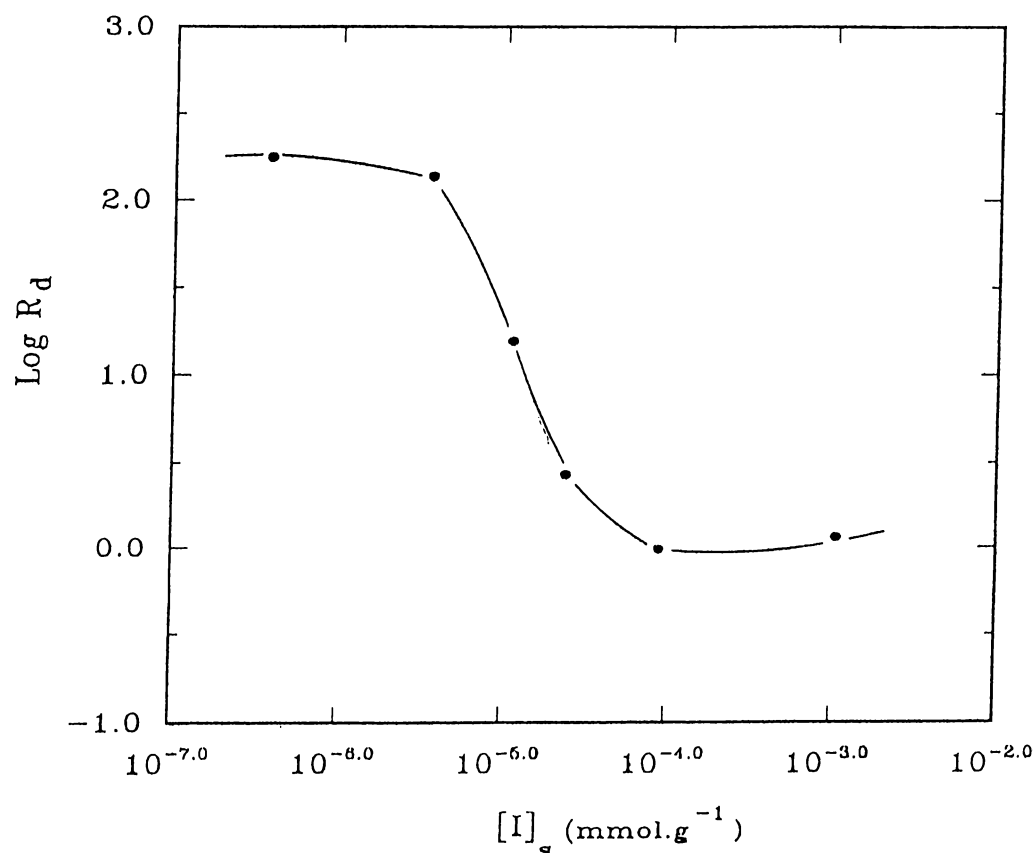


Figure 3.22: Loading Curves for sorption of radioiodine on Chlorite-Illite Clay Mixture

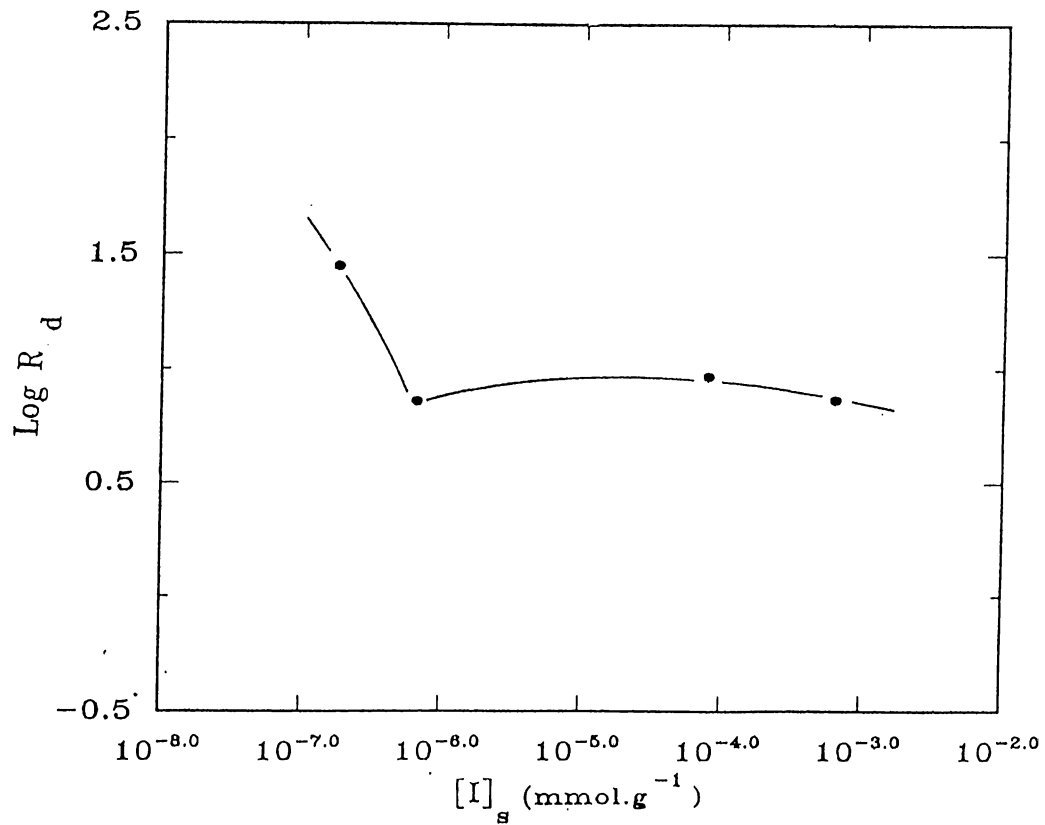


Figure 3.23: Loading Curves for sorption of radioiodine on Bentonite

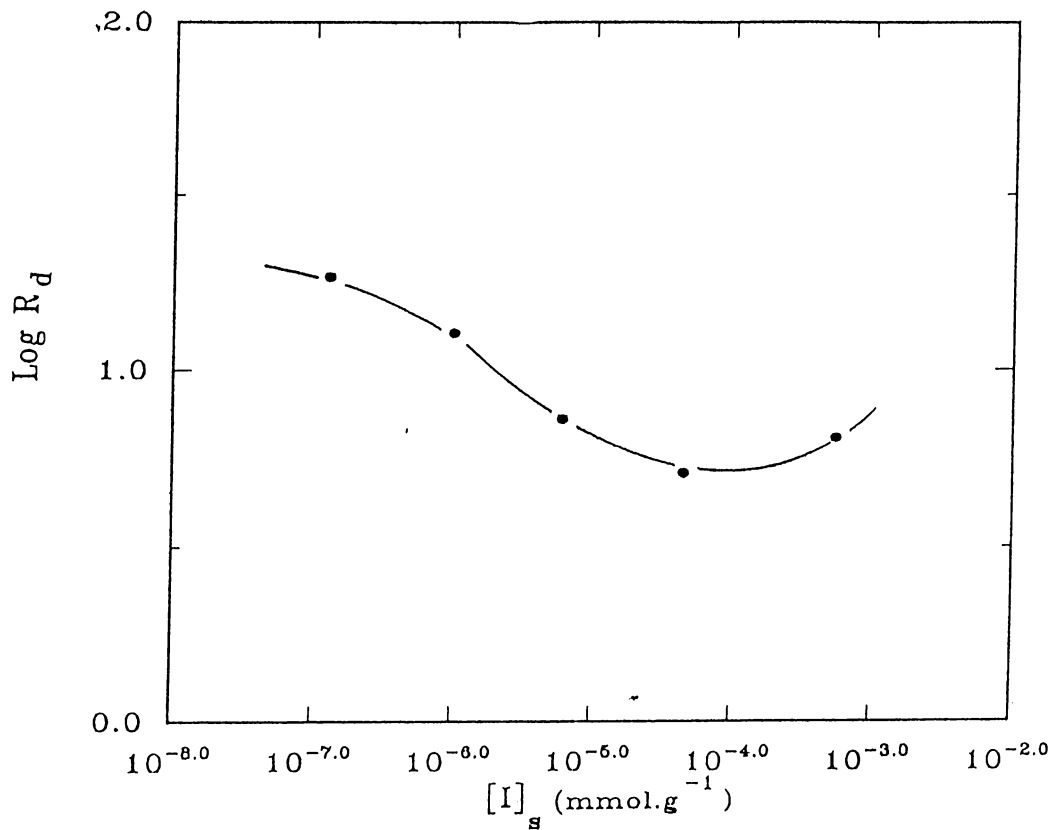


Figure 3.24: Loading Curves for sorption of radioiodine on Kaolinite

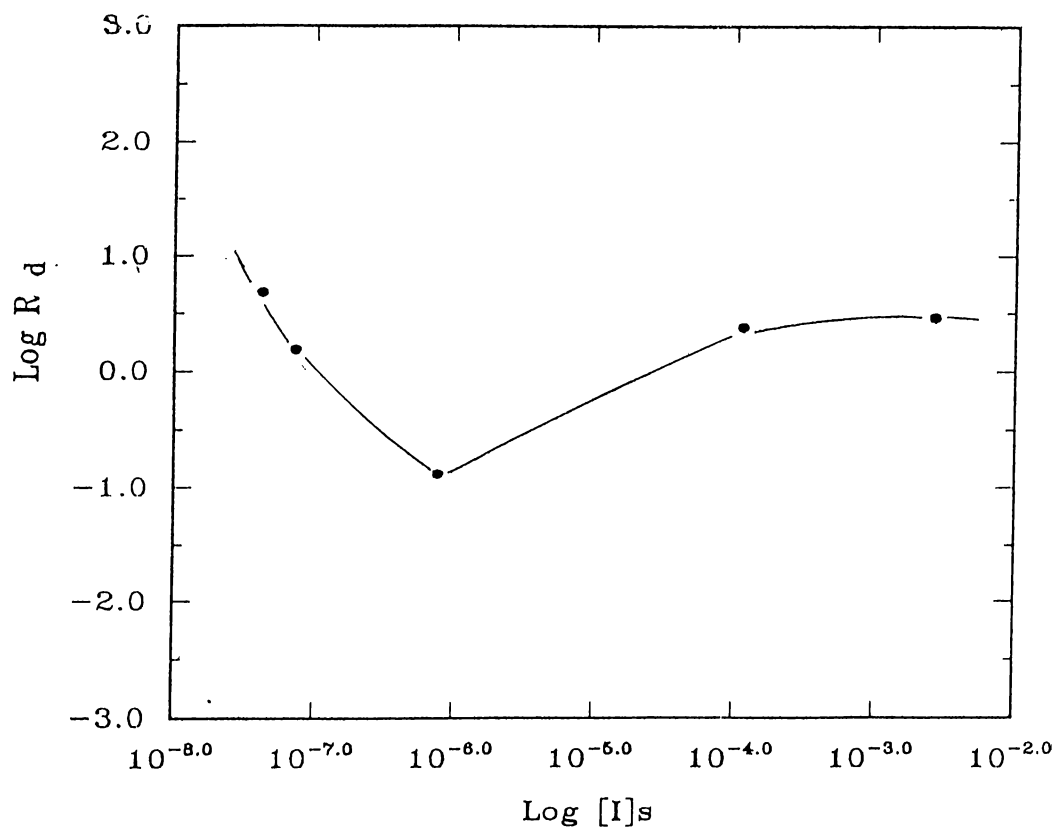


Figure 3.25: Loading Curve for sorption of radioiodine on Alumina

3.3.2 Adsorption Isotherms

The sorption data for the adsorption of radioiodine on clay minerals were fitted to the Freundlich and Dubinin-Radushkevich isotherms. The Freundlich isotherms obtained are shown in Figs. 34-37. The slopes are all below 1.00 and the curves are not linear. The Dubinin-Radushkevich isotherms are given in Figures 38-41. The curves are not linear also in these isotherms. The isotherm of Chlorite-Illite has a break in the region $[I]_s \cong 1 \times 10^{-5}$. For the other samples the isotherm seems to be linear although there appear some points far from the best line.

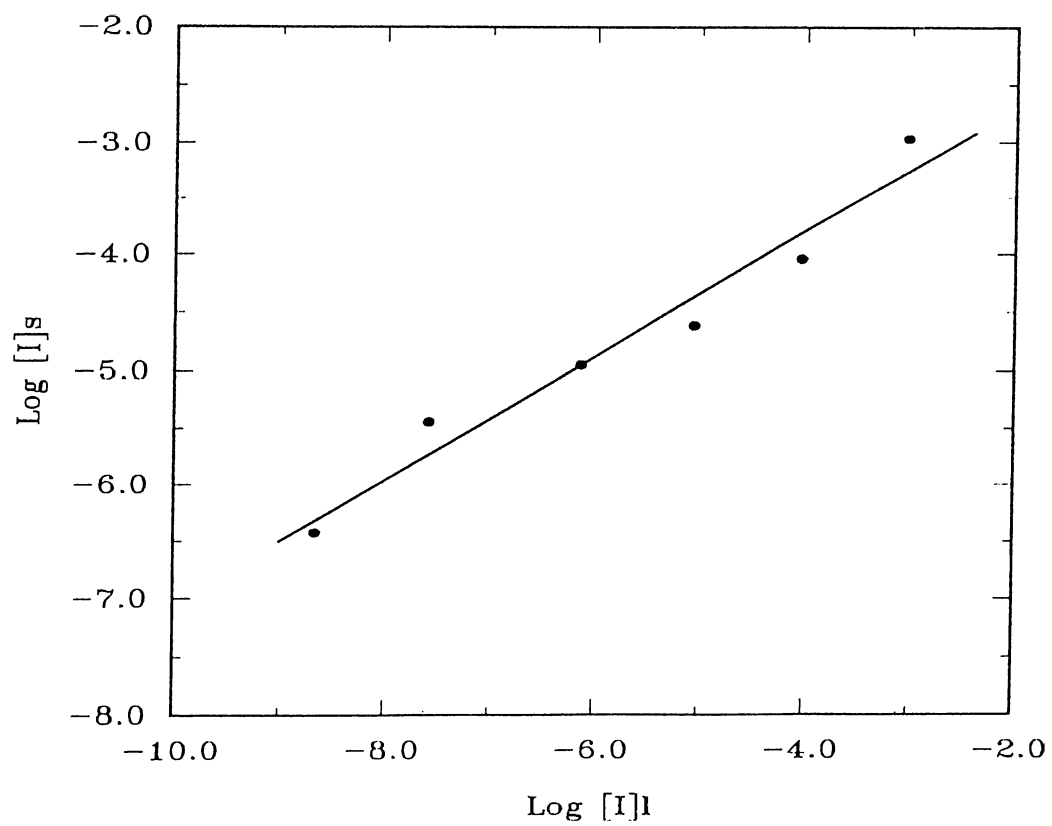


Figure 3.26: Freundlich Isotherm for Sorption of Radioiodine on Chlorite-Illite Clay Mixture

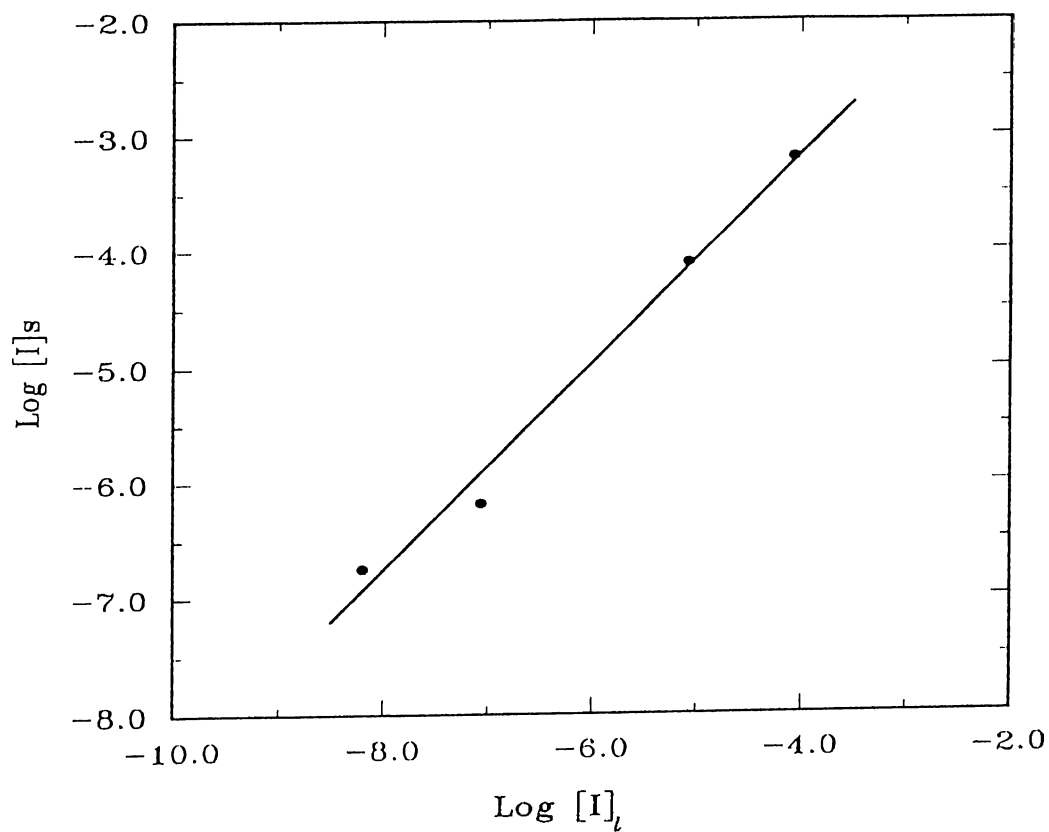


Figure 3.27: Freundlich Isotherm for Sorption of Radioiodine on Bentonite

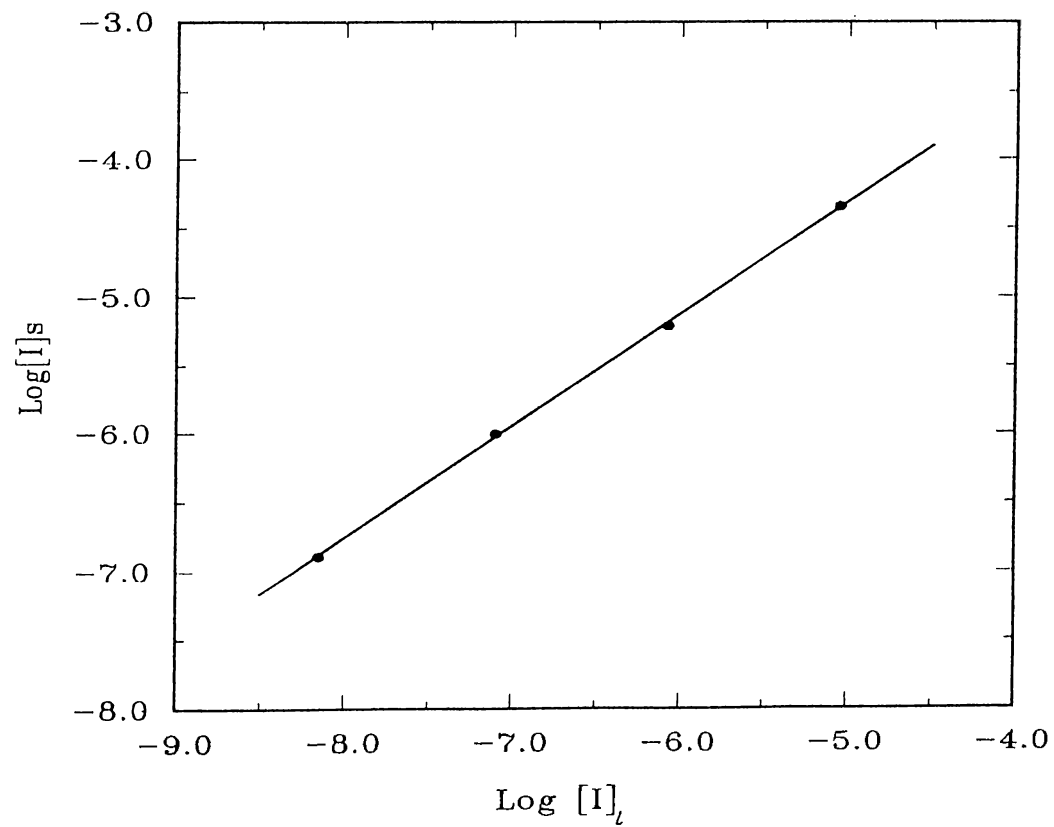


Figure 3.28: Freundlich Isotherm for Sorption of Radioiodine on Kaolinite

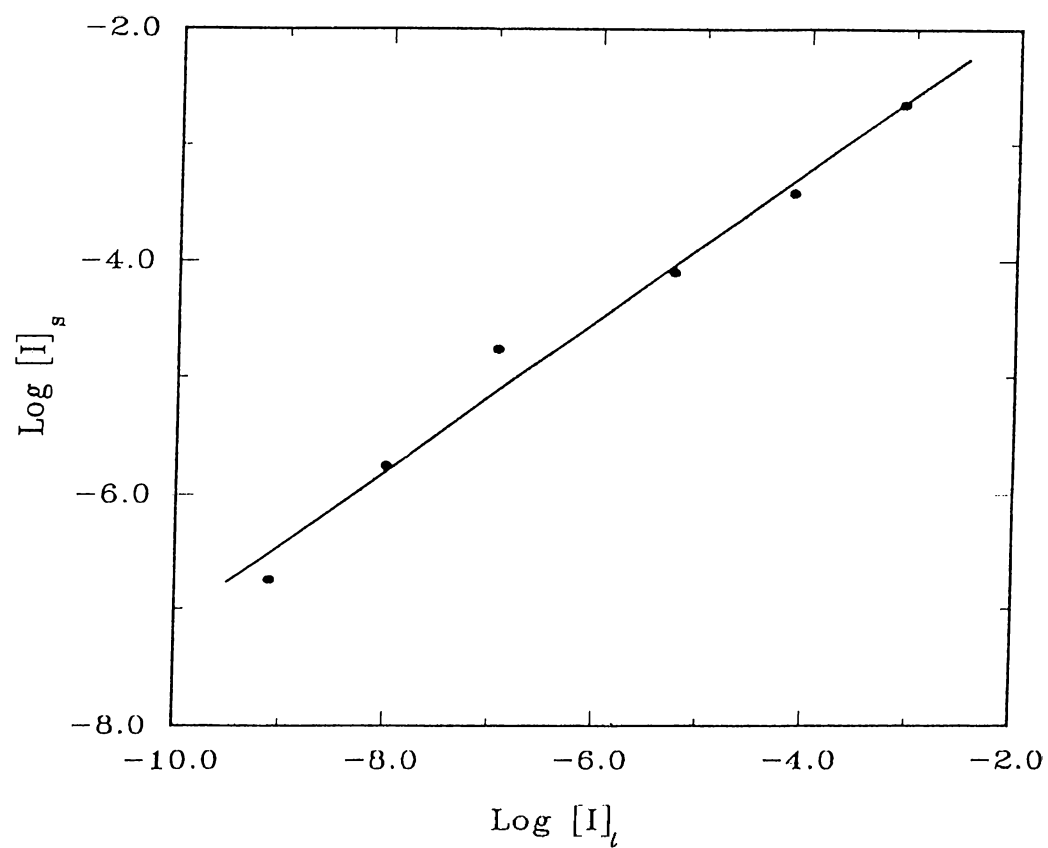


Figure 3.29: Freundlich Isotherm for Sorption of Radioiodine on Alumina

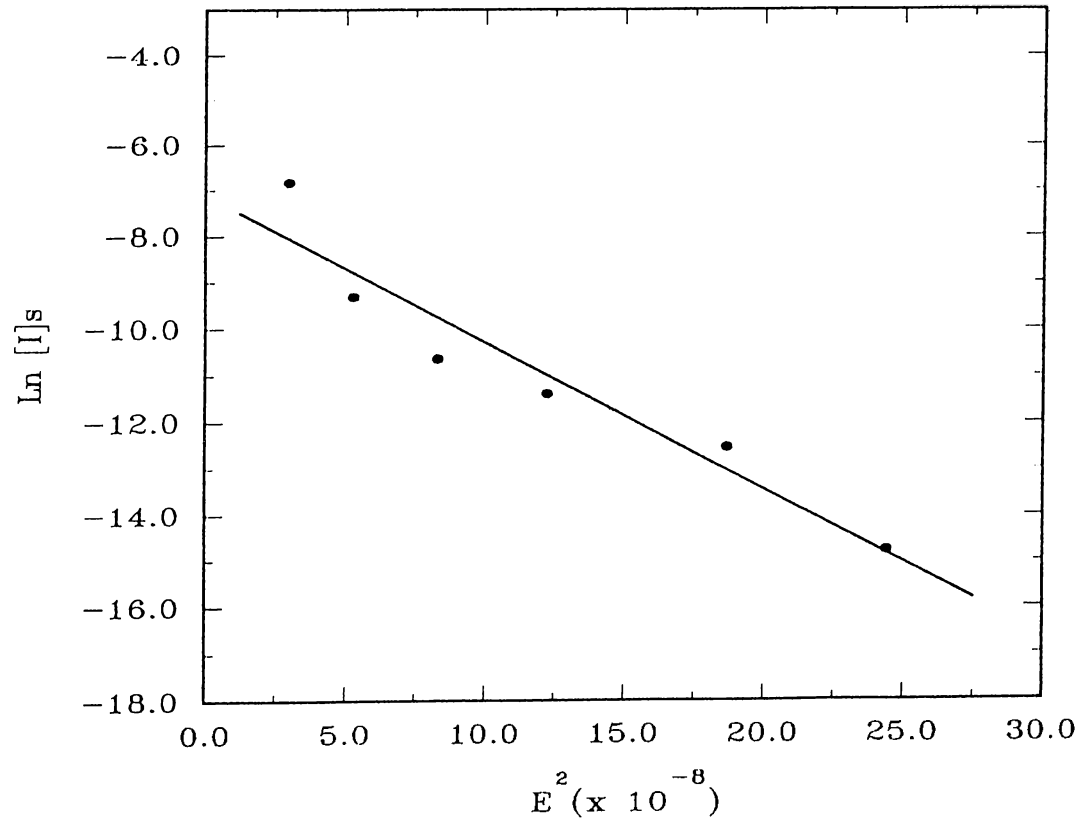


Figure 3.30: Dubinin-Radushkevich Isotherm for sorption of Radioiodine on Chlorite-Illite Clay Mixture

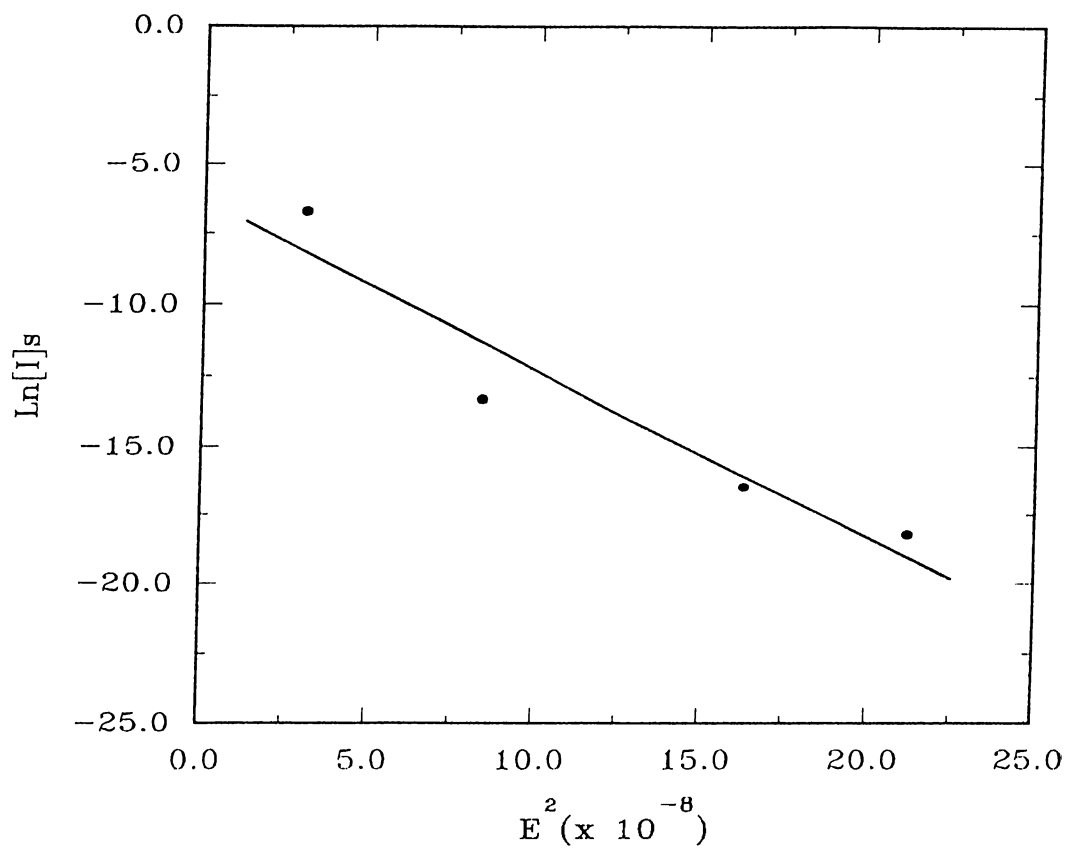


Figure 3.31: Dubinin-Radushkevich Isotherm for sorption of Radioiodine on Bentonite

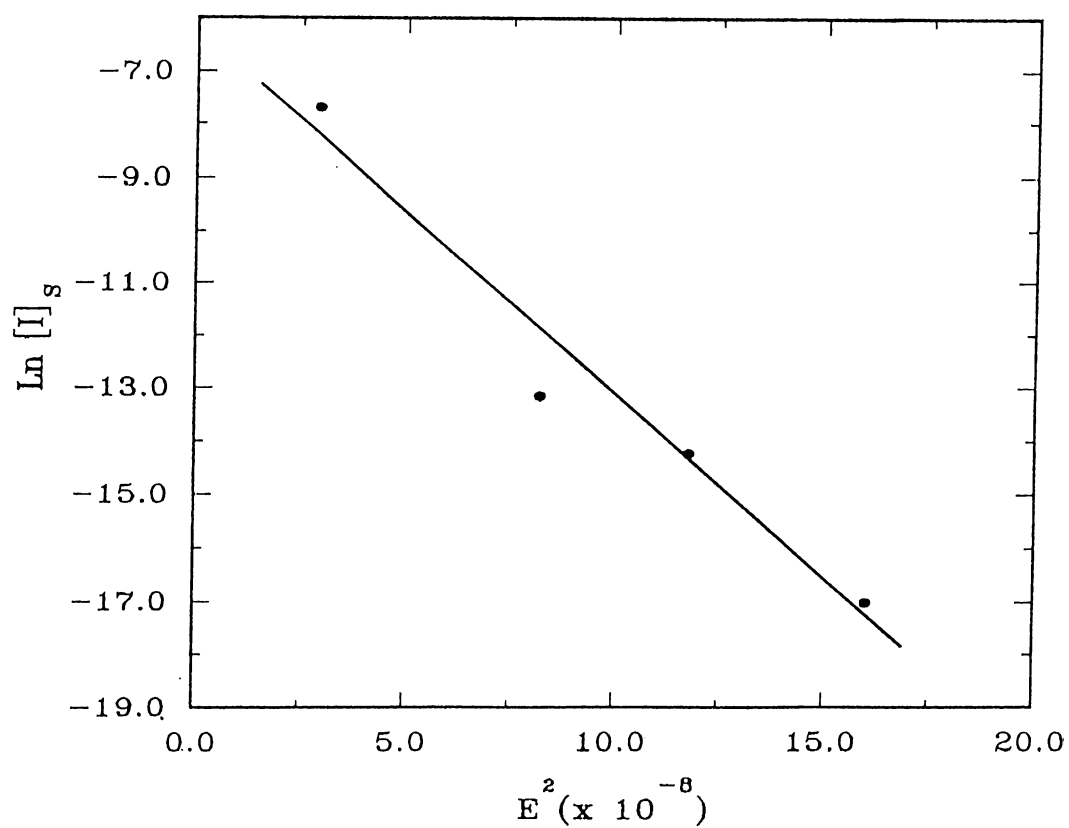


Figure 3.32: Dubinin-Radushkevich Isotherm. for sorption of Radio iodine on Kaolinite

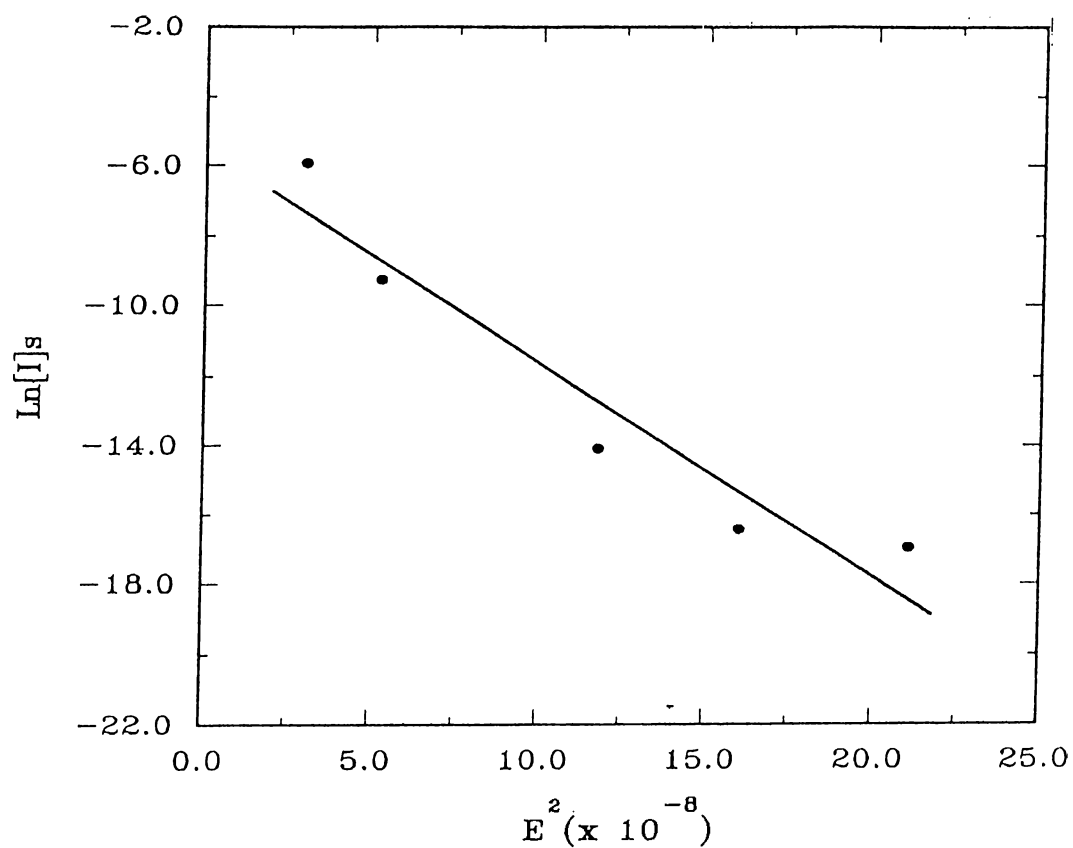


Figure 3.33: Dubinin-Radushkevich Isotherm for sorption of Radio iodine on Alumina

Sample	$[I]_i^0$ (mmole/ml)	$R_{d,(exp.)}$ (ml/g)	$R_{d,(D-R)}$ (ml/g)	$R_{d,(Fru.)}$ (ml/g)
Chlorite-Illite	1×10^{-3}	1.6 ± 0.34	0.3	0.6
	1×10^{-4}	1.0 ± 0.6	1.7	1.7
	1×10^{-5}	3.3 ± 0.6	6.6	4.9
	1×10^{-6}	19.8 ± 4.2	23.1	15.3
	1×10^{-7}	136.8 ± 19.4	83.3	70.3
	1×10^{-8}	175.7	163	220
Bentonite	1×10^{-4}	7.4 ± 1.4	2.3	1.1
	1×10^{-5}	9.4 ± 3.1	5.4	1.4
	1×10^{-6}	0.8 ± 0.1	9.0	1.8
	1×10^{-7}	7.6 ± 0.30	11.3	2.3
	1×10^{-8}	28.3 ± 6.5	9.8	3.1
Kaolinite	1×10^{-4}	6.4 ± 2.2	3.4	2.6
	1×10^{-5}	5.1 ± 0.7	7.4	4.2
	1×10^{-6}	7.2 ± 2.0	12.3	7.2
	1×10^{-7}	12.71 ± 1.5	14.7	12.3
	1×10^{-8}	18.4 ± 2.7	12.3	21.2
Alumina	1×10^{-3}	3.0 ± 0.9	0.7	0.9
	1×10^{-4}	2.4 ± 0.5	1.7	0.9
	1×10^{-6}	1.3 ± 0.2	3.1	1.0
	1×10^{-7}	1.6 ± 1.3	2.3	1.0
	1×10^{-8}	4.9 ± 0.5	1.1	1.0

Table 3.10: Experimental and Theoretical R_d Values for the Adsorption of Radioiodine on Clay Minerals. $R_{d,(exp.)}$: Experimentally obtained R_d values, $R_{d,(D-R)}$: R_d Calculated from Dubinin-Radushkevich Isotherm, $R_{d,(Fru.)}$: R_d Calculated from Freundlich Isotherm

Using equations 3.1 and 3.2, the theoretical R_d values can be calculated from the constants found from the isotherms. These values are also given in Table-3.10.

Sample	Freundlich		Dubinin-Radushkevich	
	N	A	$X_m(\text{meq/g})$	K
Chlorite-Illite	0.54	0.02	8.23×10^{-4}	3.17×10^{-9}
Bentonite	0.89	0.40	2.76×10^{-3}	5.15×10^{-9}
Kaolinite	0.77	0.31	4.09×10^{-3}	6.89×10^{-9}
Alumina	0.99	0.78	4.05×10^{-3}	4.32×10^{-9}

Table 3.11: The Constants Found From Fitting the Sorption Data to Isotherm Models for Clay Minerals

The constants found from the curve fitting of isotherms are listed in Table-3.11. The intercept of the Dubinin-Radushkevich isotherm gives information about the maximum adsorption amount and the slope enables the estimation of the adsorption energy as explained before. The energy values found are given in Table-3.12.

Sample	E (kJ/mole)
Chlorite-Illite	11
Bentonite	10
Kaolinite	8.5
Alumina	11

Table 3.12: Adsorption Energies Calculated from the Dubinin-Radushkevich Isotherm Constant K ($E = (2K)^{-1/2}$) for the Minerals

3.3.3 Site Distribution

From the constants of Freundlich and Dubinin-Radushkevich isotherms, and by considering Cl^- as the competing anion, the site distribution functions were obtained for the clay minerals as described for Bolu-Yeniçağ soil. The curves were obtained by giving arbitrary values to q , between -20 and +20. As can be seen in Figures 42-45, the sites are distributed over number of classes in the solid samples. This suggests that exchange is not restricted to one specific class of sites. In all of the samples the affinity of sites are higher for Cl^- , which is reasonable because of its smaller size, but there are also some sites which have higher affinity for iodine (positive q values). The parameters used in the calculations of the site distribution curves are given in Table-34. The highest affinity for iodide ion is observed in chlorite-Illite clay mixture and the lowest in Alumina.

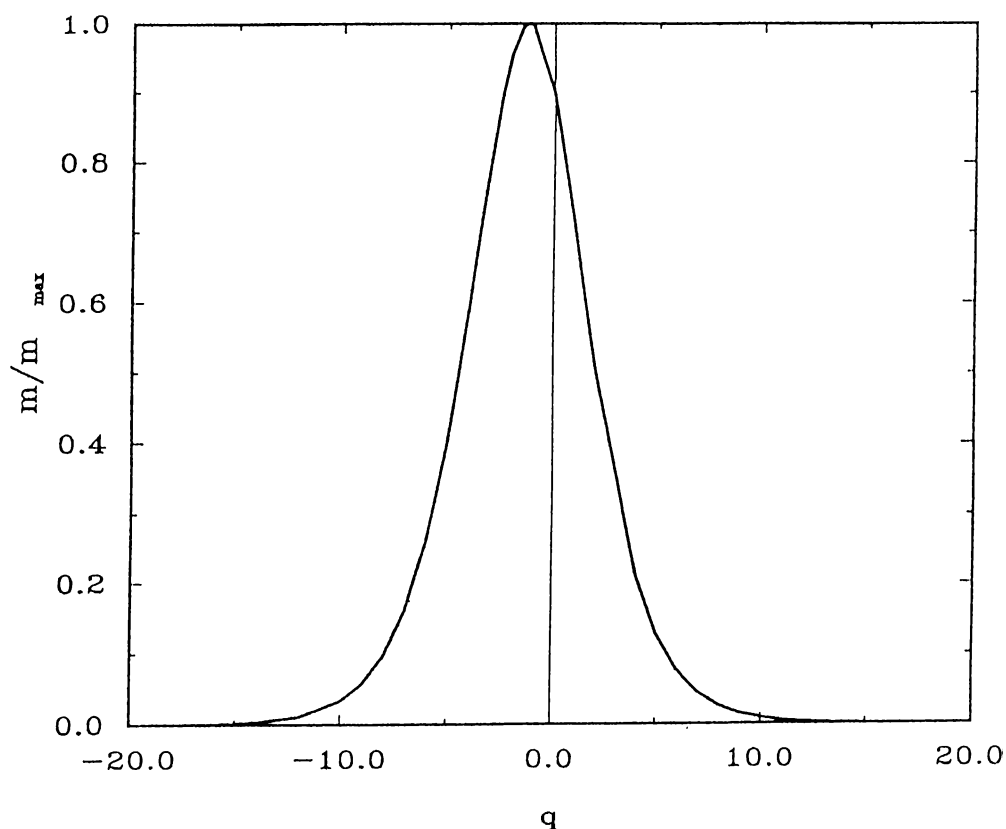


Figure 3.34: The Site Distribution on Chlorite-Illite, for the adsorption of iodine, Considering Cl^- as Competing Ion

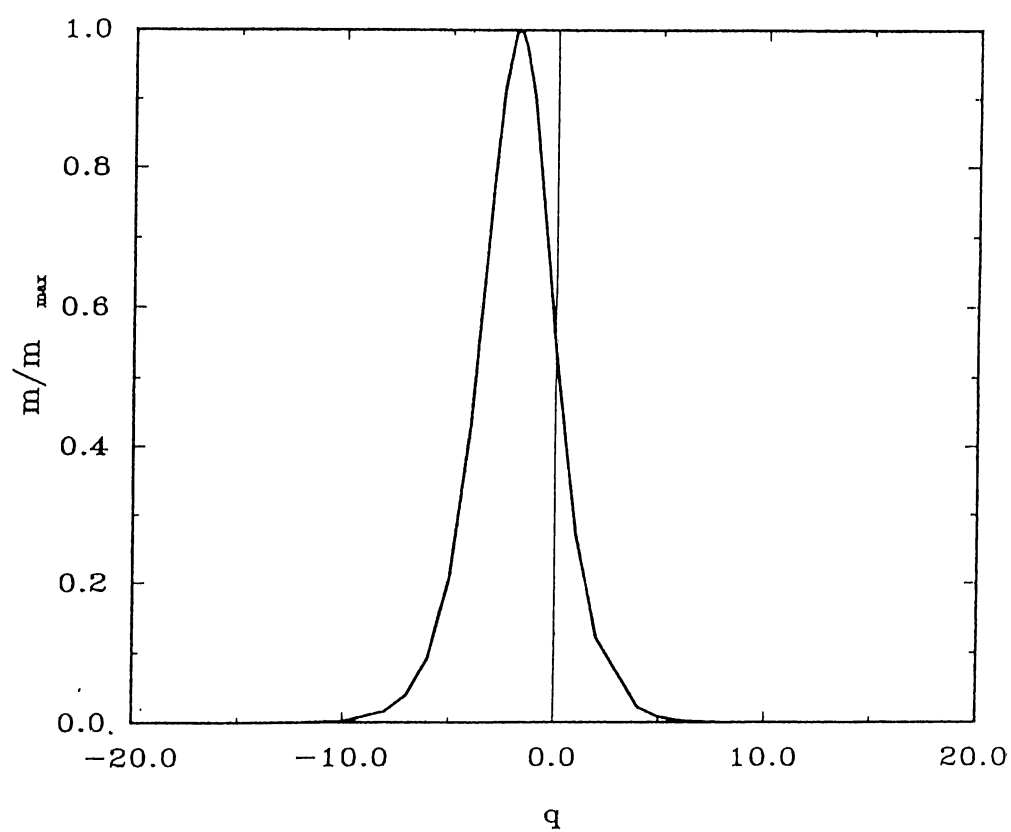


Figure 3.35: The Site Distribution on Bentonite, for the adsorption of iodine, Considering Cl^- as Competing Ion

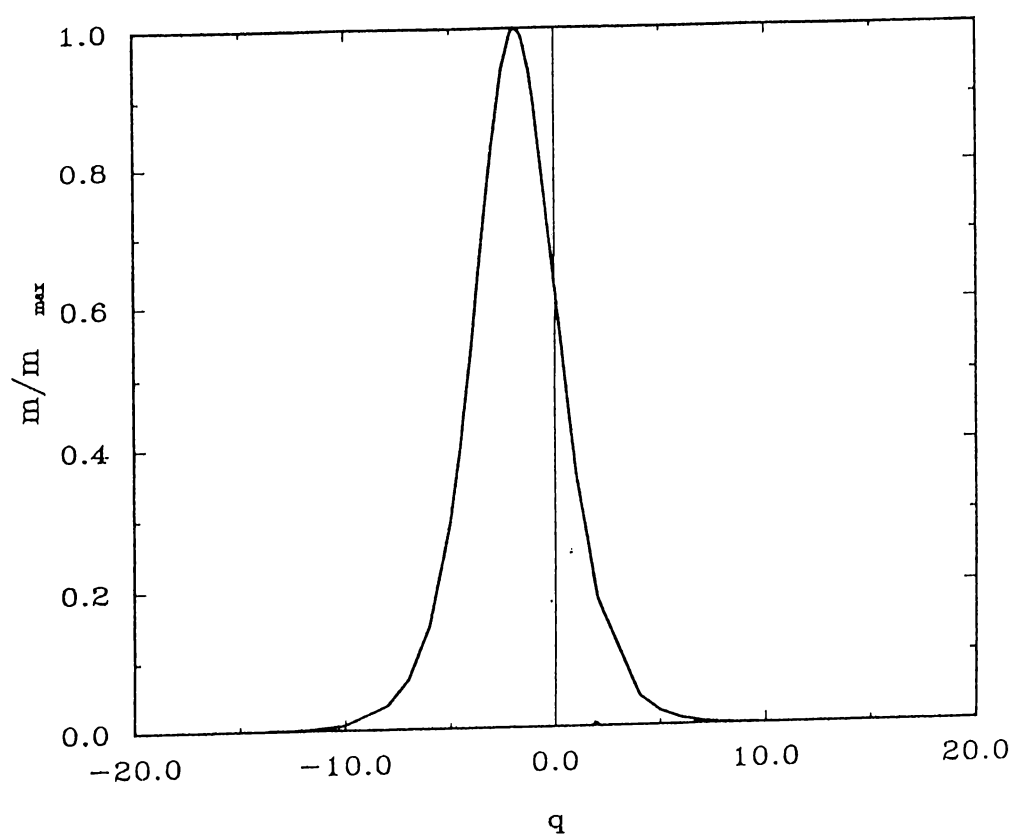


Figure 3.36: The Site Distribution on Kaolinite, for the adsorption of iodine, Considering Cl^- as Competing Ion

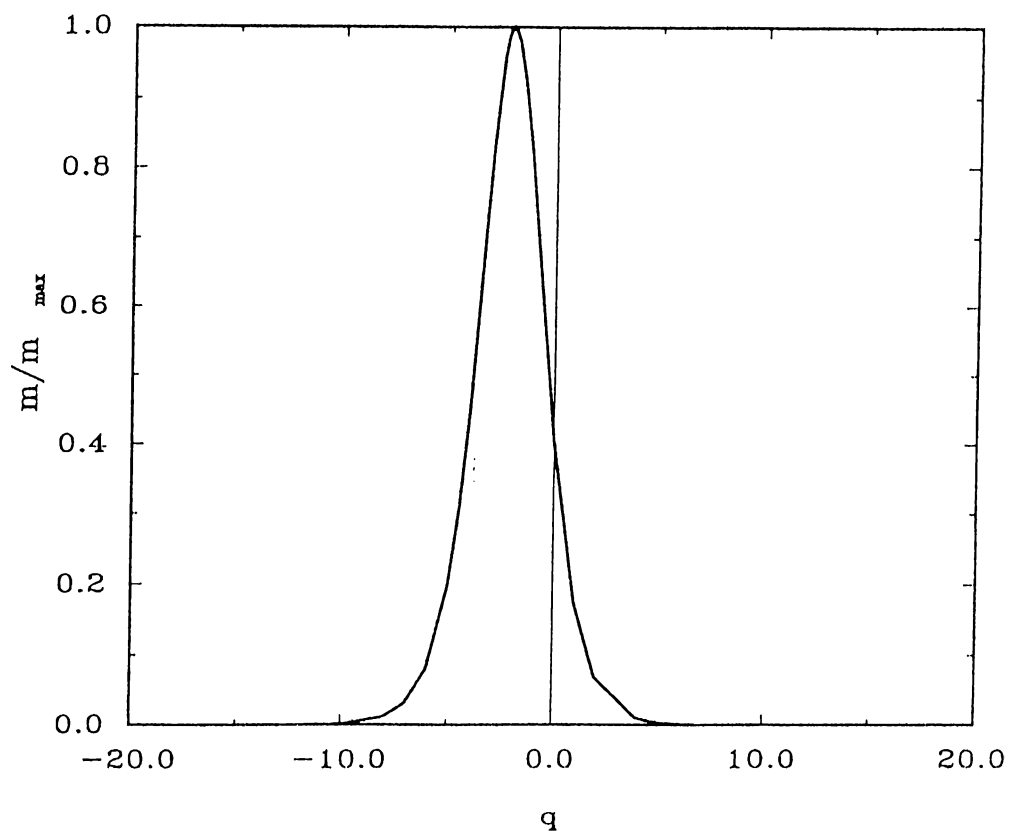


Figure 3.37: The Site Distribution on Alumina for the adsorption of iodine, Considering Cl^- as Competing Ion

Sample	α	q_{max}	k_{I^-}/K_{Cl^-}	k_{Cl^-}/K_{I^-}
Chlorite-Illite	0.52	-1.21	0.30	3.36
Bentonite	0.20	-1.83	0.16	6.24
Kaolinite	0.24	-1.85	0.16	6.35
Alumina	0.13	-2.10	0.13	7.97

Table 3.13: The Parameters Used to Calculate the Site Distribution Functions of Minerals and the Affinities Found from These Parameters for the Adsorption of Iodine on Clay Minerals

3.3.4 Effect of Complexing Agents

The effect of complexing agents on the sorption of radioiodine was examined by adding Ethylene Diamine Tetra Acetic Acid (EDTA) and Trimethyl Phenyl Ammonium Iodide (TPAI). Very low distribution ratios were found in the sorption experiments. It seems that the complexing agents occupy most of the adsorption sites in an irreversible manner. Samples pretreated with EDTA had greater distribution coefficients with respect to the samples pretreated with TPAI. The experimental Results are given in Table-3.14.

No experimental data is available for adsorption of iodine on soil or minerals pretreated with TPAI. But experiments have been done using EDTA as complexing reagent. Keiling et al. [54] have found lower results ($R_d=0.04\text{ml/g}$) for sorption of iodide on NaCl/Cement pretreated with 0.072 M EDTA at pH=12. Bors et al.[59] have done column experiments with soils pretreated with some complexing agents including EDTA and stated that the presence of these complexing agents increases the mobility of radioiodine and release radioiodine from its sorption sites. However later they performed sorption experiments with soil and clays pretreated with alkyl ammonium ions and obtained R_d values as high as 1500 ml/g for sorption of iodide ion on bentonite pretreated with hexadecyl trimethyl ammonium ion, HDPY⁺. Soil samples pretreated with the same ion, also adsorbed iodide ion in a large extent and the R_d values obtained was 900 ml/g[55].

Sample	R_d (ml/g)		
	EDTA	TPAI	untreated
Chlorite-Illite	3.0	0	175.7
Bentonite	0.8	0	28.3±6.54
Kaolinite	1.5	0.5	18.4±2.69
Alumina	1.4	0	4.9±0.45

Table 3.14: R_d Values for the Sorption of Radioiodine on Clay Mineral Samples Pretreated With EDTA and TPAI. $[I]_i^0 = 1 \times 10^{-8} \text{mmol/ml}$

Chapter 4

Discussion of Results

In this study sorption experiments were performed to observe the sorption behavior of radioiodine in different natural matrices, in accordance with the underground disposal of radioactive wastes. The main idea is to observe or predict how radioiodine distributes in the ground and to find the material which can hold radioiodine for a long time after it releases to the environment.

From the matrices used in this study the highest adsorption of iodine was observed in Bolu-Yeniçağ soil which has a high amount of organic carbon ($\approx 70\%$). The saturation time for this sample was rather long. In the studies done by Erten and Bors[36], the same effect is observed and it seems that as the amount of biomass in the sample increases, the time it has to reach saturation increases. It may be the indication of a dynamic adsorption by living microorganisms. The great lowering of R_d values by sterilization of soil can be a good reason for the high immobilization of iodine by microbial part of the soil.

The complex structure of soil organic matter, makes it difficult to make any assumptions about the sorption sites or mechanisms. Iodine may react with phenols, mono or dilignins, alcohols or proteinous materials in the humic acid. The estimation of an exact replacement or reaction is not possible in this stage without doing specified experiments with each component. Possible reactions are addition of iodine to the aromatic structure or substitution of some other molecules. It is stated by Christiansen[34] that phenol could be iodinated either by elemental iodine, hypiodous acid, or enzymatically controlled, in low concentrations of iodide ion $[I^-] = 1 \times 10^{-6}M$. It is also possible that iodide ion is converted to other forms by the organic part of the soil. Schnitzer[56] has stated that humic substances can react as oxidizing and reducing agents

Clay Mineral	OH^- Number in Unit Cell	R_d (ml/g)		
		$[I]_l^0 = 1 \times 10^{-8}$ (mmole/ml)	$[I]_l^0 = 1 \times 10^{-7}$ (mmole/ml)	$[I]_l^0 = 1 \times 10^{-6}$ (mmole/ml)
Chlorite-Illite	4+4	175.7	136.6	15.6
Kaolinite	8	18.4	12.7	7.2
Bentonite	4	28.3	7.4	0.8
Alumina	0	4.9	0.8	0.8

Table 4.1: Comparison of Distribution Ratios with the Number of OH^- ion in The Unit Cells of Clay Minerals

efficiently and Beherens has observed transformation of iodide ion to other chemical forms except iodate ion and reports a strong fixation of radioiodine by soil in these conditions[57, 58]. Most possibly the interaction of iodine with soil is not by just one site or a unique mechanism because of the structure of the soil. The sorption experiments also approve this fact by non-linearity of the isotherms and changes in the iodine loading curves.

As for the minerals the R_d values are much lower than those found for Bolu-Yeniçağ soil. The reason was related to the absence of organic compounds. Some low sorption values were observed in the clay minerals and alumina. As observed in the site distribution curves, the adsorption is not restricted to one class of sites (which would be reflected as a sharp distribution curve) and most probably there are more than one adsorption mechanism in the immobilization of radioiodine. One of them can be an anion exchange reaction and the most likely anion to be replaced is OH^- ions in the broken bonds around the edges and on the surface of the mineral particles. To have a better view, the R_d values are given for the clay minerals along with the number of OH^- ions in the unit cell.(Table-4.1)

Distribution ratios show an increasing trend by increase in number of OH^- ions in the unit cell. The R_d values for Kaolinite and Bentonite show a reverse effect at $[I]_l^0 = 1 \times 10^{-8}$ mmole/ml. But the distribution ratios obtained at $[I]_l^0 = 1 \times 10^{-7}$ mmole/ml $[I]_l^0 = 1 \times 10^{-6}$ mmole/ml, show the proposed trend. The reason for the reversal of the trend in Kaolinite and Bentonite at $[I]_l^0 = 1 \times 10^{-8}$ mmole/ml might be the double layer structure of the bentonite, compared with the single layer structure of Kaolinite. So at lower concentrations iodine can diffuse better in the interlayer and react at both sites. But for

a more convenient explanation the results must be studied in more detail. The higher R_d value obtained for Chlorite-Illite clay mixture compared to kaolinite which has the same number of OH^- ions in their unit cells, can be related to the higher amount of organics it contains, since it is a natural soil. In alumina rather low R_d values are observed. It is possible that iodine is loosely bounded to the crystal directly (to Al^{+3}) or by making complexes with the ions in the synthetic groundwater.

Anion exchange positions may also be present on the surface of clay minerals due to unbalanced charges resulting from the replacements within the lattice. As mentioned before, all the energies found from the Dubinin-Radushkevich isotherms were in the range of ion-exchange.

Hendricks[49], has stated that another factor in anion exchange is the geometry of the anion in relation to the geometry of the clay mineral structural units. Anions which have the same size and geometry of the silica tetrahedron, may be absorbed by fitting onto the edge of the silica tetrahedral sheet and going as extensions of these sheets. This possibility is low for I^- ion, since the reaction may destroy the lattice because of its large ionic size.

The higher affinity of sites for Cl^- ion enlightens another possibility. During the pretreatment step, the sites are brought to equilibrium and react with Cl^- where possible. In the sorption experiments some sites react directly with iodine and some exchange Cl^- with I^- .

The other sorption possibility is the presence of a double-layer in the solid/liquid interface. It is possible that the cations in the solution react with the anions in the surface of clays and iodine react with these bounded cations.

References

- [1] Allard, B., *Sorption of Actinides in Granite Rocks* **KBS-TR 82-81**, Swedish Nuclear Fuel Supply Co., Stockholm. (1982)
- [2] *Final Storage of Spent Nuclear Fuel* **KBS-3, SKBF/KBS Vol.I** Stockholm, Sweden (1983)
- [3] *Underground Disposal of Radioactive Waste* **Safety Series, No. 54**, Vienna (1981).
- [4] Larsson, A., Thomas, K.T., *The IAEA Program for the Underground disposal of Radioactive Wastes* **IAEA-CN-43/171** (1982)
- [5] Downs A.J, Adams C.J, *Comprehensive Inorganic Chemistry, Vol.2*, Pergamon Press (1973)
- [6] Wong G.F.T., Brewer P.G, *The marine Chemistry of iodine in anoxic basins*, **Geochim. Cosmochim. Acta Vol.41, 151** (1977)
- [7] Wiebenga E.H, Havinga E.E, and Boswijk K.H, *Advances in Inorganic Chemistry and Radiochemistry, Vol 3*, Academic Press, New York (1961)
- [8] McFadden, K.M., *Organic components of nuclear wastes and their potential for altering radionuclide distribution when released to soil*, **PNL-2563** (1980)
- [9] Whitehead D.C, *Iodine in the U.K Environment with Particular Reference to Agriculture*, **J.App.Eco. Vol.16, 269-279** (1979)
- [10] Srinivasan B., Alexander Jr. E.J and Manuel O.K, ^{129}I in terrestrial ores, **Science Vol.173, p 327** (1971)
- [11] Liu Y. and von Gunten H., *Migration Chemistry and Behaviour of Iodine Relevant to Geological Disposal of Radioactive Wastes*, **PSI- Bercht Nr. 16** (1988)

- [12] Robertson D. E., Toste, A.P., Abel K.H. and Brodzinski R.L., *Radionuclide Migration in Groundwater*, Annual Progress Report for 1982, **PNL-4773** (1982)
- [13] Waber, U., Von Gunten H.R. and Krähenbühl U., *The Impact of the Chernobyl Accident on a River/Groundwater Aquifer* (1987)
- [14] von Gunten H.R., Waber U.E and Krähenbühl U., *The Reactor Accident at Chernobyl: A Possibility to Test Colloid Controlled Transport of Radionuclides In Shallow Aquifer*, **J.of Contaminant Hydrology** (1987)
- [15] Bryant P.M., *Review of Radionuclides Released from the Nuclear Fuel Cycle and Methods of Assessing Dose to Man*, Biological Implications of Radionuclides Released From Nuclear Industries, **Vol. I, IAEA Vienna**, (1979)
- [16] R.R. Jones, R. Southwood, *Radiation and Health*, John Wiley & Sons, pp **128**, (1987)
- [17] Staley G.B., Turi G.P. and Schreiber D.L., *Radionuclide Migration from Low Level Waste*, A Generic Overview Symposium on Management of Low Level Radioactive Waste, May 13-17 1977, Atlanta, Vol II, Pergamon Press, (1979)
- [18] *Final Storage of Spent Nuclear Fuel, KBS-3, SKBF/KBS Vol.IV* Stockholm, Sweden, (1983).
- [19] Grim R.E., *Clay Mineralogy*, Mc Graw-Hill Book Company, Inc., New York, (1953)
- [20] Murray, H.H., *Industrial Characterization of Bentonites*, **Interceram**, **2**, **136**, (1967)
- [21] Kraupskoph K.B, *Introduction to Geochemistry*, Second Edition, Mc Graw Hill, (1979)
- [22] Singer F., *Industrial Ceramics*, Chapman and Hall, Cambridge University Press, London, (1979)
- [23] Kumada K, *Chemistry of Soil Organic Matter*, Japan Scientific Societies press Elsevier, (1987)
- [24] Schnitzer M, Khan S.U, *Humic Substances in the environment*, Marcel Dekker, New York, (1972)

- [25] Schnitzer M., *Soil Organic Matter-The next 75 years*, **Soil Science**, **151**, No.1, (1991)
- [26] Choppin G.R., *Humics and radionuclide migration*, **Radiochimica Acta** **44/45**, (1991)
- [27] Salter P.F, Ames L.L and Mc Garrrah J.E, *Sorption of selected radionuclides on secondary minerals associated with the Coulombia River Basalts*, **RHO-BW1-LD-43**, Rockwell Hanford Operations, Richland, Washington, (1981)
- [28] Ames L. L., McGarrarah J. E., Walker B. A., and Salter P. F., **Chem. Geol.** **35** 205 (1982)
- [29] Whitehead, D.C., *The Sorption of Iodide by Soils as Influenced by Equilibrium Conditions and Soil Properties*, **J.Sci.Fd Agric.** **24** 547-556, (1973)
- [30] Whitehead, D.C., *The Sorption of Iodide by Soil Components*, **J.Sci.Fd Agric.** **25** 73-79, (1974)
- [31] Torstenfelt B., *Migration of Fission Products Sr, Tc, I and Cs in Clay*, **Radiochimica Acta**, **39** 97-104, (1986)
- [32] Sheppard, M. I. and Thilbault D. H., *Default soil Solid/Liquid Partition Coefficients, K_{ds} , for Four Major Soil Types*, **Health Physics**, Vol59, No.4, pp471-482, (1990)
- [33] Rançon, D., *Comparative Study of Radioactive Iodine Behavior in Soils Under Various Experimental and Natural Conditions*, **Radiochimica Acta**, **44/45** 187-193, (1988)
- [34] Christiansen, J.V., and Carlsen, L., *Enzymatically Controlled Iodination Reactions in the Terrestrial Environment*, **Radiochimica Acta** **52/53**, Part II, 327-333, (1991).
- [35] Wildung R.E., Routson R.C., Serne R.J., and Garland T.R., *Pertechnetate, Iodide and Methyl iodide Retention by Surface Soils*, **BNWL- 1950**, Pt. 2, p.37, (1974)
- [36] Bors, J., Erten, H. N., Martens, R., *Sorption Studies of Radioiodine on Soils with Special References to Microbial Biomass*, **Radiochimica Acta**, **52/53**, 317-325 (1991)

- [37] Strickert R., Friedman A.M. and Fried S., *The Sorption of Technetium and Iodine Radioisotopes by Various Minerals*, Nucl. Technol. **49**, 253 (1980)
- [38] Relyea J.F and Serne R.J, *Inter laboratory Comparison of Batch K_d values*, Controlled Sample Program, Publication No.2, PNL-2872, (1979)
- [39] Meyer R.E. and Burtch F.W, *Systematic Study of metal Ion Sorption of Selected Geologic Media*, Annual Report, Oct.1978-Dec.1979, DOE/BETC/OR-14, (1980)
- [40] Bors J., *Sorption of Radioiodine in Organo-Clays and Soils*, Radiochimica Acta, **51**, 139-143 (1990)
- [41] Loomis A.G., *Grain Size of Whiteware Clays as Determined by the Andreason pipette*, Am. Cer. Soc. J., **21(11)** 393, (1938)
- [42] Norton F.H., and Speil S., *The Measurement of Particle Sizes in Clays*, Am. Ser. Soc. J. **21(3)**, 89 , (1938)
- [43] Aksoyoğlu, Ş., *Ph.D Thesis*, Middle East Technical University, Chemistry Dept., (1986)
- [44] Eylem C., *M. Sc., Thesis*, Middle East Technical University, Chemistry Dept., (1988)
- [45] Van Olphen H. and Tripiat J.J., *Data Handbook for Clay Materials and Other Non-Metallic Minerals*, Pergamon Press, London, (1979)
- [46] Jenkins R. et al., *Powder Diffraction File, Inorganic Phases*, JCPDS International Center for Diffraction Data, Swarthmore U.S.A, (1987)
- [47] Çaycı G., *Ph.D Thesis*, Ankara University, Agricultural Fac., Soil Dept., (1989)
- [48] Meier H., Zimmerhackl E., Zeitler G., Menge P. and Hecker W., *Influence of Liquid/Solid Ratios in Radionuclide Migration Studies*, Jour. of Radioanal. and Nuc. Chem. Art., Vol 109. No.1 pp 139-151, (1987)
- [49] Grim R.E, *Applied Clay Mineralogy*, Mc Graw Hill Int. Series in the Earth and Planetary Sciences, (1962)
- [50] Sposito G., *Derivation of the Freundlich equation for ion-exchange reactions in soils*, Soil Sci. Soc. Am. J. **44**, (1980)

- [51] Milton G.M., Cornett R.J., Kramer S.J and Vèzina A., *The Transfer of Iodine and Technetium Tracers From Surface Waters to Sediments* , Presented in Migration-92 , Spain (1992)
- [52] West J.M, Christofi N., Philip J.C, Arme S.C, *Investigations on the Populations of Introduced and Resident Micro-Organisms in Deep Repositories and Their Effects on Containment of Radioactive Wastes*, CEC Report, **EUR 10405 EN**, (1986)
- [53] Strack S. and Müller A., *Studies of the Microbiological Influence on the Behavior of Iodine-125 in Humus Soil*, in Proceedings of a Workshop Held in Brussels, **CEC-1984 pp 25-27** (1984)
- [54] Keiling C.H., Esser V., Marx G., *Migration and Sorption Behavior of Actinides and Fission Products in Systems of High Salinity under the influence of Organic Complexing Agents*, **Radiochimica Acta 44/45, 277-281**, (1988)
- [55] Bors, J., Martens, R. and Kühn W., *Studies on the role of Natural and Anthropogenic Organic Substances in the Mobility of Radioiodine in Soils*, **Radiochimica Acta, 44/45, 201-206**, (1988)
- [56] Schnitzer, M., *The Synthesis, Chemical Structure, Reactions and Functions of Humic Substances* , In *Humic Substances Effect on Soil and Plants* , Collection of Papers Presented Before The Eni Chem Agricultura Symposium in Milan, Italy. pp **14-28** (March 1986)
- [57] Behrens, H., *New Insights into the Chemical Behavior of Radioiodine in Aquatic Environments*, Environmental Migration of Long-Lived Radionuclides, **IAEA-SM-257/36** (1982)
- [58] Behrens, H., *Speciation of Radioiodine in Aquatic and Terrestrial Systems Under the Influence of Biogeochemical Processes*, In *Speciation of Fission and Activation Products in the Environment*, pp. **223** Elsevier App. Sc. Pub., New York, (1985)
- [59] Bors, J., Martens, R. and Kühn W., *Retention of Radioiodine in Soils Treated with Artificial Complexing Agents*, **Intern. Agroph. 3(3), pp103-111** , (1987)